Comparison of different soil water extraction systems for the prognoses of solute transport at the field scale using numerical simulations, field and lysimeter experiments

Inaugural-Dissertation

zur
Erlangung des Grades
Doktor der Agrarwissenschaften (Dr.agr.)

der
Hohen Landwirtschaftlichen Fakultät
der
Rheinischen Friedrich-Wilhelms-Universität
zu Bonn

Vorgelegt am 18.01.2005
von
Diplom Geograph Lutz Weihermüller
aus Hamburg

Überall geht ein frühes Ahnen dem späteren Wissen voraus.
Alexander von Humboldt

Vergleich unterschiedlicher Sickerwasserbeprobungssysteme zur Vorhersage einer sich verlagernden Stofffront im Feldmaßstab unter Verwendung numerischer Modelle und eines Feld- und Lysimeterexperimentes

Die ungesättigte Bodenzone beeinflußt entscheidend die Stoffdynamik und den Stoffhaushalt terrestrischer Ökosysteme. Da die meisten Reaktionen im Boden in der wäßrigen Phase ablaufen, ist die in-situ Erfassung von Bodenlösung unentbehrlicher Bestandteil der Bearbeitung vieler Fragen der Ökologie, der Wasserwirtschaft, der Landwirtschaft, des Umweltschutzes und der Validierung mathematischer Modelle. Zur in-situ Erfassung der Bodenlösung sind poröse Saugkerzen ein weit verbreitetes Mittel, wobei ihr Einfluß auf das umgebende Matrixpotential im Boden und ihr Sammelvolumen bis heute nur ungenügend erforscht sind. Diese Arbeit wurde zur Untersuchung des Saugkerzeneinflußbereiches (engl. suction cup activity domain (SCAD)), des Saugkerzenbeprobungsvolumens (engl. suction cup extraction domain (SCED)) und der Saugkerzenbeprobungsfläche (engl. suction cup sampling area (SCSA)) konzipiert. Zur numerischen Modellierung des Einflusses unterschiedlicher angelegter Saugspannungen in der Saugkerze, variierender Infiltrationsraten an der Bodenoberfläche und veränderten bodenhydraulischen Eigenschaften auf den Saugkerzeneinflußbereich, des Saugkerzenbeprobungsvolumen und die Saugkerzenbeprobungsfläche wurde das finite Elemente Programm HYDRUS-2D verwendet. Um die Fließwege im Boden zu bestimmen, die das Saugkerzenbeprobungsvolumen und die Saugkerzenbeprobungsfläche definieren, wurde der Einsatz eines Partikel-Trackers gewählt. Dadurch konnte gezeigt werden, daß der Saugkerzeneinflußbereich, das Saugkerzenbeprobungsvolumen und die Saugkerzenbebrobungsfläche primär von den hydraulischen Eigenschaften des umgebenden Bodens und der oberen Randbedingung (Infiltrationsrate), und nur sekundär von der angelegten Saugspannung in der Saugkerze abhängen. Die numerischen Befunde zeigen, daß der Saugkerzeneinflußbereich, das Saugkerzenbeprobungsvolumen und die Saugkerzenbebrobungsfläche bei höheren umgebenden Wasserleitfähigkeiten im Boden am größten ausfallen. Mit einer Zunahme der Infiltration verringern sich jedoch der Saugkerzeneinflußbereich und die Saugkerzenbebrobungsfläche. Desweiteren konnte festgestellt werden, daß das Saugkerzenbeprobungsvolumen direkt von der Beprobungsdauer abhängt. Für die räumliche Ausbreitung des Saugkerzeneinlußbereiches und der Saugkerzenbeprobungsfläche spielt die Bodenheterogenität nur eine untergeordnete Rolle, wohingegen sie bei der Extraktionsmenge von Bodenlösung und des Stoffdurchbruches einen wesentlichen Einfluß hat.

Um für verschiedene Beprobungssysteme Unterschiede in der Bodenwasserextraktion und des Stoffdurchbruches für einen konservativen Tracer und den Pestiziden Methabenzthiazuron (MBT) und Ethidimuron (ETD) zu ermitteln, wurde in einem zweiten Schritt ein Lysimeter- und Feldversuch durchgeführt. Dazu wurden keramische Saugplatten, Tensiometer, TDR-Sonden und Saugkerzen installiert und kontinuierlich über einen Zeitraum von 427 Tagen beprobt. Allgemein zeigten die Großlysimeter in der Lysimeterstation des *Forschungszentrums Jülich* vergleichbare Drainageverhältnisse über die gesamte Beprobungszeit, die sich in den Messungen der Tensiometer, TDR-Sonden und Wasserspenden widerspiegeln. Im Gegensatz zu den Großlysimetern konnten in den Beprobungsnestern auf dem Testfeld Merzenhausen niedrigere Wassergehalte über den gesamten Beprobungszeitraum ermittelt werden. Die Differenzen in den Wasser-

gehalten können auf Unterschiede in den klimatischen Bedingungen (Niederschlag und Evaporation) zurückgeführt werden, die wiederum auf mikroklimatischen Bedingungen der beiden Lokalitäten basieren. Als Konsequenz der kurzen Breprobungsperiode und des trockenen Sommers im Jahre 2003 konnte kein kompletter Bromiddurchbruch in 120 cm Tiefe ermittelt werden. Für die Testsubstanzen ETD und MBT konnte dagegen auch in einer Tiefe von 40 cm kein kompletter Durchbruch gemessen werden, was auf eine Retardation der Substanzen zurückzuführen ist. Als Folge dessen wurden die Bromiddurchbrüche in 120 cm Tiefe und die MBT- und ETD- Durchbrüche für beide Tiefen nur qualitativ beschrieben. Die Variabilität der Bromiddurchbrüche für die unterschiedlichen Sammelsysteme in 40 cm Tiefe, sowohl auf dem Testfeld Merzenhausen als auch in den Großlysimetern, spiegelt sich in den Unterschieden der effektiven Transportparameter, mittlere Porenwassergeschwindigkeit (v) und Dispersivität (λ) wider. Für die Pestiziddurchbrüche konnten dagegen für alle Sammelsysteme keine Transportparameter ermittelt werden. Im Allgemeinen wurden jedoch höhere Widerfindungen für das ETD nachgewiesen, wobei einzelne hohe Spitzenkonzentrationen für ETD und MBT auf einzelne Fließereignisse (präferentiellen Fluß) zurückzuführen sind.

Neben den effektiven Transportparametern können auch Unterschiede in den ermittelten Massenwiderfindungen und Extraktionsmengen sowohl für die Saugkerzen, als auch für die keramischen Platten, durch die vorherrschenden Bodenheterogenitäten erklärt werden. Die größere Variabilität in den Saugkerzen - im Vergleich zu den keramischen Platten - kann auf ihre kleine Oberfläche zurückgeführt werden, wodurch eine geringere Flächenintegration, und damit Mittelung, erfolgt. Da unter nichtstationären Bedingungen die Bestimmung des Saugkerzenbeprobungsvolumens und somit der Saugkerzenbeprobungsfläche nicht möglich ist, ist ein direkter Vergleich der Durchbrüche in den Saugkerzen und den keramischen Platten nur bedingt möglich. Auf Grund der genannten Variabilitäten in den Saugkerzenergebnissen ist festzustellen, daß die Installation von wenigen Saugkerzen im Labor- und Feldversuch keine aussagekräftigen Ergebnisse für die Prognose und Beschreibung des Stofftransportes bieten.

Comparison of different soil water extraction systems for the prognoses of solute transport at the field scale using numerical simulations, field and lysimeter experiments

Sampling of water and solutes in soils is of major importance to understand water movement and solute transport in soils and to validate mathematical models. Porous cups are widely used to extract soil water for monitoring solute transport. However, it is not yet clear how the suction cup influences the matrix potential in the surrounding soil and which part of the soil is sampled. This research was designed to numerically evaluate the activity domain, the extraction domain and sampling area of a suction cup under constant infiltration. A finite element model (HYDRUS-2D) was used to simulate the effect of various applied suctions at two infiltration rates on the water status in three soils (clay loam, sandy clay and sandy soil). Particle tracking was used to track the streamlines which define the sampling area and extraction domain of the suction cup. In general, the activity domain, the extraction domain and sampling area of the suction cup depend primarily on the soil hydraulic parameters and the upper boundary, and secondarily on the applied suction. The results showed that the activity domain, the extraction domain and the sampling area are largest for highest ambient hydraulic conductivities. The activity domain and the sampling area also decrease with increasing infiltration rates. Further, the extraction domain of the suction cup depends strongly on the duration of water extraction. Soil heterogeneity seems to play a minor role with respect to the activity domain and sampling area of the cup, but a major role in the amount of extracted water and solute breakthrough.

In a second step, a lysimeter and field experiment equipped with porous ceramic plates, tensiometers, TDR-probes and suction cups was conducted over a 427 day period to evaluate differences in soil water sampling and solute transport for a conservative tracer and the test compounds Methabenzthiazuron (MBT) and Ethidimuron (ETD). In general, the two lysimeters at the lysimeter station at the *Forschungszentrum Jülich* showed comparable leaching behaviour over time, reflected by the tensiometer, TDR and drainage measurements. In comparison to the lysimeters the sampling pits at the test site Merzenhausen indicate lower water contents and amounts of extracted water over the whole sampling period. These differences can be traced back to variability in the climatic data (e.g. precipitation and evaporation) caused by microclimatic distinctions at the two locations. The results of the field and lysimeter experiments show that no complete tracer breakthrough could be determined at a depth of 120 cm for the sampling pits and the lysimeters as a consequence of the short sampling time and the dry summer in 2003. As a result of retardation the breakthrough of the test substances MBT and ETD is not complete even for the samplers at 40 cm depth. Therefore, bromide breakthrough at 120 cm depth and MBT/ETD breakthrough for 40 and 120 cm depth were just described in qualitative terms. The variability in bromide tracer breakthrough at 40 cm depth for the different samplers at the two locations is reflected in the variability of the mean pore water velocity, v, and dispersivity, λ. On the other hand, no transport parameters could be determined for the pesticide breakthrough at all locations. In general, larger ETD recoveries were measured compared to the MBT for all samplers, whereby high peak concentrations in the samplers can be traced back to single events. The differences in the amount of extracted water, bromide masses, and as a result variability in transport

parameters, in the ceramic plates and the suction cups are closely related to the local heterogeneity in the hydraulic properties of the surrounding soil. The larger variability of the suction cups compared to the ceramic plates can be explained by the smaller surface area of the suction cups and, therefore, smaller integration over the sampling area and larger influence of local heterogeneity. The comparison of the breakthrough in the suction cups and the ceramic plates is not directly possible due to uncertainties in the normalization of the amount of extracted water and the lack of knowledge of the suction cup extraction domain and suction cup sampling area for transient conditions.

As a main result it was identified that the installation of such few suction cups for laboratory or field-scale experiments is not suitable for the aim of transport description by solute breakthrough.

Danksagung

Contents

List of Figures

List of Tables

Abbreviations

Institute and Organisations

FZJ	Forschungszentrum Jülich GmbH (Research Centre Jülich)
MRZ	Test site Merzenhausen

Space Indices

x	horizontal transversal direction
y	vertical transversal direction
z	longitudinal direction, mean flow direction

Instuments, Materials and Others

BTC	breakthrough curve
CEC	Cation Exchange Capacity
ETD	Ethidimuron
MBT	Methabenzthiazuron
PTFE	Teflon
PVC	Polyvinyl chloride
WP	Wettable Powder

Physical Symbols

α	[L^{-1}]	reciprocal value of the air entry value (bubble point)
α_θ	[-]	scaling factor for water content
α_h	[-]	scaling factor for pressure head
α_K	[-]	scaling factor for hydraulic conductivity
A	[L^2]	area (surface of the suction cup)
c	[LT^{-1}]	speed of light
γ	[hPa K^{-1}]	psychrometer constant
D	[L]	distance (wall thickness of a suction cup)
D_r	[L]	drainage and extracted water in the lysimeters
D_{eff}	[L^2T^{-1}]	effective dispersion coefficient
D_{hD}	[L^2T^{-1}]	hydrodynamic dispersion coefficient
D_{mD}	[L^2T^{-1}]	molecular dispersion coefficient
$D_{w_{(z)}}$	[L]	depth of water drained past depth, z
C	[cm^{-1}]	weight specific water capacity
C_E	[ML^{-3}]	equilibrium solution substance concentration
C^f	[ML^{-3}]	flux concentration
C^r	[ML^{-3}]	resident concentration
C_S	[MM^{-1}]	concentration of substance sorbed to the soil
$C_{S_{max}}$	[MM^{-1}]	maximum of sorption
E	[mm]	evaporation
e	[L]	actual vapour pressure
e_s	[hPa]	saturated vapour pressure
ET	[L]	evapotranspiration or latent heat flux λE
Δ	[hPa K^{-1}]	slope of the saturated vapour pressure curve
Δt	[T]	time intervall
Δts	[T]	travel time of an electromagnetic wave
f	[%]	relative humidity
$f_{(v)}$	[m^{-1}kPa^{-1}]	wind speed function
G	[W m^{-2}]	soil heat flux
h	[L]	pressure head
J_c	ML^{-2}T^{-1}	particle velocity (convection)
J_{hd}	[ML$^{-2}T^{-1}$]	hydrodynamic dispersion
J_{md}	[ML$^{-2}T^{-1}$]	molecular diffusion
J_s	[M L^{-2}T^{-1}]	solute flux density
J_w	[LT^{-1}]	water flux density
K	[L T^{-1}]	hydraulic conductivity
Ka	[-]	dielectric constant
K_F	μg$^{1-\frac{1}{n}}$(cm^3)$^{\frac{1}{n}}$g^{-1}	*Freundlich* constant with $\frac{1}{n} = $ *Freudlich* exponent
K_{oc}	μg$^{1-\frac{1}{n}}$(cm^3)$^{\frac{1}{n}}$g^{-1}	organic carbon partitioning coefficient
K_ψ	[L T^{-1}]	hydraulic conductivity as a function of matric potential, ψ
$K_{(\theta)}$	[L T^{-1}]	hydraulic conductivity as a function of water content, θ
K^A	[-]	dimensionless anisotropy tensor
K^A_{ij}	[-]	component of a dimensionless anisotropy tensor K^A
K_D	[L^3M^{-1}]	partition coefficient

K_p	$[L^{-1}]$	probe constant
K_r	$[\text{-}]$	relative hydraulic conductivity
K_s	$[L\ T^{-1}]$	saturated hydraulic conductivity
K_u	$[L\ T^{-1}]$	unsaturated hydraulic conductivity
L	$[mm;\ cm;\ m]$	lenght
La	$[L]$	apparent probe lenght
$L_{Br_{(z)}}$	$[M\ L^{-2}]$	mass of bromide leached past depth z per unit area
l	$[\text{-}]$	tortuosity
L_n	$[J\ kg^{-1}]$	latent heat of vaporization
λ_{eff}	$[L]$	dispersivity
λ_f	$[L]$	correlation lenght
μ	$[T^{-1}]$	first-order rate coefficient for degradation
μ_M	$[L]$ or $[T]$	1. moment
m	$[\text{-}]$	*van Genuchten* parameter
M	$[M]$	solute mass
M_{app}	$[ML^{-2}]$	applied mass per unit area
M_o	$[ML^{-2}]$	sampled mass per unit area
n	$[\text{-}]$	*van Genuchten* parameter
σ	$[Sm^{-1}]$	bulk electrical conductivity
ρ	$[\text{-}]$	reflection coefficient
q	$[L^3\ T^{-1}]$	volumetric water flow into the suction cup
R	$[\%]$	mass recovery (0. moment)
Rn	$[W\ m^{-2}]$	net radiation
R_s	$[\text{-}]$	calculated reflection coefficient
r_m	$[L]$	maximum suction cup radius
S	$[T^{-1}]$	sink term for consideration of the evaporation
S_e	$[L^3L^{-3}]$	effective water content
T	$[sec;\ min;\ h;\ a]$	time
t	$[K]$	temperature
t_a	$[K]$	mean air temperature $\frac{t_{min}-t_{max}}{2}$
θ	$[L^3L^{-3}]$	volumetric water content
θ_ψ	$[L^3L^{-3}]$	water content as a function of matric potential, ψ
θ_r	$[L^3L^{-3}]$	residual water content
ψ	$[L]$	matric potential, ψ or ψ_m, expressed as equivalent height
ψ_w	$[L]$	total water potential
ψ_g	$[L]$	gravitational potential
ψ_s	$[L]$	osmotic potential
ψ_{tp}	$[L]$	tensiometer pressure potential
v	$[LT^{-1}]$	mean pore water velocity
V	$[L^3]$	volume
V_s	$[L^3]$	volume of sampled water
$V_{wi_{(z)}}$	$[L^3]$	ith sample volume at depth z
χ	$[L]$	characteristic lenght of soil matric
Zc	$[\Omega]$	cable impedance

Chapter 1

Introduction

The benefits of the green revolution in agriculture have been immense. With increasing inputs of fertilizer, water and pesticides, new crop strains and technical innovations the global agricultural production has doubled in the last 40 years (*Food and Agricultural Organization of the United Nations*, 2001). World population is projected to increase well in the next decades and, therefore, global food production must keep pace to sustain the future population. This increased production needs to be realized with a constant land surface available for agriculture. This will put pressure on the natural resources soil and water. The main environmental pressures of agriculture stem from conversion of natural ecosystems to agricultural land, from agricultural nutrients and pesticides that pollute aquatic and terrestrial habitats as well as drinking water resources. If we consider that the use of pesticides increased by a factor of 32 in the last 50 years (*Food and Agricultural Organization of the United Nations*, 2001) the problem of drinking water contamination may become more urgent.

Therefore, European and national concepts for plant protection products (PPP) registration with a tiered approach regarding the estimation of groundwater contamination were established. In the German registration procedure three steps in the risk assessment for groundwater can be destinguished. The first tier uses intrinsic parameters of the compounds. The second step uses computer-aided model calculations for the prediction of their mobility. In the third tier evidence relevant to authorization should be given, in particular through the use of lysimeter studies or field experiments, about the possibility and the extent of ground water contamination by a PPP after application according to good agricultural practice (*Winkler et al.*, 1999). The main aim of the approach is to exclude potentially mobile PPPs exceeding an average value of 0.1 μg L^{-1} in the leachate at the bottom of the soil profile and of 0.5 μg L^{-1} for the sum of all PPPs (*Trinkwasserverordnung*, 2001).

The fate of PPPs and their mobility after application are affected by their chemical and physical properties, the site characteristics such as soil, geology, vegetation, and the handling practice of the pesticide user. Pesticides may be transformed by degradation processes or transported by runoff, volatilization, wind erosion and the movement through the soil into the ground water with percolating water.

To monitor the transport of PPPs in the soil different methods are available. The most common one used in pesticide registration and solute transport studies is the lysimeter concept (*Führ et al.*, 1998). For the experiments on a field scale, soil coring is one

widely-used technique, whereby each soil core shows a singular characteristic for the single time of extraction. For in-situ monitoring of the leaching process by soil water extraction capillary wicks, porous plates, and suction cups are widley used. The advantage of these methods resides in the high temporal resolution of the solute transport in comparison to the lysimeter concept and the possibility of solute extraction in different soil depth or horizons. Additionally, the installation of in-situ water extraction systems is less expensive than the installation of a lysimeter. Recent studies investigated the difference between porous plates and lysimeters in structured soils in terms of soil water movement and solute transport (*Kasteel et al.*, 2004). Various authors studied in field experiments the differences in solute transport determined by suction cups (e.g. *Barbee and Brown* (1986), *Williams and Lord* (1997), *Caron et al.* (1999)), or investigated the interaction between soil water extraction via suction cups and the influence on the natural flow field (e.g. *Warrick and Amoozegar-Fard* (1977), *Tseng et al.* (1995) and *Hart and Lowery* (1997)). However, the sampling volume and the imposed changes in the natural flow patterns are not well known up to now, and a generall comparison with lysimeter and porous plates is not available. As stated by *Litaor* (1988), there is no single device that will perfectly sample soil solution in all conditions encountered in the field. It is therefore of interest to reach an understanding of methodological differences, and to have criteria to select the appropriate sampling methods with respect to the objectives.

1.1   Aims and scope

To date, the understanding of processes, factors, and interactions that influence the amount of extracted water and the solute composition sampled with suction cups is limited. But this information is required for process description of solute transport in natural soils. Improved system understanding can lead to a low cost and easy to install water sampling system which can help to predict solute transport in natural soils for the benefit of environmental protection.

The main objectives of this work were to perform numerical simulations with different boundary conditions and to implement the findings in the interpretation of the lysimeter and field experiments.

In a first part of this thesis, theoretical considerations on the processes affecting the spatial influence of a suction cup in soil and changes in solute transport initiated by the suction cups are presented, including testing and validation of available model and experimental approaches. In the second part, a detailed experimental study was conducted to obtain data for the comparison of the different soil water sampling systems. Finally, the numerical experiments of the suction cup influence were used for the interpretation of the experimental data.

The main goals are summarized as follows:

- Characterization of the suction cup activity domain (SCAD), suction cup extraction domain (SCED) and suction cup sampling area (SCSA) of active suction cups (definitions are given in Chapter 6).

- Determination of the boundary conditions and soil properties [e.g. infiltration, applied suction, duration of water extraction, soil hydraulic properties and soil

heterogeneity] affecting the activity domain, extraction domain and sampling area of a suction cup.

- Identification of processes that change the travel time and travel time variance of solutes extracted by suction cups.

- Validation of the numerically derived data with analytical and experimental data from literature.

- Comparison of the experimental data obtained from the various soil water extraction devices and application of the results from numerical simulations.

Chapter 2

Soil solution sampling with suction cups

Porous suction cups are used to monitor solute concentration in soil water with time and depth. The problems that occur during operation were widely discussed throughout the last decades (see Table 2.1). A serious limitation, however, resides in the fact that the sampling volume and the imposed changes in natural flow pattern are not well known (*Grossmann and Udluft*, 1991). In the following a literature review will give a closer insight into the monitoring technique and the problems occured.

2.1 Terminology

Various terms have been used to describe the same sampling device. A few of these terms are porous tube device (*Krone et al.*, 1951), deep pressure vacuum lysimeter (*Parizek and Lane*, 1970), vacuum extractor, porous ceramic candle, or porous cup as well as suction cup (*Duke and Haise*, 1973). Since the suction or porous cup (*Saugkerze)* is only part of the whole system (the small porous body at the top end) the term suction probe (*Saugsonde*) is proposed for the sampling system (*DVWK*, 1990) and the term suction-cup method (*Saugkerzen-Methode*) for the soil water sampling technique (*Grossmann and Udluft*, 1991). Subsequently, we will use the term suction cup for the porous device.

2.2 The suction cup

As stated above porous cups provide a simple and direct method for the collection of soil water samples in the vadose zone. Moreover, the advantage of the porous cup method in comparison to other soil water sampling techniques is a negligible physical disturbance of the surrounding soil and as a consequence a minor change in the natural percolation process. The most important advantage is the possibility to sample soil water at different depths to record time and spatial variable data, with low installation and financial effort.

The principle of the porous cups was first described by *Briggs and McCall* (1904). They suggested that porous cups can be used as artifical roots to study soil water availability to plants as well as its composition. Since then, porous cups are widely used in

different surveys to collect soil water for analytical purpose (*Krone et al.*, 1951; *Reeve and Doering*, 1965; *McGuire and Lowery*, 1994; *Williams and Lord*, 1997, etc.)

Different kinds of porous cups made out from diverse materials are described in the literature by e.g. *Czeratzki* (1971), *Barbee and Brown* (1986) and *Hart and Lowery* (1997) but in general they all consist of a porous cup sealed to a tube. Inside this tube a small tube is installed to collect the extracted soil water (Figure 2.1). Different sintered materials like aluminum-oxide, nickel-sinter, glass-sinter as well as plastic and membrane filters are in use as porous cups (*DVWK*, 1990). The porous cup should be in direct contact to the soil water (soil capillary system) and an applied suction is the driving force for water to move into the porous cup.
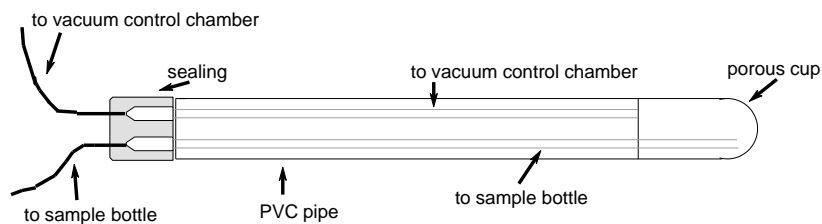
Figure 2.1: **Design of a suction cup without shaft collection.**

2.3   Installation of a suction cup

The installation of the suction cup into the soil profile is rather simple compared to other soil water sampling systems. In general, three installation modes can be distinguished: horizontal, vertical non-shaft and vertical in 45° installation. In the case of vertical installation a vertical hole is drilled by means of a soil auger with a diameter similar to that of the probe up to a specific depth. Soil material from upper horizons should be prevented from falling into the hole. To get good hydraulic contact between the suction cup and the soil a slurry of the auger material is refilled into the hole before inserting the suction probe. For coarse sand and gravel the larger fraction are removed from the slurry material by sieving, or fine quarz silt can be used instead. During the installation of the probe the slurry begins to move upwards between the shaft and the soil and fills any gaps. To obtain reliable results water should be prevented from seeping along the shaft as this causes hydraulic short cuts (*DVWK*, 1990; *Grossmann and Udluft*, 1991).

For a horizontal installation it is also advantageous to install the probe in a slight angle to provide water percolating away from the suction cup. For a vertical installation *Mitchell et al.* (2001) proposed a 45° angle to the soil surface for the suction cup. Another possibility is the use of non-shaft cups and a refilling of the borehole with the soil material. With respect to the soil heterogeneity it seems reasonable to install several suction probes within a small area to record a mean percolation front (*Starr*, 1985). At the same time, the space between the single devices should be larger than the influence of each probe on the natural flow field.

2.4   Operation of a suction probe

To move an infinitesimal volume of water within porous media it is neccesary to generate a gradient of energy (soil water potential) between two reference points (*Roth*, 1996). If the potential within the suction cup is lower than in the surrounding soil water flows through the finely-pored hydrophilic suction cup material until the potential gradient is at equilibrium. Finally, the hydraulic conductivity of the suction cup material should be higher than the surrounding soil to get reliable results (*DVWK*, 1990; *Grossmann and Udluft*, 1991). The suction to be applied in the porous cup depends on the soil type, the
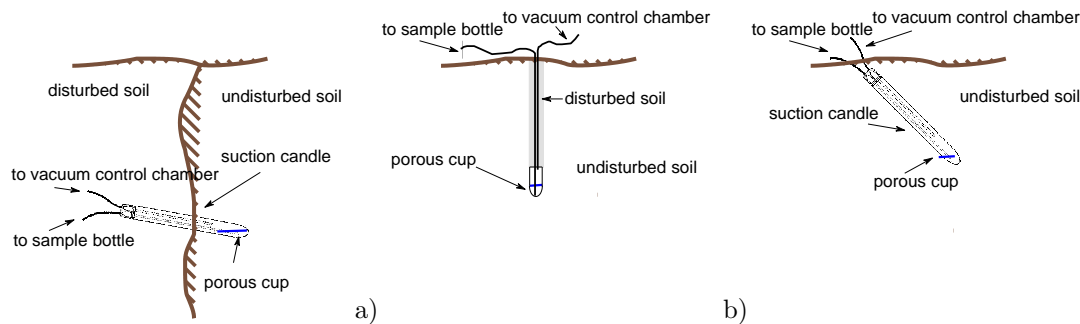
Figure 2.2: a) Horizontal, b) vertical non-shaft and c) vertical in 45° angle installation of a suction cup into the soil.

specific amount of water required for analysis, the actual soil water content, and the time of applied suction, whereby the suction is closely connected to the soil water sampling method (*DVWK*, 1990). In general, the potential gradient should be as small as possible to minimize the impact on the natural percolation front. For the extraction of soil water with porous cups two modes of operation are possible. For a continuous operation mode a potential gradient is applied, which depends on the actual pressure head in the undisturbed soil measured by tensiometers, and a predefined pressure offset. The advantages of the tensiometer-controlled continuous operation mode are the continuous collection of water samples, an accurate assessment of the drainage water front (*Magid et al.*, 1992; *McGuire and Lowery*, 1994) as well as the small withdrawal of water from the soil per time and, therefore, a minimization of changes of the natural water flow pattern (*Grossmann and Udluft*, 1991). The continuous water flow also reduces sorption processes in the cup material and only low potential gradients are necessary to collect adequate amounts of water for analysis. The disadvantages of this operation mode are the initialisation of preferential flow path to the cup, a high manpower for maintaining the system, and the possibility of probe alteration between sampling (*DVWK*, 1990). However, the main problem is that the suction cup influence cannot be defined over a specific area (*Brandi-Dohrn et al.*, 1996).

   For the discontinuous operation mode water collection will take part at short-time intervals. This operation mode is used to indicate the presence of solutes at specific time intervals (*Linden*, 1977b). The advantages are just temporary disturbances of the natural flow field, and reduced maintainance time. The disadvantage is a nonpermanent flow through the cup material which can result in high sorption. Therefore, it is useful to discharge the first water sampled. The biggest disadvantage is that short-time intervals

during periods of rapidly changing concentrations of solutes caused by heavy rainfall and preferential flow are not recordable (*DVWK*, 1990).

The interpretation of sampled concentrations with suction cups is still a matter of debate in literature. *Kreft and Zuber* (1978) defined the flux concentration, C^f $[ML^{-3}]$, as the mass of solute per unit volume of fluid passing through a given cross section at a given time intervall, and the resident concentration, C^r, as the mass of solute per unit volume of fluid contained in an elementary volume of the system at a given instant. The resident concentration, C^r $[ML^{-3}]$, can be calcualted by Equation 2.1:

$$C^r(z,t) = \frac{M}{V} \tag{2.1}$$

where M is the solute mass [M], z ist the sampling depth [L], t is the time of sampling [T], and V the elementary soil volume (L^3). The flux concentration, C^f, is defined as (*Jury and Roth*, 1990):

$$C^f(z,t) = \frac{J_s}{J_w} \tag{2.2}$$

with J_s the flux of solute [M L^{-2}T^{-1}], and J_w the flux of water [LT^{-1}]. Water collection of resident or flux concentration is directly linked to the operation mode. The continuous operation mode rather collects flux than resident concentrations, and the discontinuous operation mode rather samples resident than flux concentrations.

2.5 Problems of soil water extraction

Soil physical and chemical properties show a variability in space and time typical for each region, location, plot, and also depth. This must be taken into account when planning and conducting suction cup experiments. Such variabilities exist both in space and time and depend on inhomogenities in texture and structure (*Grossmann and Udluft*, 1991; *Schmidt-Eisenlohr*, 2001). Differences in mineral and organic composition caused by flora and fauna activity also lead to soil heterogeneity. Each single factor as well as a combination result in a spatial variability of the hydraulic properties of the media and affect the soil water extraction with suction cups. Other reasons for variability of the amount and the chemical composition of the extracted soil solution can be found in changes in the soil water content, the intensity of biological activity and the measurement depth. Methodological reasons for the variability can be the permeability of the suction cup or mistakes during sampling or analysis (*Grossmann*, 1988; *Grossmann and Udluft*, 1991).

The chemical and mass variabilities of soil water extracted by porous cups (an overview, without having the intention to be complete, is given in Table 2.1), as well as the heterogeneity of the physical soil properties (e.g. *Hajrasuliha et al.* (1980), *Dahiya et al.* (1984), *Dahiya et al.* (1985), *Roth* (1995), and *Schmidt-Eisenlohr* (2001)) were widely discussed in literature during the past decades.

Table 2.1: Chronological literature review for the variability of soil water extracted by porous cups.

Author and year of publication		
Wagner (1962)	*Starr* (1985)	*Lord and Shepherd* (1993)
Reeve and Doering (1965)	*Smith and Carsel* (1986)	*Magid and Christensen* (1993)
Shimshi (1966)	*Rasmussen et al.* (1986)	*Perrin-Garnier et al.* (1993)
Wolff (1967)	*Joslin et al.* (1987)	*Simmons and Baker* (1993)
Grover and Lamborn (1970)	*Montgomery et al.* (1987)	*Vetterlein et al.* (1993)
Parizek and Lane (1970)	*Barcelona et al.* (1988)	*Webster et al.* (1993)
Bell (1974)	*Creasey and Dreiss* (1988)	*Andersen* (1994)
Dazzo and Rothwell (1974)	*Debyle et al.* (1988)	*Djurhuus and Jacobsen* (1995)
Hansen and Harris (1975)	*Raulund-Rasmussen* (1989)	*Flemming and Butters* (1995)
Severson and Grigal (1976)	*Bredemeier et al.* (1990)	*Wenzel and Wieshammer* (1995)
Alberts et al. (1977)	*Morrison and Lowery* (1990)	*Brandi-Dohrn et al.* (1996)
Levin and Jackson (1977)	*Hughes and Reynolds* (1990)	*Perrin-Garnier et al.* (1996)
Linden (1977a)	*Swistock et al.* (1990)	*Marques et al.* (1996)
Barbarick et al. (1979)	*Swistock et al.* (1990)	*Wenzel et al.* (1997)
Hetch et al. (1979)	*Hendershot and Courchesne* (1991)	*Spangenberg et al.* (1997)
Silkworth and Grigal (1981)	*Maitre et al.* (1991)	*Tischner et al.* (1998)
Morrison (1982)	*Beier and Hansen* (1992)	*Potschin* (1999)
Nagpal (1982)	*Beier et al.* (1992)	*Patterson et al.* (2000)
Bottcher et al. (1984)	*Guggenberger and Zech* (1992)	*Wessel-Bothe et al.* (2000)
Schimmack et al. (1984)	*Magid et al.* (1992)	*Siemens and Kaupenjohann* (2003)
Grossmann et al. (1985)	*McGuire et al.* (1992)	
Neary and Tomassini (1985)	*Koch and Grupe* (1993)	

2.6   Representativity of the collected soil water

Adsorption of compounds by the porous cup, sealing material and tubes, affecting the variability in quality and quantity of collected soil water were reported by several authors (see Table 2.1). *Hansen and Harris* (1975) assessed the representativity of soil solution sampled by porous cups, whereby substantial bias and variability in the chemical composition were found. Some of the sources of sample bias were sorption, leaching, diffusion, and filtering of substances by the cup material. They appraised the sorption tendencies of the cup material as problematic only if the sorption capacity differs from the surrounding soil, due to the fact that the suction cup substitutes the natural soil with its own sorption capacity. Even though sorption is significant, soil water extraction shows reliable results after a sufficient conditioning period of the suction cup within the soil (*Hansen and Harris*, 1975). Some changes of the sampled soil water composition were ascribed to filtering effects. Various studies attempted to analyze and describe sorption tendencies for different cup materials (see Chapter 2.5 and Table 2.1), whereby some materials indicate lower changes for individual substances and assessments. In the following, some examples show the broad spectrum of research with respect to filtering, sorption, material choices, and changes in the amount of extracted water.

Bell (1974) investigated the possibility of collecting microorganisms with the suction cup method and figured out that such a sampling system cannot be usefully applied to studies requiring enumeration of the soil microflora or other organisms. As expected the soil moisture sampler acted as a bacterial filter, reducing the number of organisms in suspension passing through the porous ceramic. A similar case is described by *Dazzo and Rothwell* (1974) for bacteriological sampling with ceramic cups. *Grossmann et al.* (1985) examined the applicability of nylon- and polyvinylidene fluoride membrane filters for the construction of suction cups. Results of the sorption tests indicate lower sorption of heavy metals compared to commercial aluminum oxide sinter cups. *Wessel-Bothe et al.* (2000) studied the sorption of pesticides and dissolved organic carbon (DOC) on glass and ceramic suction cups, whereby the borosilicate-glass suction cups tend to lower sorption. *Zimmermann et al.* (1978) pointed out that the sorption tendencies depend on the cup material, whereby ceramic cups indicate higher changes in filtrates for nutrients compared to Teflon cups. Experiments conducted by *Silkworth and Grigal* (1981) showed that soil solution collected with small samplers were significant higher in ion concentration than those collected by larger ones. However, it is not entirely clear why contamination and sorption are more pronounced for the small samplers. Apart from the filter material the manufacturing process determines the quality of the extracted soil water. *Hansen and Harris* (1975) correlated the variability of ion concentration within the percolate with the intake rate, which is determined by the pore-size distribution and the sampler size. A pure pore-size dependent sorption by the cup material is described by *Grossmann* (1988). Colloides (oxides) and macromolecules (humic substances or clay minerals) can be adsorbed by the material, and reactive ions may sorb to these complexes resulting in a depletion in the sampled soil water (*Grossmann and Udluft*, 1991; *Tischner et al.*, 1998). Besides the material properties, the physico-chemical characteristics of the soil solution have an essential influence on the sampled percolate. A dependency of the pH-value on the sorption of the suction cup material and the contamination of the percolate is shown by *Neary and Tomassini* (1985), *Creasey and Dreiss* (1988), *Grossmann*

(1988), and *Grossmann et al.* (1990). The contaminants leached from different suction cup materials changed with pH-values in composition and as well as in abundance during the cleaning procedure. Overall highest release was found at lower pH-values (*Creasey and Dreiss*, 1988). The length of extraction time is also significant. It is reasonable to use suction cups with uniform intake rate, same age, and same operation time. Solute samples collected with differently aged suction cups cause significant differences in the sorption and percolate volume. If samplers are left in the soil for a longer time period (month or years), the hydraulic conductivity may change due to clogging with mineral particles, chemical compounds or micro-organisms. To obtain similar results all suction cups should have the same age or should be acid-leached and flushed with distilled water before installation (*Debyle et al.*, 1988). *Morrison and Lowery* (1990) suggested that the cumulative sample volume is significantly affected by the type and the height of applied suction, and as expected, the total percolate volume collected with a constant head was always larger than with transient suction. The percolate volume is also determined by cup conductance, cup surface area and cup length. Next to the absolute age of the cups *Lord and Shepherd* (1993) detected a dependency between the time after installation (month or years) and the sampled percolate. They ascribed this effect to the disturbance of the soil with installation (preferential flow in the vicinity of the sampler shaft). *Van der Ploeg and Beese* (1977) stated that the extraction rate of a suction cup can be several times higher than the percolation rate through undisturbed soils, depending on the suction applied. They explained this findings by the loss of the hydraulic head in the zone of contact between suction and the surrounding soil which was not taken into account in the model calculation. *Severson and Grigal* (1976) and *Moutonnet and Fardeau* (1997) pointed out that changes in chemical composition are related to two factors. First, the percolate sampled in very short time intervals represents solutions draining through soil 'macropores'. This percolate approximates the solution moving through the soil system in the field. Second, percolate extracted over longer periods may present soil water held at lower pressure heads. *Grossmann et al.* (1985) argued that soil solution out of this finer pores does not take part at the drainage process and, therefore, analysis will mislead in understanding soil water drainage. It is recommended to apply minimal suctions in the cups to obtain representative soil water from larger pores and macropores (*Severson and Grigal*, 1976). A fundamental aspect to account for the chemical composition and the amount of the percolate is the spatial and temporary heterogeneity of the investigated soils. Information on the origin of the extracted soil water and its chemical composition is widely discussed in literature. *England* (1974) assumed that 'loosly bound' seepage water from larger pores extracted at low applied suctions may have a chemical 'quality' that is different from that extracted from micropores. However, *Grossmann and Udluft* (1991) pointed out that the potential gradient generated by the suction cup acts on all pores, and therefore, water movement takes place in all pores with flow velocities depending on the pore-diameter. They stated that the pores of all sizes are closely interlinked (except macropores in structured soils) and, therefore, existing concentration gradient between small and large pores is reduced by dispersion and diffusion. Due to the soil heterogeneity some kind of 'chanelling effect' of the seepage water movement in areas with larger pore structures can occur. If there is a concentration gradient in the soil, caused by a downward- moving seepage front, the potential gradient can have an influence on the composition of the sample, due to the proportionately too high influx from

coarser pores. At the same time concentration gradients between different pores are not compensated by diffusion or dispersion processes due to the rapid drainage of the water front with macropore or preferential flow (*Grossmann and Udluft*, 1991). Some authors found evidence of solute bypass of the cups in a well-structured soils (*Shaffer et al.*, 1979; *Barbee and Brown*, 1986; *Caron et al.*, 1999). *Jury and Flühler* (1992) suggested that samplers (particularly shallow ones) may be unreliable in soils with preferential flow, whereby recording of bypass flow might be a fundamental weakness of the sampler or a result of having too few samplers for adequate sampling the flow regime. Therefore, it is an open question how many samplers would be required and whether it is practical to install and monitor the required number of suction cups (*Flemming and Butters*, 1995). In structured soils, porous cup samplers may be completely circumvented by the channeling of water and chemicals due to poor hydraulic contact between macropores and cup (*Shaffer et al.*, 1979; *Barbee and Brown*, 1986; *Caron et al.*, 1999). *Starr* (1985) annoted that the soil water collected by suction cups may be extracted from deeper in the soil profile with low rainfall and high potential evapotranspiration during the summer month, resulting in little or no percolation. These samples tend to show less variation than infiltration water due to longer soil contact time. *Patterson et al.* (2000) pointed out that a combination of soil coring and suction cup monitoring has the potential to improve estimates of both migration and mass loss rates. They also showed that differences in migration rates occur due to the installation method, whereby vertically installed suction cups substantially overestimate migration rates due to possible formation of preferred pathways (channeling) and disturbance and/or removal of the higher organic top-layer during installation. In addition, *Grossmann* (1988) accentuated that results obtained from laboratory experiments cannot be directly extrapolated to field conditions. Various boundary conditions like pH-value, humic substance content, concentration of different elements, applied pressure, temperature, and extraction rate will vary in field situations. A selection of the suitable suction cup material for the different fields of application is a necessity to minimize sorption and to quantify the desired compounds.

Narasimhan and Dreiss (1986) used a numerical technique based on the integral finite different method (IFDM) to predict the suction cup influence and the amount of water extracted by the cup for the falling head method by combining the IFDM with the Boyle's law to estimate the changing effective suction in the sampler. The computed water extracted by the suction cup is a function of time with a decrease of the flow rate with time due to the decrease of applied suction. *Talsma et al.* (1979) pointed out that experimental results led to lower extraction rates in comparison to model calculations due to specific natural conditions in the soils, hydraulic properties of the suction cup (e.g. plugging) and disturbances (compaction of the natural soil in direct vicinity of the cup and lowered hydraulic conductivity) during suction cup installation. *Tseng et al.* (1995) showed in numerical simulations that suction cup devices decreased the peak concentration and increased the mean and variance of travel times to varying degrees, but the activating process was not identified.

Chapter 3

Theory of water flow and solute transport in porous media

3.1 Water flow

Water in natural soils is rarely in a static state. Water flow is driven by differences in potential states at different locations, whereby the total potential, ψ_w [L], consists of the sum of partial potentials (e.g. Equation 3.1).

$$\psi_w = \psi_g + \psi_s + \psi_m \tag{3.1}$$

with the gravitational potential, ψ_g [L], the osmotic potential, ψ_s [L], and the matric potential, ψ_m [L], (*Marshall and Holmes*, 1988; *Roth*, 1996). Percolation of soil water in the unsaturated zone is dominated by the matric potential, ψ_m, and is generally described by *Buckingham-Darcy's* law:

$$J_w = -K(\theta) \frac{d\,\psi_w}{d\,z} \tag{3.2}$$

The relationship between ψ_m and θ is a characteristical function for each single soil known as soil water retention function or the soil water characteristic. The shape of this function depends on structure and texture of the soil. Notice that $\psi_m < 0$ for the unsaturated zone. Under transient condition the potential gradient varies with time, resulting in a water flux, J_w [LT^{-1}]. *Buckingham* (1907) postulated that *Darcy's* law (*Darcy*, 1856) is also valid under unsaturated conditions. $K(\theta)$ can also be expressed as the unsaturated hydraulic conductivity in dependency of the pressure head $K(\psi)$ and has the dimension of a velocity [LT^{-1}]. K decreases with a decrease of θ. The gradient $\frac{d\,\psi_w}{d\,z}$ describes the change of the water potential, ψ_w, with depth, z. For a two-dimensional isothermal heterogeneous and variable saturated rigid porous medium and under the assumption that the air phase is continuous, the flow equation is given by the *Richards'* equation (*Richards*, 1931) (Equation 3.3):

$$\frac{\partial \theta}{\partial t} = \frac{\partial}{\partial x}\left[K(\psi)\frac{\partial \psi}{\partial x}\right] + \frac{\partial}{\partial z}\left[K(\psi)\left(\frac{\partial \psi}{\partial z}\right) + 1\right] \tag{3.3}$$

where θ is the volumetric water content [L^{3}L^{-3}], ψ is the matric potential in head units [L], x and z are spatial coordinates [L] in horizontal and vertical direction, respectively, and $K(\psi)$ is the unsaturated hydraulic conductivity [LT^{-1}].

3.2   Solute transport

To describe solute transport in porous media various conceptual models are available. For example the stochastic stream tube model in which the soil is conceptualized as a set of stream tubes in which transport is described as a one-dimensional process which is independent of the transport in other stream tubes , which implies no lateral mixing (*Vanderborght*, 1997). The stochastic continuum model in which the flow and transport equation, and as a direct consequence also the variables, are described by stochastic functions in space or random space functions, which represent the spatial heterogeneity of these parameters and variables (*Vanderborght*, 1997). The mobile- immobile model (*van Genuchten and Wierenga*, 1976) which consists of the assumtion of a water-conducting (mobile) phase and a stagnant (immobile) phase, and finally the physically based convection-dispersion-equation (CDE). In this study the CDE was chosen for the calculation of the solute transport due to the fact that the used HYDRUS-2D (*Simunek et al.*, 1999) code also solves the CDE.

A simple form of the Convection-Dispersion-Equation (CDE) for a one-dimensional (1D) transport without interaction of the solute with the soil matrix and no sinks or sources in a rigid homogeneous porous medium is given by:

$$\frac{\partial(C\theta)}{\partial t} = -\frac{\partial(v\theta C)}{\partial z} + \frac{\partial}{\partial z}\left(D\theta\frac{\partial C}{\partial z}\right) \tag{3.4}$$

where D $[\mathrm{L^2 T^{-1}}]$ is the dispersion coefficient, v $[\mathrm{L\ T^{-1}}]$ is the average pore water velocity, and C is the solute concentration $[\mathrm{M\ L^{-3}}]$.

The first term on the right hand side in the CDE describes the convective transport by the soil water. In a one-dimensional view the solute flux without spreading and mixing, J_c, is proportional to the concentration, C (*Hillel*, 1998):

$$J_c = J_w C \tag{3.5}$$

Since J_w $[\mathrm{L\ T^{-1}}]$ (*Darcy velocity*) is usually expressed as volume of liquid flowing through an area per time, and C a mass of solute per volume of solution, J_c is given in terms of mass of solute passing through a cross-sectional area of a soil body per unit of time. To estimate the travel distance of a solute the mean pore water velocity $v = \frac{J_w}{\theta}$ $[\mathrm{ML^{-3}}]$ has to be considered (*Hillel*, 1998). After substitution of J_w with $v\theta$ in Equation 3.5 J_c leads to:

$$J_c = v\,\theta\,C \tag{3.6}$$

To consider dispersion in the transport mechanism a second term is introduced into the CDE. The hydrodynamic dispersion, J_{hD}, is a result of two different principles at the pore-scale (*Beese*, 1982; *Roth*, 1996).

1. Dispersion: The dispersion describes the variation in flow velocity within a capillary and between different pore radii by the law of *Poisseuille*.

2. Tortuosity: The soil's pore passages are tortuous so that the actual path length of diffusion is significant larger than the apparent straight-line distance

The hydrodynamic dispersion, J_{hd} [$ML^{-2}T^{-1}$], can be described by *Fick's* first law:

$$J_{hD} = -D_{hD}\theta \frac{\partial C}{\partial z} \tag{3.7}$$

where D_{hD} [L^2T^{-1}] is the hydrodynamic dispersion coefficient. The longitudinal dispersion coefficient is normally larger than the transversal dispersion coefficient (*Forrer et al.*, 1999) and the field-scale dispersion is larger than the local-scale dispersion due to heterogeneities in the flow field.

Molecular diffusion is a consequence of the random thermal motion (*Brownian motion*) and repeated collisions and deflections of molecules in the fluid or gas phase (*Hillel*, 1998). If solutes are not distributed uniformly throughout a soil solution, concentration gradients exist and solutes tend to diffuse from zones with higher concentrations to zones with lower concentrations. For the one-dimensional view in bulk water at rest, the rate of molecular diffusion, J_{mD} [$ML^{-2}T^{-1}$], is also proportional to the gradient of the concentration C:

$$J_{mD} = -D_{mD}\theta \frac{\partial C}{\partial z} \tag{3.8}$$

where D_{mD} [$L^2\ T^{-1}$] is the diffusion coefficient for a particular solute diffusing in bulk water, and $\frac{\partial C}{\partial z}$ is the effective concentration gradient (*Hillel*, 1998). In some cases the diffusion in the liquid phase can be negligible small in comparison to the water movement.

Because of the similarity in effect (not in mechanism) between diffusion and dispersion and the problem of experimental discrimination of both terms, a combination into one single term, called effective dispersion coefficient, D_{eff}, is possible (Equation 3.9).

$$D_{eff} = D_{mD} + D_{hD} \qquad \Longleftrightarrow \qquad D = D_{mD} + \lambda v \tag{3.9}$$

D_{eff} is for a 1-dimesional case the longitudinal dispersion coefficient. The dispersivity, λ [L], is the normalized dispersion coefficient, D_{eff}, with the mean pore water velocity, v.

Certain solutes react within the soil (immobilisation), other solutes may disappear from soil by plant uptake or microbial degradation. To account for such sinks and sources a composite souce-sink term, S, is included in Equation 3.4:

$$\frac{\partial(C\theta)}{\partial t} = -\frac{\partial J_s}{\partial z} + S \tag{3.10}$$

where J_s is the solute mass flux density [$ML^{-2}T^{-1}$]. Solutes may also be sorbed to the soil matrix. Basically two assumptions with respect to the sorption process are considered in literature: equilibrium and non-equilibrium sorption. The left-hand side of Equation 3.10 can be substituted by $\frac{\partial(C\theta+\sigma_s)}{\partial t}$, with $\sigma_s = \rho_b C_s$ and ρ_b as the bulk density [ML^{-3}]. The time derivative of σ_s (namely, $\frac{\partial \sigma_s}{\partial t}$) expresses the rate of increase of storage outside the solution phase for the solute under consideration. In general, three main sorption isotherms are in use. Equilibrium sorption is usually described by three sorption isothems:

1. Henry isotherm with a constant ratio of C_S (C_S [MM^{-1}] = concentration of substance sorbed to the soil) and C_E (C_E [ML^{-3}] = equilibrium solution substance concentration), with $C_S = K_D C_E$, and K_D [L^3M^{-1}] as the linear partition coefficient.

2. Freundlich isotherm with an exponential ratio of C_S and C_E, with $C_S = K_F C_E^{\frac{1}{n}}$. K_F [L^{3}M^{-1}] is the Freundlich-constant, and $\frac{1}{n}$ [-] is the Freundlich-exponent with the index n of the sorption intensity (normally <1.0 for most pesticides). The Freundlich-exponent characterizes the slope of the function in the linear form $log(C_S) = log(K_F) + \frac{1}{n} log(C_E)$.

3. Langmuir isotherm which is characterized by a nonlinearity and the ambition to reach a threshold value. In contrast to the Freundlich isotherm, the Langmuir isotherm exhibits a maximum of sorption. The Langmuir isotherm can be expressed by $C_S = C_{S_{max}} \frac{C_E}{C_{0.5} + C_E}$, with $C_{S_{max}}$ as the maximum of sorption [MM^{-1}], and $C_{0.5}$ as the half-concentration-value [ML^{-3}] (point where C_S is the half of $C_{S_{max}}$).

What kind of isotherm fits best depends on the sorption of each substance.

For many cases equilibrium conditions are not obtained requiring kinetic approaches (e.g. *Jaekel et al.* (1996), *Fortin et al.* (1997), *Streck* (1998), *Streck and Richter* (1999), *Vereecken et al.* (1999), *Altfelder et al.* (2000) and *Altfelder et al.* (2001)). So far, no assumptions were made regarding degradation or decay. The degradation is the possibility of chemicals to decay in water as well as in the adsorbed phase. For many transport problems it is not possible to determine meaningful individual degradation parameters. Notice that different variables influence decay, e.g. temperature, water content, or density of microbiological population. Therefore, the number of degradation pathways and associated coeffcents should be reduced. For the characterization of the degradation the DT50 (50 reflects the time it takes for a chemical to decay to half its amount) and DT90 values. Finally, a comprehensive equation of transient-state solute dynamics including convective-dispersive-diffusive movement as well as sources, sinks, and storage changes is given by:

$$\frac{\partial(\theta c + \sigma_s)}{\partial t} = \frac{\partial}{\partial z}\left(\theta D \frac{\partial C}{\partial z}\right) - \frac{\partial(J_w C)}{\partial z} + S - \mu C \theta \qquad (3.11)$$

with μ [T^{-1}] as the rate coefficient for the decay. If retardation, R, is considered Equation 3.11 can be postulated as:

$$\frac{\partial \theta C R}{\partial t} = \frac{\partial}{\partial z}\left(\theta D \frac{\partial C}{\partial z}\right) - \frac{\partial(J_w C)}{\partial z} + S - \mu C \theta \qquad (3.12)$$

where R is the retardation factor $R = 1 + \frac{\rho_b}{\theta} \frac{\partial C_s}{\partial C_E}$ or for linear sorption $R = 1 + \frac{\rho_b}{\theta} K_D$. θ, C, S and J_w are functions of depth and time, and D is a function of θ and the average pore-water velocity v. For complex systems Equation 3.12 cannot be solved analytically. In contrast to the method of moments (Chapter 4.8) the CDE is a description of breakthrough curves or concentration profiles with an assumption of the underlying physically based processes (complete lateral mixing, convection, and dispersion).

Chapter 4

Methods and Materials

4.1 Test site Merzenhausen

The test site Merzenhausen is located 10 km northwest of the *Forschungszentrum Jülich* (Germany) between *'Haus Brühl'* and the country road L14. DGK 5 (1 : 5.000) maps *Engelsdorf* and *Barmen*. In geomorphological terms the area is located on a weakly inclined and structured high terrace of the river Rur bassin, the upper 'Rurscholle' respectively. The elevation is 93.0 m above sea level and groundwater depth is around 78.0 m above sea level. The seasonal fluctuation of the water table of up to 5 m depends on the climatic water balance of the area. A full description of the test site is given by *Pütz* (1993), or *Kaiser* (2002) and *Dressel* (2003). The markedly profound loess from fluviatil origin is dated to the Pleistocen/Holocen, whereas the original eolian sediment
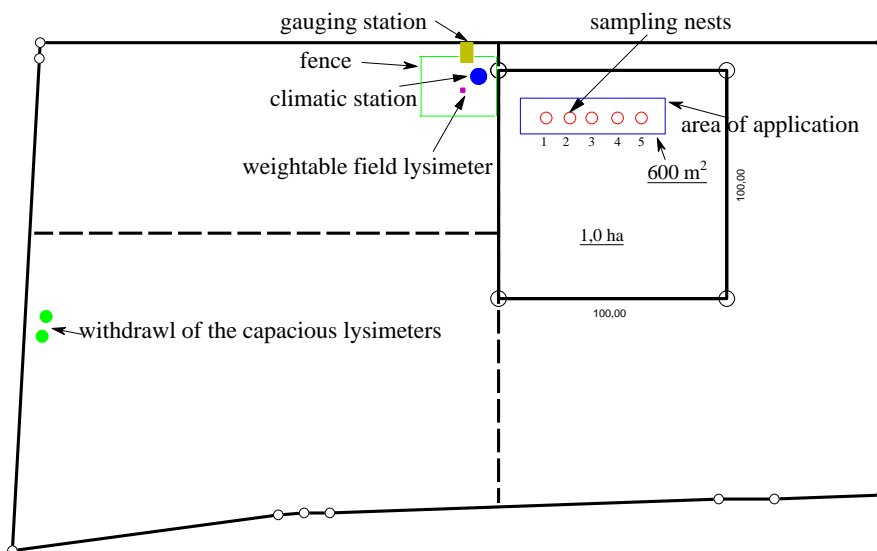
Figure 4.1: Test site Merzenhausen with climatic station, sampling pits, weighable field lysimeter, treated area, and withdrawal of the lysimeters. All unit length in meters.

was transported through the water. According to the soil map sandy pepply sediments of the main terraces of the river Rhein and Maas occur in deeper layers and lower elevations (vale of the Merzbach) (*Geologisches-Landesamt-Nordrhein-Westfalen*, 1972) but a drilling at the test site up to the depht of 5 m showed just loess. In addition colluvial processes are assumed which were dependent on geomorphology and agricultural practice. As a result of erosion and the variability of the grain size distribution soil subtypes like *Parabraunerde*, *Braunerde-Parabraunerde*, *Parabraunerde-Braunerde* and typical *Braunerde* occur aside the colluvials.

The soil at the sampling location in described as an orthic luvisol (FAO) (see Table 4.1).

The whole profile is composed of fluvial deposed loess, whereas up to a depth of 165 cm small gravel can be found. The profile is free of carbonate up to a depth of 225 cm. After carbonate depletion and browning a downward movement of clay took place and the recent lessivation is quite distinctive. The Al-horizon is, as far as it is not degradated through agricultural practice (plowing) or erosion, brighter in colour and can mostly only be determined through grain-size distribution. In the Bt-horizon coarse prismatic structures and redbrown clay cutanes on the surfaces of the aggregates indicate the clay enrichment. The clay leaching is possibly of a recent date and is connected to shrinking cracks up to the Btv-horizon.

The Btv-horizon points out fine but clear layers with a maximum in a depth of 110 - 130 cm. Underneath 120 cm a clay enriched layer interrupts free drainage and the profile shows a high bulk density. Earthworm and root channels were detected to a depth of up to 200 cm, but they may occur even in deeper sections. The depth of 225 cm of decarbonisation is an indicator of an undisturbed soil development because calculations estimated a depth of about 2 m. Carbonate concretions in form of small lenses above the C-horizon indicate a secundary carbonate enrichment of the Bcv-horizon through ascending water.

4.1.1   Soil sampling

After removal of the lysimeters a characterization of the soil profile was carried out on the lysimeter cavity. Soil sampling in the cavity was performed in a fresh profile wall on the 13/11/2001. The sampling was based on predefined horizons in the 3 m deep cavity. Disturbed samples for physicochemical analysis and undisturbed soil samples (using stainless-steel rings with 100 cm^3 volume) for determination of hydraulic properties were taken with six replicates per horizon.

4.1.2   Soil physical parameters

The texture analysis distribution was carried out by sieving and sedimentation (Köhn-method) after treatment with sodiumphyrophosphate. No destruction of the organic substance was carried out due to its low absolute content. The particle density was appraised by helium-pycnometry and the dry-matter after drying at 105°C, whereby the loss of water can be used to determine the soil's field capacity. The maximum water content of the probes was determined through total saturation and following drying at 105°C (memorandum LUFA Speyer).

Table 4.1: Physico-chemical soil parameters for the test site Merzenhausen. Soil types after *AGBoden* **(1994). All units based on mass of dry matter except field capacity, (FC), based on saturated soil.**

Parameter	*Horizon*						
	Ap	*Al*	*Bt*	*Btv*	*Bv*	*Bcv*	*C*
	0 - 35	35 - 47	47 - 97	97 - 150	150 - 210	210 - 225	225 - 280
	[cm]	[cm]	[cm]	[cm]	[cm]	[cm]	[cm]
clay (<2 μm) [%]	13.4	18.0	22.7	18.0	16.0	12.7	13.1
silt (2 - 63 μm) [%]	81.9	78.9	74.9	79.4	81.1	82.8	81.9
sand (>63 μm) [%]	4.7	3.1	2.4	2.6	2.9	4.5	5.0
soil	Ut3	Ut4	Ut4	Ut4	Ut3	Ut3	Ut3
bulk density $[g\ cm^{-3}]$	1.48	1.53	1.54	1.56	1.52	1.45	1.59
particle density $[g\ cm^{-3}]$	2.62	2.64	2.64	2.64	2.65	2.67	2.67
FC [%]	39.2	42.2	39.5	39.2	38.0	37.1	35.0
pH-value $(CaCl_2)$	7.1	7.1	7.1	7.0	6.8	7.6	7.6
humus [%]	1.8	0.6	0.4	0.2	0.1	0.2	0.3
CEC $[meq\ 100\ g^{-1}]$	10.5	10.5	11.9	16.3	12.5	10.0	15.0
S-value $[meq\ 100\ g^{-1}]$	13.56	11.58	14.29	14.41	11.60	14.10	17.39
carbonate $[\%\ CaCO_3]$	0.5	0.4	0.4	0.3	0.4	11.9	15.6

With a content of about 80 % silt is the main textural fraction, whereby the coarse silt dominates with about 50 %. The clay content is about 20 % and the total sand content is lower than ≤ 5 % within all horizons. The Ap-horizon is characterized as a clay silt (Ut3), the Al, Bt and Btv-horizon as a high clayic silt (Ut4), underlayed by a mediocre clayic silt (Ut3)(*AGBoden*, 1994) in the Bv, Bcv and C-horizon (see Figure 4.2). This grain-size distribution is typically for the genesis of the eolian sediment loess.

The homogeneity in all horizons is confirmed by the nearly constant soil bulk density of 1.48 for the top layer to 1.59 for the C-horizon (see Figure 4.3).
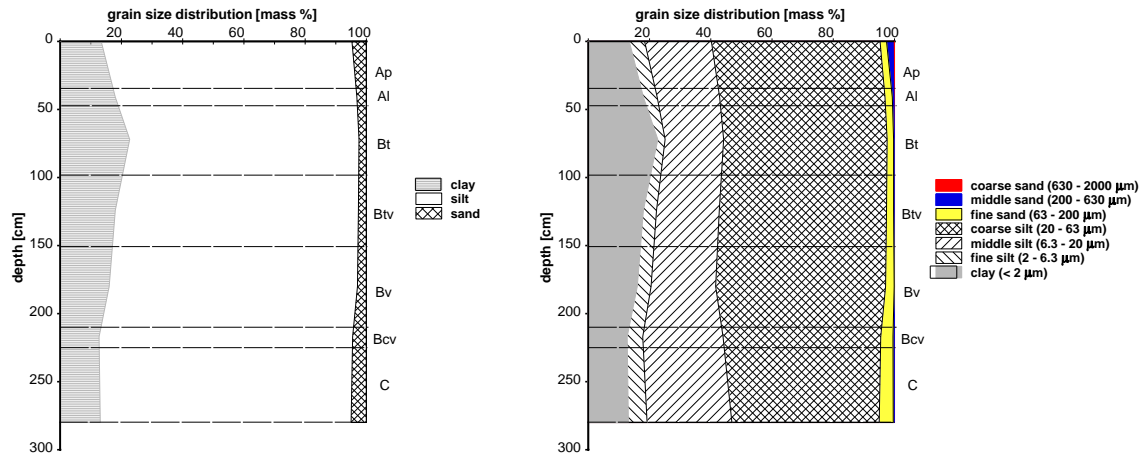
Figure 4.2: Grain size distribution for the test site Merzenhausen. All data are expressed in mass percentage.

The soil hydraulic properties were measured with the porous pressure plate extractor method. The pressure steps were set to pF 0, 1, 1.3, 1.6, 1.8, 2, 2.5, 3.0, 3.5, and 4.2, respectively. For each soil horizon six replications per horizon were conducted and a mean was calculated. The program RETC (*van Genuchten et al.*, 1991, version 6.0) was used to determine the parameters in the *Mualem and van Genuchten* function (Equation 4.10). The saturated hydraulic conductivity and the saturated water content were taken from *Schmidt-Eisenlohr* (2001). For the Bt, Btv, Bv, Bcv, and C-horizons the measurement point of 1 cm was neglected due to a dual porosity pore-size distribution and resulting problems in parameter estimation. The resulting parameters n, m, α, and θ_s (θ_r was set to 0) (Table 4.2) were calculated using Equation 4.11 to receive the hydraulic conductivity function depict in Figure 4.4. The soil chemical parameters are shown in Annex A.1.1.

4.2 Measurement equipment

4.2.1 Sampling pits

The sampling pits at the test site Merzenhausen (Chapter 4.1) were constructed as subsurface soil water sampling cavities. They consist of steel tubes with a diameter of 160 cm, a length of 250 cm, and a wall thickness of 10 mm which were vertically pressed into the soil and later digged out in the inside. A detailed description of the sampling
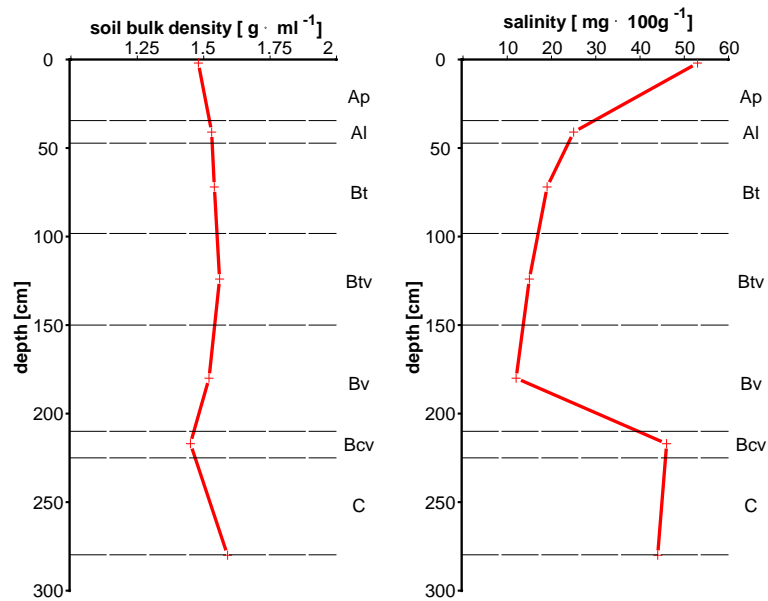
Figure 4.3: Bulk density in g ml^{-1} and salinity in mg 100 g^{-1} dry matter for the test site Merzenhausen.
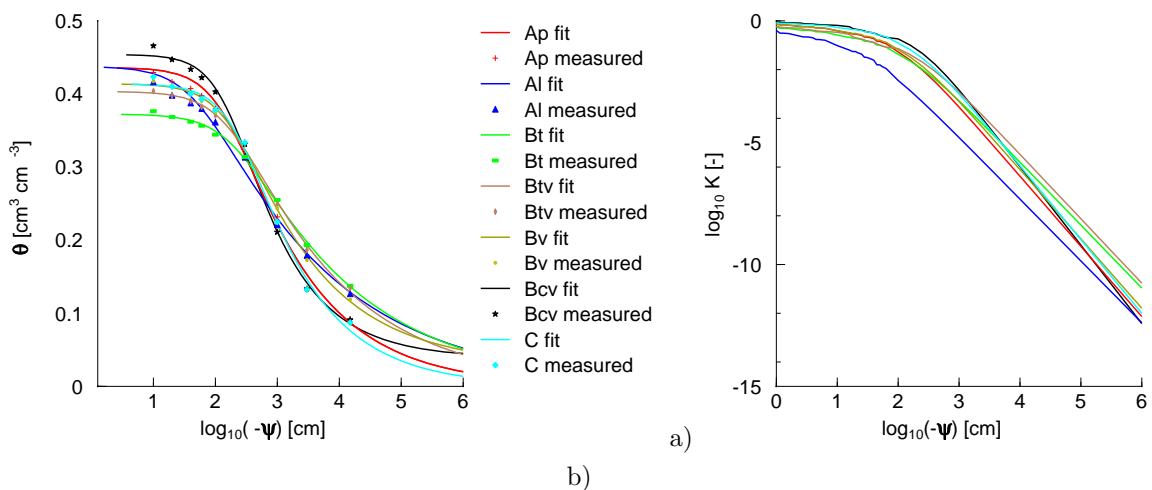
Figure 4.4: Soil hydraulic properties of the test site Merzenhausen. a) soil water retention curve fitted with RETC (*van Genuchten et al.*, 1991). b) relative hydraulic conductivity function calculated with Equation 4.11.

Table 4.2: The soil hydraulic properties for the test site Merzenhausen. Parameters θ_s, n, and α, were based on *Mualem and van Genuchten* fitted with RETC (*van Genuchten et al.*, 1991). K_s was taken from *Schmidt-Eisenlohr* (2001). θ_r was set to 0 for all fits.

	Horizon						
	Ap	**Al**	**Bt**	**Btv**	**Bv**	**Bcv**	**C**
	0 - 35	35 - 47	47 - 97	97 - 150	150 - 210	210 - 225	225 - 280
	[cm]	[cm]	[cm]	[cm]	[cm]	[cm]	[cm]
θ_s [$cm^3\ cm^{-3}$]	0.436	0.438	0.372	0.403	0.414	0.454	0.414
n [-]	1.353	1.215	1.234	1.259	1.338	1.490	1.411
α [cm^{-1}]	0.0064	0.0195	0.0048	0.0056	0.0053	0.0056	0.0041
K_s [$cm\ h^{-1}$]	1.8629	0.1615	0.0595	0.05625	0.05625	0.05625	0.05625

pits is given by *Dressel* (2003). 12 ceramic plates (six at a depth of 40 cm and six at a depth of 120 cm) were installed in each sampling pit. Six tensiometers (three at 40 cm and three at 120 cm depth) completed the installation. Compared to the survey of *Dressel* (2003), the system was enhanced by four suction cups at a depth of 40 cm and six at a depth of 120 cm (see Figure 4.5).
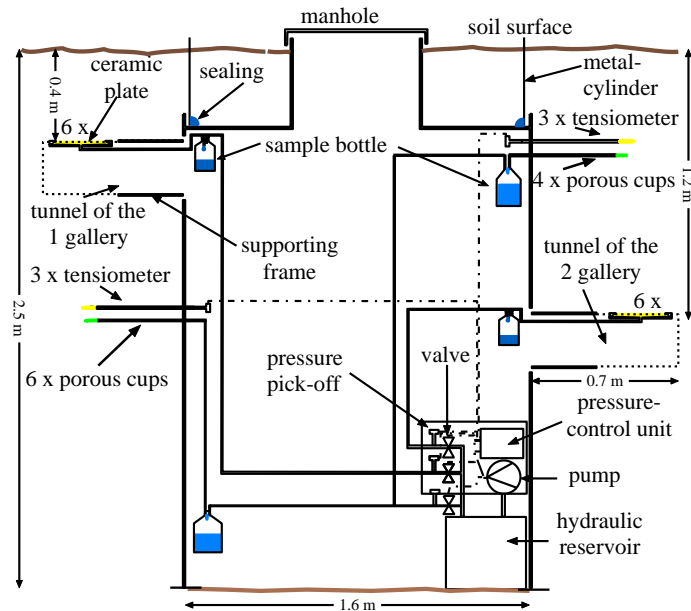
Figure 4.5: Sampling pit at the test site Merzenhausen.

4.3   Lysimeters

A standard zero-tension field lysimeter was installed at the test site Merzenhausen in 1993. It is a quadratic lysimeter with a depth of 120 cm and a surface of 1 m². A detailed description of the lysimeter is given by *Wüstemeyer* (2000) and *Dressel* (2003). Standard lysimeters collect soil water in free or forced drainage mode. Simple zero-tension or free-drainage lysimeters cause water saturation at the lower boundary which affects the travel time of solutes and water. Forced drainage by applying suction at low potential overcomes the saturation problem and removes drainage water (*Cole*, 1958). In addition standard lysimeters (0.5 to 1 m² surface area) might not capture large scale soil heterogeneities and short time evaporation rates are not available. To solve these problems two weighable capacious lysimeters were also used in this study.

4.3.1   Weighable lysimeters

The withdrawal of the soil monoliths in the lysimeters at the test site Merzenhausen took place in June 2001 with cylindrical V_2A-vessels with a diameter of 160 and a depth of 250 cm. A detailed description of the test site is given in Chapter 4.1. The lysimeter castings consist of 10 mm V_2A-steel, which are grinded spiky at the bottom to achieve a better filling and to compress the soil into the lysimeter cylinders. The shape of these spiky bottom results in the compression of one part of the soil into and the other part on the outside of the lysimeter cylinder (*Steffens*, 1990). The moulding of the lysimeters took place according to the lysimeter principles of the *Landesumweltamt Nordrhein-Westpfahlen* using a hydraulic press. After moulding, the lysimeter cylinders were dug out and a shearing device was horizontally installed to drag a porous sintered V_2A-steel plate underneath the cylinder. Finally, the porous sintered V_2A-steel plate was screwed to the cylinder bottom. These transportable units were transfered to the *Forschungszentrum* and were stored on the areal of the Agrosphere Institute before they were equipped with measurement devices and finally settled down into the 'lysimeter station' during August 2002.

   To collect the percolate at the bottom of the lysimeters special collection pans with eight separated segments were constructed (Figure 4.6). The size of each inner and outer segment is 1046 cm² and 3954 cm², respectively. The overall area is 20000 cm². These pans were hermetically closed versus the lysimeter cylinders with a tube sealing and a suction of about 10 cm was imposed at the lysimeter bottom (Figure 4.6). The lysimeters are weighted on a balance with a measuring range of 0 to 12 t and a resolution of 100 g m⁻². The whole lysimeter cellar is airconditioned on the basis of a reference temperature measured at 150 cm depth at the test site Merzenhausen. For soil water collection three suction cups were installed horizontally at the depth of 40 cm and four at 120 cm. To describe the matric potential and to controll the suction in the porous cups three tensiometer were installed analogous at each depth of the suction cups.

   Porous cups and tensiometers were installed at a distance of 35 and 55 cm, respectively, from the cylinder wall for all depths. Additionally, 22 TDR-probes (in duplication) were installed in vertical intervals of 15 cm up to a depth of 120 cm. Below this depth a larger interval of 60 cm was chosen. For the measurement of the internal temperature of the lysimeters six soil thermometers (PT100 devices) were installed in several
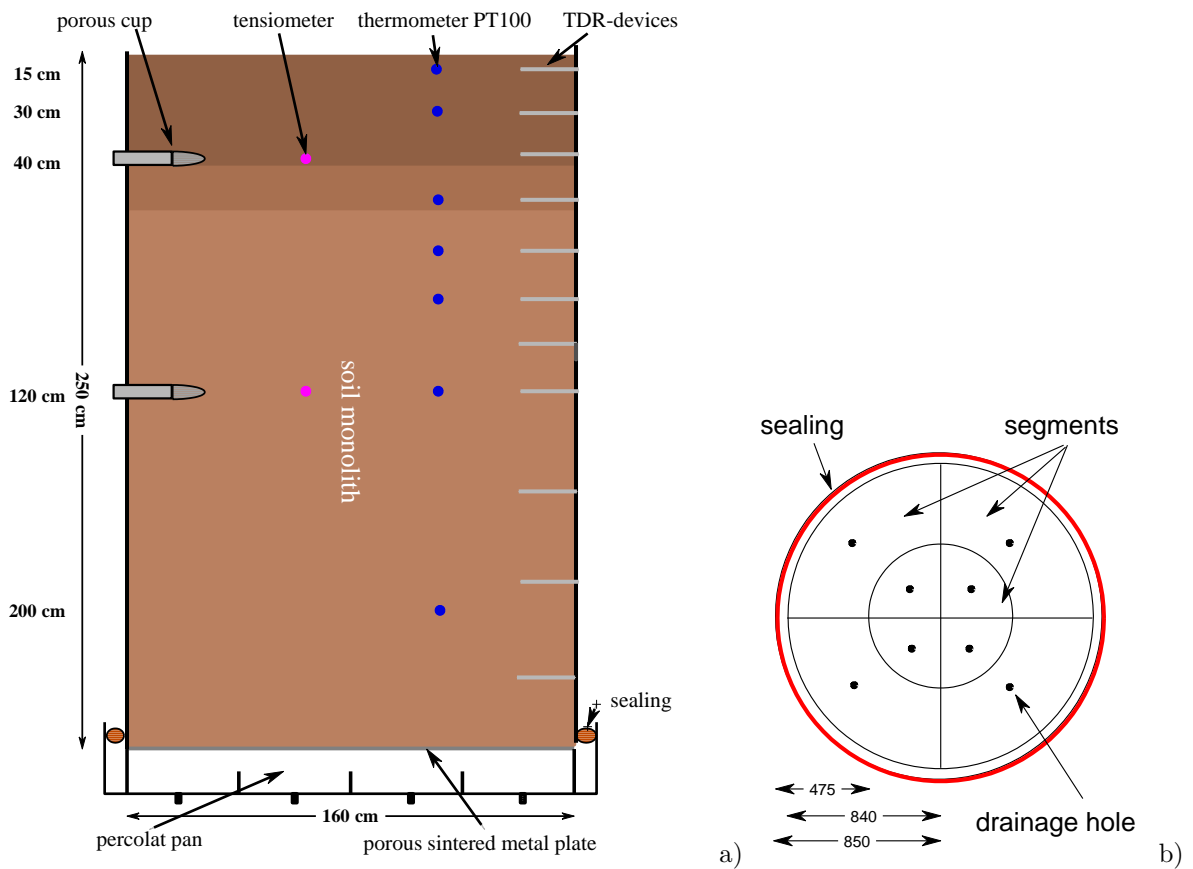
Figure 4.6: a) Design of the lysimeters and b) the percolate pan. Percolate pan: all units in mm.

depths. An overview of all installations is given in Figure 4.7. A detailed description of all measurement equipment is given in Chapter 4.3.2.
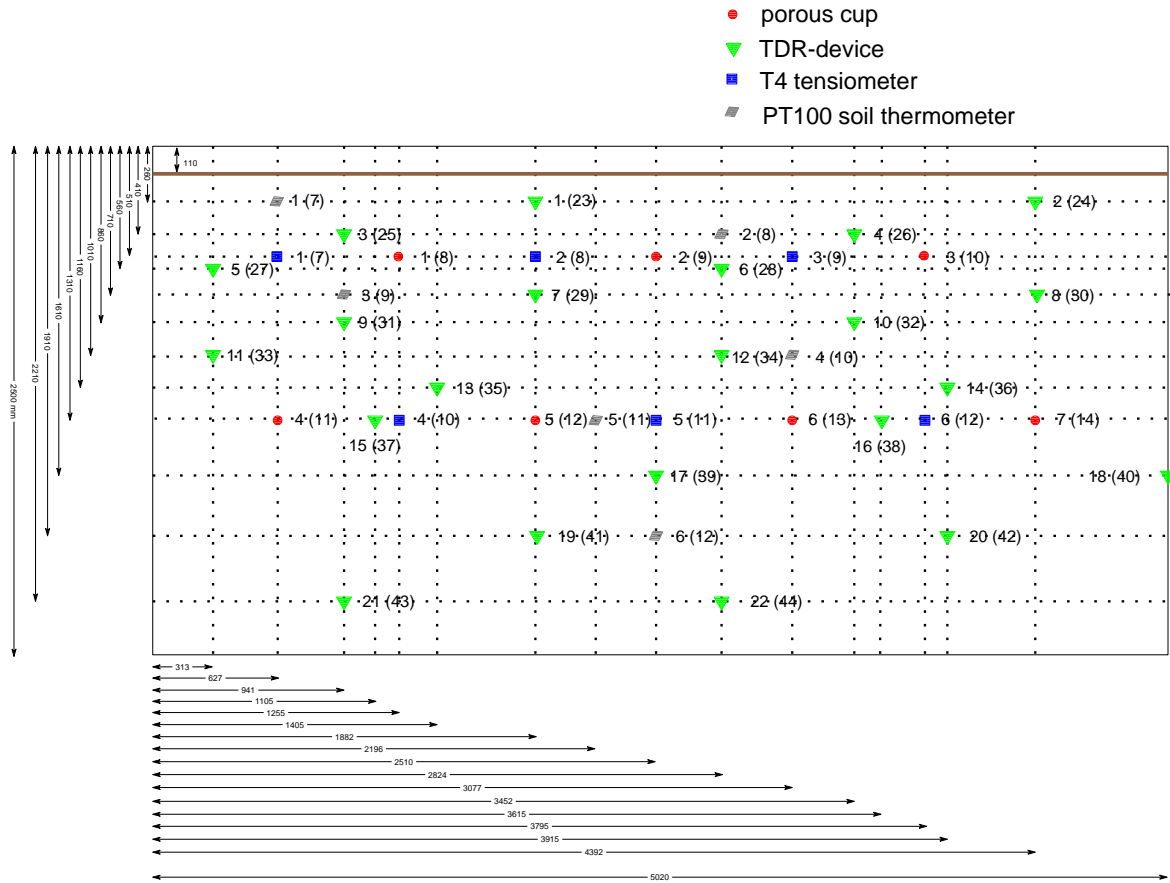
Figure 4.7: Overview of the measurement devices in the lysimeters with labelling. In parentheses: devices lysimeter 2. All units in mm.

In order to prevent water from leaking outside of the cylinder and to reduce local water changes all open spaces in the lysimeter wall and the measurement equipment were sealed with Elch polyurethane solution adhesive P1 (Rhodia Silicon GmbH, Leverkusen).

All agricultural practice on the capacious lysimeters and on the test site were accomplished at the same time. A detailed chronological set of practices before the experiment is shown in Annex A.7.

4.3.2   Measurement of soil water dynamics

Tensiometers, TDR-devices and PT100 soil thermometers were used to read continuously soil water dynamics in the lysimeters and the sampling pits. Borosilicate-glass suction cups and porous ceramic plates were used for soil water extraction.

TDR-devices

For the assessment of solute transport within the vadose zone it is indispensable to determine the change of volumetric water content with time. For this aim TDR-probes (*Time Domain Reflectometry*) were installed into the capacious lysimeters. The measurement principle of a TDR-probe is based on the speed with which an electromagnetic wave travels through a parallel transmission line. The propagation velocity depends on the dielectric constant, (Ka), of the material surrounding the transmission line (*O'Conner and Dowding*, 1999). Soil is composed, in general, of air, mineral and organic particles, and water with dielectric constants of one, two to four, and 80, respectively. Because of the large difference in the dielectric constant of water from the other soil constituents, the speed of travel of a electromagnetic wave depends largely on the water content of the soil. Changes in impendance in the transmission line and surrounding material cause some of the energy to be reflected back through the line. When the pulse reaches the end of the transmission line, virtually all the remaining energy in the pulse is reflected back through the line. These characteristics make it possible to measure the time required for a pulse to travel through a known length of transmission line, referred to as 'waveguides', buried in the soil (*Soilmoisture*, 1993). The apparent dielectric constant, Ka, of the soil can be determined by Equation 4.1 (*Vanderborght et al.*, 2000):

$$Ka = \left(\frac{c\,\Delta ts}{2L} \right)^2 \tag{4.1}$$

where L is the length of the waveguides [L], Δts is the 'travel time' of an electromagnetic wave along the TDR rods [T], and c is the speed of light [LT^{-1}]. The factor 2 is introduced because the electromagnetic wave travels twice the length of the wave guides (*Vanderborght*, 1997). Equation 4.1 can be simplified to express the apparent dielectric constant as the ratio of the apparent probe length ($L_a = \frac{c\Delta ts}{2}$) to the real probe length.

$$\sqrt{Ka} = \frac{L_a - L_{offset}}{L} \tag{4.2}$$

To accurately determine K_a, a probe offset, L_{offset}, was determined by the measurement of the wavelength in distilled water with different probe length. The resulting wavelengths [-] were fitted with a linear equation with an intercept of 4.757 (Figure 4.8). This intercept leads to an offset of 4.757 cm. The relationship between dielectric constant, Ka, and volumetric water content, θ, was described by *Topp et al.* (1980) and *Ledieu et al.* (1986) in an empirical fashion using both polynominal and linear relationship, respectively. *Roth et al.* (1990b) developed a physically based 'dielectric mixing model' to describe the volumetric water content. In this work the volumetric water content was calculated using *Topp*'s Equation:

$$\theta = -5.3 \cdot 10^{-2} + 2.92 \cdot 10^{-2} K_a - 5.5 \cdot 10^{-4} K_a^2 + 4.3 \cdot 10^{-6} K_a^3 \tag{4.3}$$

All TDR measurements were carried out using a Campbell$^{\text{TM}}$computer controlled multiplexing system (Campbell Scientific, Inc. North Logan, Utah, USA) which retrieved, stored and analyzed TDR wave forms. As the TDR-system a TDR-100 device, eight SDMX50 multiplexers and a CR10X datalogger were used. A RS232 interface was connected to a local computer to obtain data from the logger. The TDR-100 system was
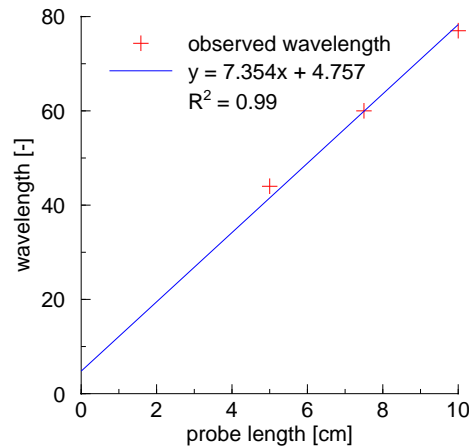
Figure 4.8: TDR wavelength for different probelength (10, 7.5, and 5 cm) in distilled water and linear fit.

operated with the datalogger software PC208W. The waveforms were analyzed with a C-routine developed at the Agrosphere Institute.

PT100 temperature-devices

The PT100 temperature devices relay on the principle that the resistance of a metal (platin) increases with temperature. The specified resistance of the metal is $100\ \Omega$ at $0°C$. They are extremely resistant and precise with a maximum deviation of $\pm\ 0.1$ K.

Tensiometers

A tensiometer measures the matric potential in the surrounding soil. The basic components of a tensiometer include a porous ceramic cup, a plastic body tube, and a vacuum gauge. The vacuum inside the tensiometer body equilibrates with the soil water tension, and the dial gauge provides a direct readout. The used T4 tensiometers (UMS Umweltanalytische Meß-Systeme, München) are high resolution tensiometer for continuous data recording in the unsaturated soil profile. A possibility of refilling through an intregrated cannula is given for easy and longterm field application (*UMS*, 2001). An overview of the technial data is given in Annex A.1.

Porous cups

The applied sampler consists of a 1000 hPa air entry value porous borosilicate-glass, 32 mm in diameter and 60 mm long, glued to a polyvinyl chloride (PVC) pipe (ecoTech ™ Umwelt-Meßsysteme GmbH, Bonn), which were especially developed for the survey of dissolved organic substances. A general description of the functionality of porous cups is shown in Chapter 2. The used suction cup is made of borosilicate-glass with a special porosity. As a result of the physico-chemical characteristics (small inner surface and a low exchange capacity) the filter material shows lower sorption tendencies compared to the widespread used ceramic and plastic suction cups. For the fritting of the glass cup no additives and bonding agents are necessary, and, therefore, contamination of the

sampled water is low (*ecoTech*, 2001). A detailed overview of the technical data of the cups is shown in Annex A.2.

Furthermore, the porous cup device is provided with a vacuum control chamber for inspection of the applied vacuum within the cup. The porous cups were connected to a multichannel SCS-6 vacuum-control-unit to sample water (Chapter 4.3.2). Six tensiometers (three per suction cup level) determine the applied suction in the cups. A datalogger is integrated into the system to store tensiometer values.

Porous ceramic plates

Porous ceramic plates were used to sample soil water within the sampling pits. The nominal data of the porous ceramic plates type *High Flow* (Soil Moisture Equipment Corp.; Goleta, USA) are shown in Annex A.3.

To sample soil water the ceramic plates where connected to a SCS-6 vacuum-control-unit (Chapter 4.3.2). A detailed description of the installation of the porous ceramic plates within the sampling pits, their feedforward control and their sorption tendencies for ETD and MBT is given by *Dressel* (2003).

Vacuum control unit

For the soil water sampling of the suction cups and the ceramic plates a SCS-6 vacuum-control-unit (UMS, Umweltanalytische Meß-Systeme, München) was used. Each single sampling pit at the test site Merzenhausen and each lysimeter at the lysimeter station at the *Forschungszentrum Jülich* was connected to one vacuum-control-unit. A detailed description of the vacuum-control-unit is given by *Dressel* (2003). During the experiment the applied vacuum was determined by a linear function of the measured tensiometers and an offset of 30 hPa up to the internal maximum of 400 cm pressure. It was programmed with control intervals of one minute, a one minute record of the measurement readings and a calculation of the mean value for each minute. An exclusive criteria for single tensiometer values for the calculation of the mean tension value (target value) was set at 25 percent and/or 30 hPa absolute deviation of the mean value. The internal datalogger of the SCS 6 logged data in maximum 60 minutes intervals, or if changes within the tension of 4 percent and/or 6.0 hPa from the last logged value occurred.

4.4   Measurement of climatic data

Climatic stations were installed at both, the test site Merzenhausen and the lysimeter station of the *Agrosphere Institute*. The measurement equipment of the stations is shown in Annex A.6. All data, except for precipitation, were detected in measurement cycles of 5 to 10 seconds and logged as 10 minute means with a datalogger MAC 19 (Schuehle, Ravensburg). The data were transferred from the datalogger onto portable PCMCIA-cards and regular transferred to a local computer.

Humidity

Two approaches are available to determine the relative humidity, f, of the air. The first approach is based on direct measurements with a hair-hygrometer. The second one uses the wet and dry air temperature to calculate the relative humidity, f, according to:

$$f \ = \ e_s - \frac{t_d - t_w}{2} \ \cdot \ 100 \tag{4.4}$$

where t_w is the wet air temperature, and d_d the dry air temperatur. The multiplicator 100 is introduced to receive relative percentage data (*Zmarsly et al.*, 1999). The saturated vapour pressure, e_s, is calculated after the Magnus Equation (4.5):

$$e_s \ = \ 6.1 \ \cdot 10^{\left(\frac{7.5 \cdot t_d}{t + 237.2^\circ C}\right)} \tag{4.5}$$

with the empirical factor 6.1 hPa and 237.2 K.

Evaporation

Evaporation, E, or latent heat flux, (λE), is mostly driven by the humidity difference between the atmosphere and the soil surface. The magnitude of this flux is also modified by the degree of turbulence in the atmosphere and by the rate at which water can be transported towards the surface atmosphere interface. Numerical models require potential evaporation, which is the evaporation over a saturated soil surface. In case soil hydraulic properties become limited for water flux, the actual evaporation is reduced. Various models are in use to calculate potential evaporation. The common ones are the physically based equation after *Penman* (1948) and the Penman-Monteith-equation after *Monteith* (1965). A full description and comparison of the different methods is given by *Dressel* (2003). For our input data of the HYDRUS-2D simulations and for the calculation of the potential evaporation the *Penman-* Equation (4.6) was used:

$$ET_{pPenman} \ = \ \frac{\Delta}{\Delta + \gamma} \frac{Rn - G}{L_h} + \frac{\gamma}{\Delta + \gamma} \ f(v) \left(e_s \left(t_a\right) - e\right) \tag{4.6}$$

$ET_{pPenman}$ is the potential evaporation $[mm]$, Δ is the slope of the saturated vapour pressure curve [hPa K^{-1}], γ is the psychrometer constant [hPa K^{-1}], Rn is the net radiation [W m^{-2}], G is the soil heat flux [W m^{-2}], L_h is the latent heat of vaporization [W kg^{-1}], $f(v)$ is a wind speed function [m^{-1}kPa^{-1}], e_s is the saturated vapour pressure at mean air temperature t_a [K] in [hPa], and e is the actual vapour pressure at mean air temperature t_a [hPa]. The mean air temperature t_a is defined as:

$$t_a = \frac{t_{min} - t_{max}}{2} \tag{4.7}$$

with the minimum air temperature, t_{min}, and maximum air temperature t_{max} [$^\circ C$].

4.5   Application of test compounds and water tracer

For the field and lysimeter experiments the heterocyclic ureas Methabenzthiazuron (MBT) (Annex A.6.1) and Ethidimuron (ETD) (Annex A.6.2) were used. Their influence on plant growth was first described by *Thompson et al.* (1946). The development

of these ureas led to different substances for a widespread of applications and are still important on the market of herbicidal chemicals (*Schmidt*, 1996). Bromide as a conservative tracer was applied to gain a better understanding of the physical mixing processes and the solute transport in the soil.

Table 4.3: Specification of the potassium bromide (KBr) applied on the test site and lysimeters.

Potassium bromide	
manufacturer	Merck KGaA, Darmstadt
mol. weight	119.01 g mol^{-1}
purity	>99.5 %

Test site Merzenhausen

The experiment was performed on a rectangular field of about 570 m^2 on the test site Merzenhausen (Chapter 4.1 and Figure 4.1). A computer-assisted Dubex (model Nestor, year of manufacture 1999) field sprayer with a tank volume of 3200 liter was used for the pesticide and tracer application. The boom (width: 27 m in total; divided in 9 sections of 3 m) was equipped with 54 nozzles (Turbo Drop TD 025; Dubex), whereby only 9 meters were used. The concentration of the test substances within the spray solution was measured by taking samples from the reservoir tank before application. Driving speed and spray pressure were controlled electronically resulting in a total spray volume of 328.5 L ha^{-1}. At the day of application, the soil coverage was low due to tillage and low spring temperatures. During the application on the 03/04/2003 between 9^{02} am and

Table 4.4: Application details for the sampling pits on the test site Merzenhausen.

Substance	*MBT*	*ETD*	*Bromide*
formulation	wettable powder	wettable powder	salt
	(70 % a.i.) [†]	(70 % a.i.) [‡]	
nominal applied [§]	230.3 mg m^{-2}	161.7 mg m^{-2}	24.507 g m^{-2}
net applied [¶]	142.9 mg m^{-2}	100.3 mg m^{-2}	15.202 g m^{-2}
applied water	L ha^{-1} (total volume: 179 l applied on field spot)		

[†] commercial product Tribunil^{TM}Bayer AG

[‡] commercial product Ustilan^{TM}Bayer AG

[§] calculated values related to the applied total amount 200.522 g Tribunil^{TM}, 140.792 g Ustilan^{TM}and 22246.5 g potassium bromide (14936.935 g Br^{-}) dissolved in 179 l water

[¶] determined by dish sampling during spay process

9^{25} am westerly winds with an average wind speed of 3.2 m s^{-1} were observed. The sky was cloudy and the top soil was moderately wet due to slightly rainfall during the night.

To control the homogeneity of the spraying process and to determine the initial amount of the test substances 63 petri dishes with a diameter of 8.52 cm and a surface of 57.01 cm^2 construed with 2 layers of filterpaper (Schleicher & Schuell, Dassel; 589^3 Blauband Rundfilter; Ref. No. 300209) were layed out within a regular grid (Figure 4.9). The petri dishes were washed out and the filter paper was eluated with destilled water. From the washing and eluated water aliquotes were taken and bromide was analyzed. Preliminary experiments for rinsing of the bromide from the petri dish and filterpaper were conducted and led to a recovery of $\geq$ 99 % of the applied bromide. Based on the assumption that the spray solution was homogeneously mixed with all test substances the detection of bromide also leads to an acceptable distribution pattern of the pesticides MBT and ETD. The overall average amount of bromide was calculated by the results of the petri
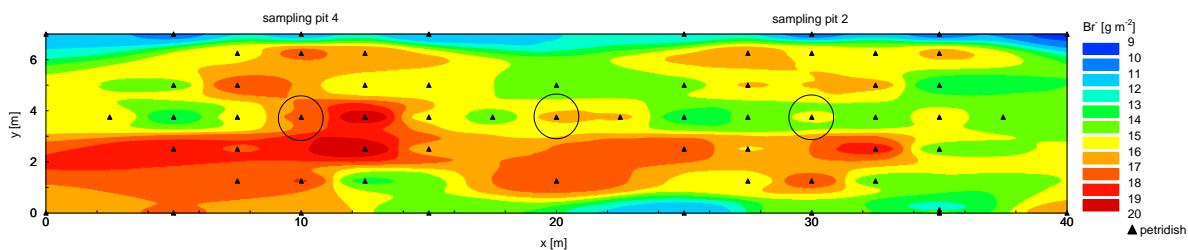
Figure 4.9: Distribution of the 63 petri dishes and homogeneity of the spraying process of bromide on the test site Merzenhausen.

dish-experiment and yielded to an application amount of 15.20 g m^{-2} with a standard deviation of 2.29 g m^{-2}. Figure 4.9 shows the spatial distribution of bromide on the test spot with the variation between sampling pit 2 and 4. Due to these variations an average initial amount for each sampling pit was calculated on the basis of the 13 surrounding collecting points. This leads to an average bromide application of 15.39 g m^{-2} (standard deviation = 1.80 g m^{-2}) for sampling pit 2 and 16.67 g m^{-2} (standard deviation = 2.14 g m^{-2}) for sampling pit 4. The low total amounts for the whole test spot as well as for the single sampling pits compared to the calculated nominal application masses may result from wind drift, volatilisation, airborne particles (long range transport) as well as from technical problems occuring during the spraying process.

Weighable lysimeters

Weighable field lysimeter

The application of bromide on the field lysimeter was carried out after field application on the 03/04/2003 between 9^{40} am and 10^{00} am. For the determination of the application loss aluminum foil was layed out at the lysimeter castings and flanged over the frame. The spraying was carried out with a hand sprayer set onto a laboratory round-bottom flask. A 5 ml aliquot was withdrawn from the spray solution for bromide analysis. After application of 24.507 g bromide (36.5 g KBr) solved in 292 ml tap water the aluminum foil and the hand sprayer were stored in a sealed plastic back. Aluminum foil, plastic bag and hand sprayer were washed out with distilled water and the bromide content was analyzed to determine the spraying loss. The spraying loss of 7.85 % led to a net total bromide amount of 20.57 g m^{-2}.

Weighable lysimeters *Agrosphere Institute*

The MBT, ETD and bromide application on the lysimeters at the *Agrosphere Institute* took part in the afternoon of the 03/04/2003 between 1^{30} pm and 1^{50} pm. The same spraying procedure as on the field lysimeter was used to apply 49.01 g Br^-(73 g KBr), 658.0 mg Tribunil^{TM}(460.6 mg MBT) and 462.0 mg Ustilan^{TM}(323.4 mg ETD) solved in 584 ml tap water. Two 5 ml aliquots were withdrawn from the spray solution for bromide and MBT/ETD analysis. The spraying loss was determined using the same method as for the field lysimeter. The calculated spraying loss for the lysimeter 1 and lysimeter 2 was 5.8 % and 4.0 %, respectively, which led to a net total spraying amount of 20.99 and 21.71 g m^2, respectively. Gross applied amounts of MBT, ETD and bromide and calculated net amounts are listed in Table 4.5.

Table 4.5: Application details for the lysimeters at the *Agrosphere Institute* and field lysimeter at the test site (*Merzenhausen.*

Substance	*MBT*	*ETD*	*Bromide*
formulation	wettable powder (70 % a.i.) [†]	wettable powder (70 % a.i.) [‡]	salt
nominal applied [§]	230.3 mg m^{-2}	161.7 mg m^{-2}	24.51 g m^{-2}
lysimeter 1 net applied [¶]	216.94 mg m^{-2}	152.32 mg m^{-2}	20.99 g m^{-2}
lysimeter 2 net applied [¶]	212.10 mg m^{-2}	155.23 mg m^{-2}	21.71 g m^{-2}
field-lysimeter net applied [¶]	-	-	20.57 g m^{-2}
applied water		292 ml m^{-3}	

[†] commercial product Tribunil^{TM}Bayer AG

[‡] commercial product Ustilan^{TM}Bayer AG

[§] calculated values related to the applied total amount 658 mg Tribunil^{TM}, 462 mg Ustilan^{TM}and 73 g potassium bromide (49.014 g Br^-) dissolved in 584 ml water

[¶] calculated in consideration of spray losses and aliquot withdrawal

4.6 Irrigation

The irrigation system at the test site Merzenhausen and the lysimeters at the *Agrosphere Institute* was installed to consider low natural rainfall during spring and summer 2003. The aim of the irrigation is to force the breakthrough of the test compounds.

For the field irrigation two quadrangle garden sprinklers (Gardena Polo Viereckberegner) were choosen. Water was pumped from a reservoir with a maximum volume of 80 l min^{-1} to the sprinklers. To observe the homogeneity of the sprinkling process and to calculate the total irrigated water 24 plastic beakers (diameter = 62 mm) were set up in a regular grid of 1.25 m (Figure 4.10). The total applied water was calculated as a mean of the inner eight measurement points. The same amount of water was used for the manual irrigation of the field and capacious lysimeters. For a better infiltration of the applied water the upper 3 to 5 cm were tilled. All irrigation data are shown in Annex
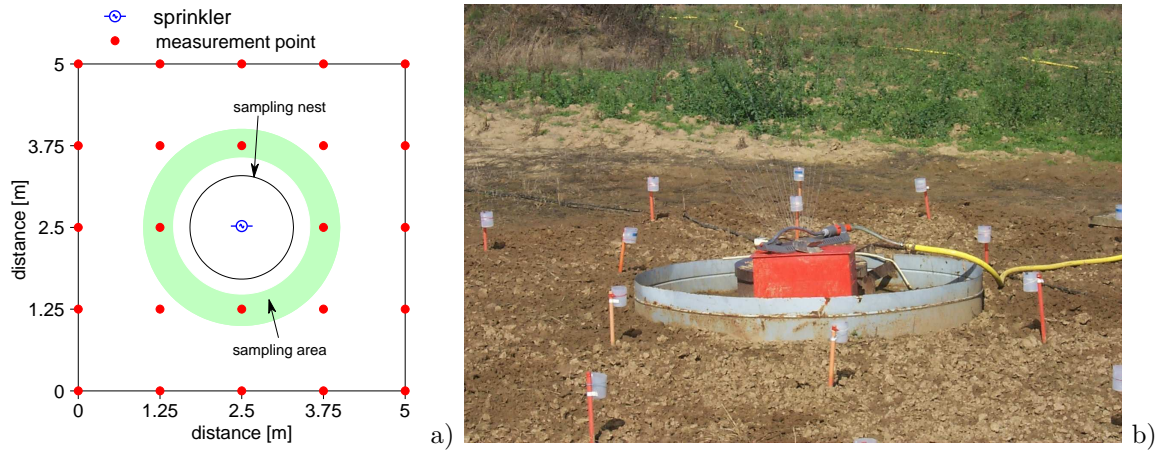
Figure 4.10: Irrigation of the sampling pits at the test site Merzenhausen. a) grid of 24 plastic beakers, location of the sprinkler system, and the sampling area of the ceramic plates and suction cups (grey contour). b) the sprinkler system at work.

A.8. As an average 129.3 mm of water were irrigated on the test site Merzenhausen and on the lysimeters at the *Agrosphere Institute*, whereby sampling pit 2 was irrigated with an average of 127.2, and sampling pit 4 with 129.3 mm, respectively. The homogeneity of the irrigation is shown in Annex A.4.

4.7 Simulation of soil water fluxes

For the simulation of the soil water fluxes in a lysimeter and field soil the HYDRUS-2D (*Simunek et al.*, 1999) code was used, which numerically solves the Richards' equation (Equation 3.3) for saturated-unsaturated water flow and the convection-dispersion equation (Equation 3.11) for heat and solute transport.

4.7.1 Parametrization of the soil water characteristic

The unsaturated soil hydraulic properties $\theta(h)$, and $K(h)$, in Equation 3.3 are in general highly nonlinear functions of the pressure head. Closed-form analytical expressions for prediction the unsaturated hydraulic conductivity have been developed by several investigators but the most common are the *Brooks and Corey* (1964) and the *Mualem - van Genuchten* approach which was used in the simulations. *van Genuchten* (1980) used the statistical pore-size distribution model of *Mualem* (1976) to obtain a predictive equation for the unsaturated hydraulic conductivity function in terms of soil water retention parameters. For the parametrization of the retention of *Brooks and Corey* (1964), *van Genuchten* (1980) used the saturated volumetric water content, θ_s, and the residual water content, θ_r. These two parameters determine the range of the volumetric water content (see Equation 4.8).

$$S_e = \frac{\theta - \theta_r}{\theta_s - \theta_r} \begin{cases} 1 & \psi \geq 0 \\ (1 + |\alpha\psi|^n)^{-m} & \psi < 0, \ \alpha, n, m > 0 \end{cases} \tag{4.8}$$

For the *Mulaem-van Genuchten* approach a S-shaped function is characteristic, which is described by the parameters α $[\frac{1}{cm}]$ (reciprocal value of the air entrance value or bubbling pressure), n [-] and m [-]. The parameters m and n are shape parameters. m is related to n by:

$$m = 1 - \frac{1}{n} \tag{4.9}$$

To obtain the weight specific water capacity C_ψ $[\text{cm}^{-1}]$ for a predetermined matric potential (ψ) for the *van Genuchten* (1980) parametrization Equation 4.8 must be solved toward θ. The derivation from θ versus ψ results in Equation 4.10.

$$C_\psi = (\theta_s - \theta_r)\frac{m\,n\,|\alpha|^n\,|\psi|^{n-1}}{(1+|\alpha\psi|^n)^{m+1}} \qquad \psi < 0, \;\; \alpha\,m > 0, \;\; n > 1 \tag{4.10}$$

Assuming that the turtuosity factor $\lambda = 0.5$ the *Mualem-van Genuchten* approach leads to the unsaturated hydraulic conductivity function given by Equation 4.11.

$$K_r(\psi) = K_s\frac{\left[1 - (\alpha\psi)^{mn}\left\{1+(\alpha\psi)^n\right\}^{-m}\right]^2}{\left[1+(\alpha\psi)^n\right]^{\frac{m}{2}}} \tag{4.11}$$

4.8   Moment analysis of breakthrough curves

One approach to analyze beakthrough curve data is to use the method of moments to provide some basic informations about the movement of solutes in soils. The method of moments is only a descriptive tool for the comparison of different breakthrough curves without any assumption concerning the underlying processes.

In a first step the relative mass recovery, R, which describes the proportion of the sampled mass τ_o in n probes - defined as the 0. moment - to the total applied mass M_{app} is determined by using Equation 4.12.

$$R = \frac{\tau_o}{M_{app}} \cdot 100 \tag{4.12}$$

with the 0. moment:

$$\tau_0(x) = \int_0^\infty c(x,t)dt \tag{4.13}$$

Prerequisite of the method of moments is that the complete breakthrough curve or concentration-profile is sampled. Differences in the mass balance can be traced back to sorption, sampling error and, circumventing of the sampling system.

In a second step the BTCs measured in individual samplers were analyzed, whereby the first two normalized temporal moments, $\tau_1(x)$ $[T]$ and $\tau_2(x)$ $[T^2]$ of a BTC measured at location x were used. The centroid of concentration $\tau_1(x)$ or μ [L] or [T] - defined as the 1. moment - corresponds to the arithmetic mean and describes the mean travel time. The 1. moment is calculated with Equation 4.14.

$$\tau_1(x) = \frac{\int_0^\infty tc(x,t)dt}{\int_0^\infty c(x,t)dt} \tag{4.14}$$

The normalized 2. moment $\tau_2(x)$ $[T^2]$ corresponds to the spread of the observed BTC and describes the dispersion of solutes in time or space. The 2. moment can be calculated using Equation 4.15.

$$\tau_2(x) = \frac{\int_0^\infty t^2 c(x,t) dt}{\int_0^\infty c(x,t) dt} \tag{4.15}$$

The variance σ^2 [T] can be calculated by (*Jury and Sposito*, 1985):

$$\sigma^2 = \tau_2 - \tau_1^2 \tag{4.16}$$

For transient conditions the time, t, can be substitute by the normalized cumulative amount of water I $[L]$.

Chapter 5

Preliminary experiments

In this section experimental results providing information on the sorption behaviour of suction cups and the determination of saturated hydraulic conductivity are presented.

5.1 Sorption behaviour of suction cups

Two different laboratory tests were conducted to investigate the potential sorption behaviour of the borosilicate-glass suction cups. On one hand the sorption of the raw material of the suction cup was analyzed and on the other hand the cleaning procedure of the suction cup was performed.

5.1.1 Sorption of raw material of the suction cups

A detailed description of the sorption of pesticides and DOC on glass suction cups is given by *Wessel-Bothe et al.* (2000). Nevertheless, sorption experiments with the raw material of the suction cups were conducted to analyze the sorption behaviour of various elements. Therefore, 10 g of the fine grained raw borosilicate-glass material was added either to 60 ml of destilled water, 1M $HCl_{(aq)}$, 1M $NaOH_{(aq)}$ or an artifical soil water solution containing traces of Fe, Ca, Mg, Mn, Na, K, NO_3, S and the potential tracer substances Cl, Br and I. The probes were shaken for 48 hours and filtered with a paper-filter afterwards. Changes in the solvent concentrations were analyzed and are presented in Annex Figure A.5. In contrast to the other anions, changes in bromide concentration are relatively low. A direct transfer of the results to the potential sorption tendency of the whole porous cup is not valid due to the larger reactive surface of the raw material in comparison to the sintered material of the suction cup.

5.1.2 Cleaning procedure of suction cups

Suction cups require special preperation prior to installation. A recommended procedure (*DVWK*, 1990; *Grossmann and Udluft*, 1991) includes rinsing with distilled water, one liter of 1 N $HCl_{(aq)}$, followed by one liter of 1 N $NaOH_{(aq)}$ and again rinsing with some liters of distilled water. To check whether this procedure is applicable for the borosilicate-glass suction cups we applied this procedure, whereby the percolate was sampled in short time intervals ($\Delta t = 90, 180, 270, 360, 1260$ and 1350 min) and its ion content was

analyzed. The suction was -22 mbar to ensure low percolation and long reaction times. For the final rinsing with distilled water a suction of -500 mbar was chosen to reduce the percolation time. Impurities of the solvent are shown in Annex Figure A.6. These results indicate that a sufficient cleaning took part. The high contamination at the beginning of the rinsing procedure might be a result of dust and other surface contaminations due to the manufacturing process. The small increase at the end of the cleaning procedure might be caused by probe contamination after sampling or by analytical inaccuracy.

5.2 Assessment of the saturated hydraulic conductivity of suction cups

To predict the saturated hydraulic conductivity, K_s, for the borosilicate-glass suction cups, distilled water was sucked through the system at a defined constant suction. The bulk-percolate was determined gravimetrical. After flow equilibrium was established the percolate was measured within a time interval of 60 minutes.
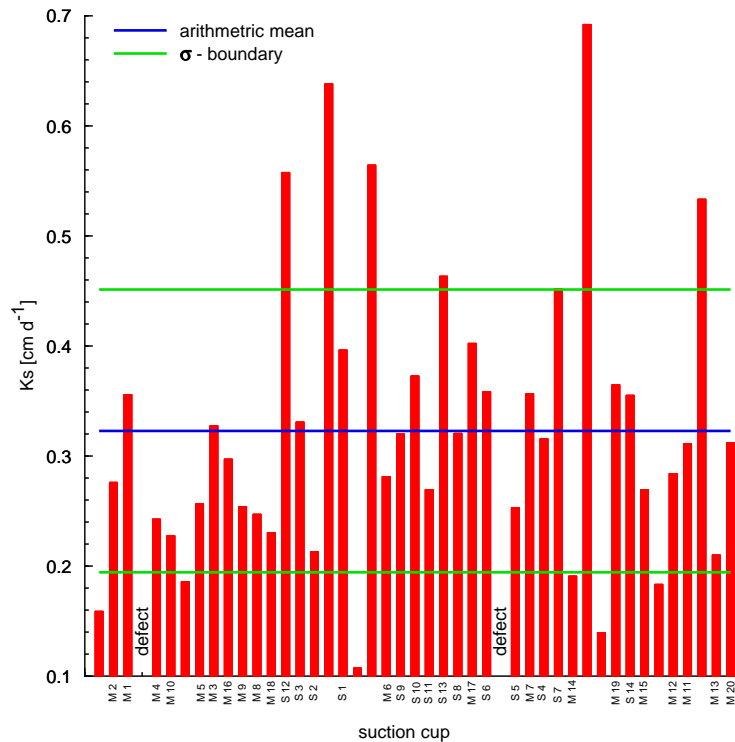
Figure 5.1: Saturated hydraulic conductivity, *Ks*, with mean value and standard deviation for the borosilicate glass suction cups. Labelling: S = installation in the lysimeters, and M = installation in the sampling pits at the test site Merzenhausen.

The saturated hydraulic conductivity was calculated by:

$$K_s = \frac{V \cdot D}{A\,t\,(h_a - \tau_h)} \qquad (5.1)$$

where V the volume of percolate [L^3], D the thickness of the suction cup wall [L], A the surface area of the suction cup [L^2], h_a the applied pressure head [L] and τ_h the maximum tube height from the bottom of the suction cup [L]. The saturated hydraulic conductivity as well as the arithmetic mean and the standard deviation (σ-boundary) are plotted in Figure 5.1. The data show large differences in hydraulic conductivity between the suction cups. Only cups with a hydraulic conductivity within the σ-boundary were used for the installation. Each suction cup position in the sampling pits and lysimeters was recorded.

Chapter 6

Simulation of suction cup behaviour: literature overview

In this section the state of the art in the field of analytical and numerical solutions concerning the suction cup behaviour are summarized. To provide a consistent bias for the interpretation of the analytical and numerical solutions of the suction cup behaviour three new cup characteristics are introduced:

1. The suction cup activity domain (SCAD)(see Figure 6.1) is defined as the spatial extension [L] of the difference in matric potential between the initial situation without applying suction and the conditions where suction is applied to the cup. It represents the area of influence in matric potential distribution of the natural flow field after suction is applied. For a better comparison between different cases, the activity domain will be plotted as a horizontal transect through the cup.

2. The suction cup extraction domain (SCED) (see Figure 6.1) is an area [L^2], for a two-dimesional case, or volume [L^3], for a three-dimensional case, from which water and solute can be extracted by a suction cup within a certain time of applied suction. If the sampling time is set to infinity, the suction cup extraction domain will eventually reach the soil surface and in the limit will be equal to the suction cup sampling area (SCSA).

3. The suction cup sampling area (SCSA) is defined as the area at the overlying soil surface from which water could be captured by the suction cup under a continuous application of tension. It is expressed in unit length [L], for the two-dimensional case, or unit area [L^2], for the three-dimensional case.

6.1 Analytical solutions of suction cup behaviour

The interaction between soil water extraction and flow field has been studied using analytical solutions e.g. *Warrick and Amoozegar-Fard* (1977) and *Hart and Lowery* (1997). For the calculation of the influence with analytical solutions three soil types with different hydraulic properties were chosen - a clay loam, a sandy clay and a sandy soil. The hydraulic properties of the three soils is given in Chapter 7.1.

differences in matrix potential [cm]

a)

sampling area (SCSA)

extraction domain (SCED)

suction cup

b)
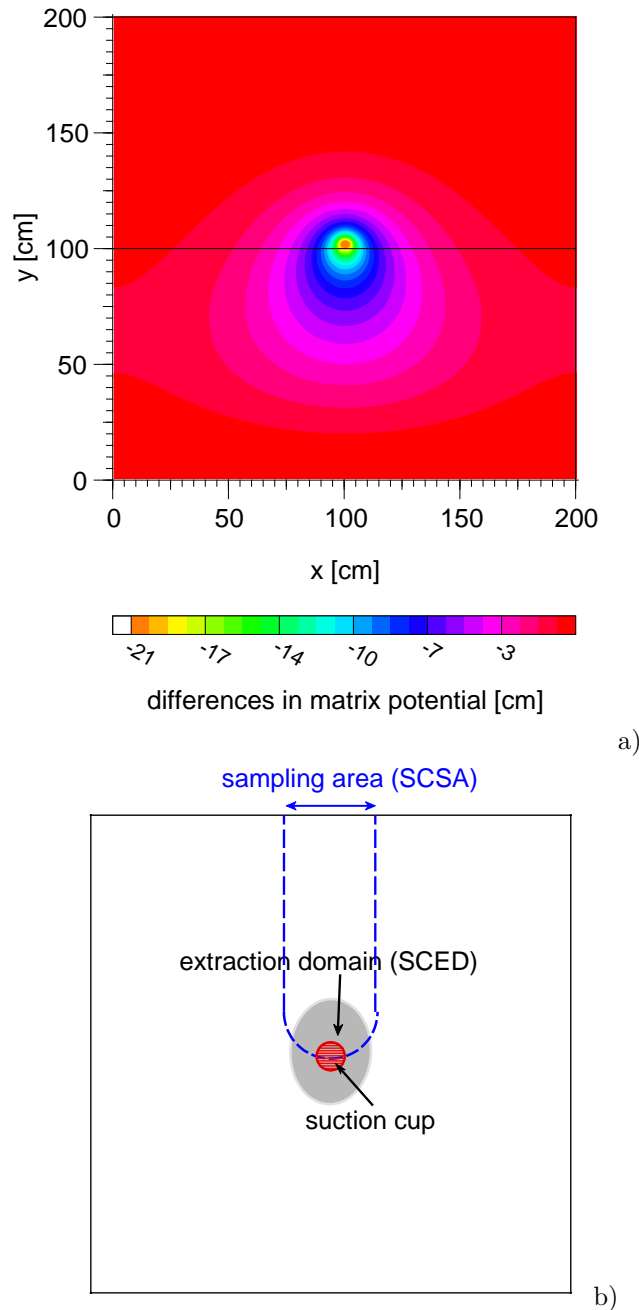
Figure 6.1: Definitions of a) suction cup activity domain (SCAD) b) the suction cup sampling area (SCSA) and suction cup extraction domain (SCED).

Warrick and Amoozegar-Fard (1977) give a general analytical solution based on the combination of *Darcys'* law and the hydraulic conductivity function after *Philip* (1968) and *Raats* (1971) for the spatial extent of the suction cup activity domain depending on the soil properties and the suction cup radius, r_o. As a boundary condition the flow site is assumed to be far away from any boundaries and a unit gradient exists away from the cup. The normalized matric flux form for steady state conditions in Darcy flux, J_w, and extraction rate, q, in the suction cup are given by Equation 6.1:

$$\phi_N = (1 - \frac{R_o}{p})^{(Z-p+R_o)} \tag{6.1}$$

where ϕ_N is the matric flux [-] normalized by the suction cup radius, r_o), R_o [-] is $\frac{\alpha r_o}{2}$ with α [cm^{-1}] for the slope of the hydraulic function curve (*Thomas et al.*, 1976), Z [-] is $\frac{\alpha z}{2}$ with z [cm] for the vertical distance, and p [-] is $\sqrt{R^2 + Z^2}$ with R [-] $= \frac{\alpha r}{2}$ with r [cm] for the horizontal distance. To calculate the normalized matric flux potential for the three given soils the slope α was fitted on the hydraulic conductivity function (see Figure 7.2). The fits yielded values for $\alpha = 0.0236$ for the clay loam, 0.0279 for the sandy clay, and 0.0978 cm^{-1} for the sandy soil, respectively. The suction cup radius r_o was 2 cm. The highest decrease in ϕ_N occurs near the sink (the value at the cup surface is zero and forty percent of the decrease occur inside the 0.4 surface, which is roughly the sphere of the suction cup activity domain)(see Figure 6.2).
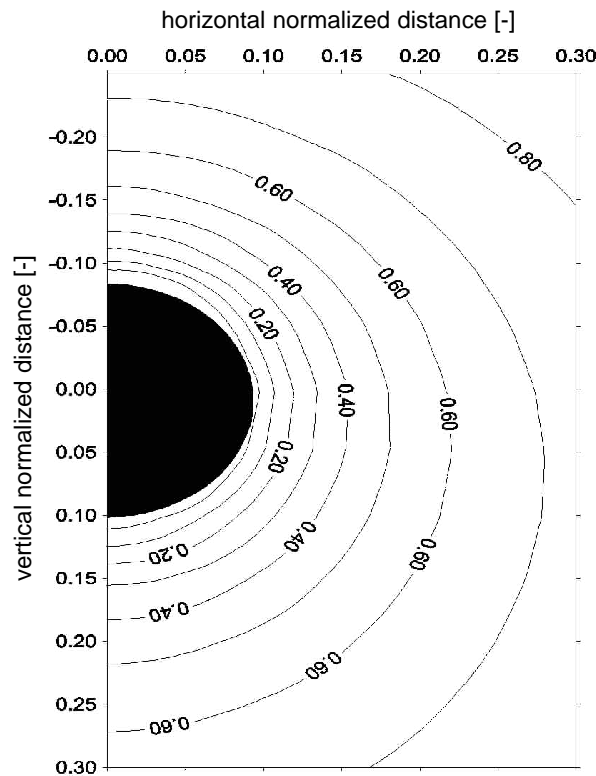
Figure 6.2: Matric flux potential normalized by the suction cup radius, r_o, for a sand with $\alpha = 0.0978$ cm $^{-1}$ and a suction cup radius of 2 cm (calculated using Equation 6.1). The black area illustrates the location of the suction cup.

The equi-potential lines of matric flux potential are plotted in Figure 6.2 for a sand soil with $\alpha = 0.0978$ cm^{-1}. The results of the spatial extent of the suction cup activity domain given by the analytical solution indicate a vertical unsymmetry, but the maximum extent of the suction cup activity domain cannot be calculated. To solve this problem *Warrick and Amoozegar-Fard* (1977) give an analytical solution for the maximum cylindrical distance of line sinks from which flow can be intercepted (Equation 6.2):

$$SCED_m = [(\frac{\alpha^2 q}{4\pi\,K_s})^{-(\alpha\psi_1)}]^{0.5} \qquad (6.2)$$

where $SCED_m$ is the maximum suction cup extraction domain [-], q is the volumetric water flow into the sampler or extraction rate [L^3T^{-1}], the saturated hydraulic conductivity K_s [LT^{-1}] and α [cm^{-1}] are constants appropriate for a given soil. ψ_1 is the pressure head at large distances [L]. The calculations of the maximum extraction domain R_m for a clay loam, a sandy clay and a sandy soil are listed in Table 6.1. The differences in the calculated maximum SCED for each single soil are directly linked to the amount of extracted soil water, with larger SCED for larger amounts of extracted water. The high SCED-values for the sandy clay, which do not correspond to the results of the numerical simulations presented in Chapter 7.1, might be caused by uncertainties in Gardner-α parameter estimation.

To determine the lines of equal hydraulic head (H = h - z) and the normalized *Stokes* stream function ($\frac{\psi}{q}$) for the three soils Equation 6.3 (*Warrick and Amoozegar-Fard*, 1977) was used.

$$\frac{\psi}{q} = \frac{4\pi\,K_s\,\exp(\alpha\psi_1)}{\alpha^2 q}\,R^2 + 0.5*(1+\frac{Z}{p})\,\exp(Z-p) \qquad (6.3)$$

The results are shown in Figure 6.3.
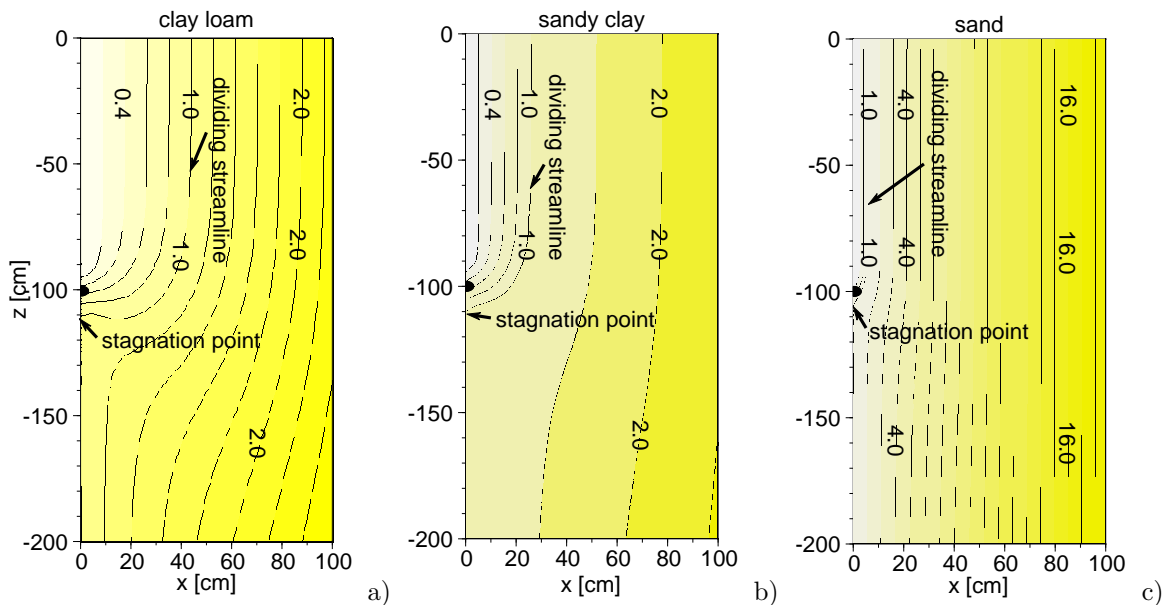
Figure 6.3: Flow net of the streamlines for a suction cup with dividing streamlines $\frac{\psi}{q} = 1.0$ **for an applied suction of 100 cm for a) a clay loam, b) a sandy clay and c) a sandy soil. All calculations were done using Equation 6.3 and input parameters listed in Table 6.2.**

The streamlines form an orthogonal set, whereby the dividing streamline labeled $\frac{\psi}{q} = 1.0$ separates the water going into from that which passes the cup. Therefore, the dividing streamline directly determines the SCSA at the soil surface. Figure 6.3 shows that the highest extraction rates correlate with a larger suction cup sampling area. As seen before, the extraction rates depend on the hydraulic conductivity of the soils and, therefore, the analytical solution for the sampling area of the cups does too.

Table 6.1: Suction cup extraction domain (SCED) for a clay loam, a sandy clay and a sandy soil calculated using Equation 6.2. Note that Gardner-α was fitted on data listed in Table 7.1, K_s was taken from Table 7.2 and ψ_1 from axisymmetrical calculations presented in Chapter 7.1.1.

Input parameters:

| | α | K_s | ψ_1 |
	$[cm^{-1}]$	$[cmh^{-1}]$	$[cm]$
clay loam	0.0236	0.26	-31.2
sandy clay	0.0279	0.12	-7.2
sand	0.0.0978	29.7	-20.5

| *soil* | *q* | $\boldsymbol{R_m}$ |
	[ml]	*[-]*
clay loam	2764	29.4
	2914	30.2
	3014	30.7
	3034	30.8
	3044	30.9
sandy clay	2764	94.9
	2804	95.6
	2834	96.1
	2864	96.6
	2874	96.7
	2874	96.7
sand	2694	2.6
	2724	2.6
	2734	2.6
	2734	2.6
	2734	2.6
	2744	2.6

Table 6.2: Input parameter for the calculation of the streamlines for a clay loam, sand and sandy clay.

Soil type	*Gardner-*α [†]	*Flux rate (q)* [‡]	K_s [§]	ψ_1 [¶]
	[cm^{-1}]	*[cm$^{-3}h^{-1}$]*	*[cm h^{-1}]*	*[cm]*
clay loam	0.0236	2914	0.26	-31.2
sand	0.0978	2734	29.70	-20.5
sandy clay	0.0279	2834	0.12	-7.2

[†] Gardner-α fitted on Mualem van Genuchten hydraulic conductivity function

[‡] Extraction rate of the point sink taken from axisymmetrical simulation with constant upper boundary flux $J_w = 0.013$ cm h^{-1}

[§] saturated hydraulic conductivity taken from HYDRUS-2D soil cataloque

[¶] matric potential of the undisturbed soil - taken from axisymmetrical simulation with constant upper boundary flux $J_w = 0.013$ cm h^{-1}

As stated above, the analyses presented are for steady-state conditions. Since the time-dependent solution is unknown, the authors assume that the extraction rate approaches rapidly to an equilibrium state. This might be true for small extraction rates, in which only a slight pertubation of a uniform flow exists (as if there was no sink), but not for large extraction rates. The sample withdrawal might also be expected to originate from approximately the same soil volume for steady-state and transient conditions (*Warrick and Amoozegar-Fard*, 1977). *Hart and Lowery* (1997) assumed that the porous cup collects a soil solution sample from a columnar soil volume, V_s, surrounding the sampler body and porous cup. Furthermore, the sampler was assumed to collect all water percolating through its axial extraction domain, although this water may be subsequently replaced by water outside this effective extraction domain. For transient-state conditions the extraction domain can be calculated by (*Hart and Lowery*, 1997):

$$SCED_m = \left[\frac{\sum_{i=1}^{s} V_{wi_{(z)}}}{D_{w_{(z)}}} \frac{1}{\theta_{(z)}} \frac{1}{\pi} \right]^{0.5} \tag{6.4}$$

where $SCED_m$ is the estimated axial-radius of the extraction domain [L] based on the water volume collected by a sampler at depth z [L]. $V_{wi_{(z)}}$ is the ith sample volume at depth z [L^3], s is the total number of samples, $D_{w_{(z)}}$ is the depth of water drained past depth z [L], and $\theta_{(z)}$ is the volumetric water content at depth z [L^3 L^{-3}]. $V_{wi_{(z)}}$, $D_{w_{(z)}}$, and $\theta_{(z)}$ have unique distributions with time, or the sampling period (*Hart and Lowery*, 1997). In a further step, an equation was developed for the extraction domain of a conservative tracer (bromide) in a similar manner to that of Equation 6.4:

$$R_{Br_{(z)}} = \left[\frac{\sum_{i=1}^{n} M_{i_{(z)}}}{L_{Br_{(z)}}} \frac{1}{\theta_{(z)}} \frac{1}{\pi} \right]^{0.5} \tag{6.5}$$

where $R_{Br_{(z)}}$ is the axial-radius based on the bromide collected by the sampler at depth z. Equation 6.5 is based on the mass [M] of bromide collected by the sampler at depth z ($M_{i_{(z)}}$), and the mass of bromide leached past depth z per unit area, $L_{Br_{(z)}}$ [M L^{-2}]. The first term on the right side of Equation 6.4 and 6.5 represents the gross area within the sampler collects soil solution. The second term represents the effective porosity of the soil, which has to be included to give reliable estimates of the extraction domain. *Hart and Lowery* (1997) point out that their calculations of the suction cup extraction domain for steady-state conditions are in good agreement with calculations derived by *Warrick and Amoozegar-Fard* (1977) (data not shown).

6.2 Numerical simulations of suction cup behaviour

The interaction between soil water extraction and flow field has been studied using numerical simulations e.g. *Germann* (1972), *Van der Ploeg and Beese* (1977),*Talsma et al.* (1979), *Barbee and Brown* (1986), *Grossmann* (1988), *Wu et al.* (1995) and *Narasimhan and Dreiss* (1986)), whereby just the approaches of *Germann* (1972), *Van der Ploeg and Beese* (1977) and *Grossmann* (1988) give general information about the impact of soil water extraction on the SCAD and SCED.

Germann (1972) developed a model to predict the local change in water content during water extraction with a suction cup. The basic principles were *Darcy's* law, the water retention curve $\psi_{(\theta)}$, and the hydraulic function $K_{(\psi)}$. Furthermore, isotropy and homogeneity was assumed. The applied suction in the cup as well as the undisturbed matric potential in the soil were given. For the discritization of the flow field a cylindrical and spherical model were available. The results of the simulations for a suction cup with the radius $r_o = 2.5$ cm in one soil are listed in Table 6.3.

Table 6.3: Input data and results of the simulation after *Germann* **(1972) for one soil† and a suction cup radius $r_o = 2.5$ cm.**

Model	*matric potential* [cm]	*applied suction* [cm]	*SCAD t = 600 sec* [cm]	*SCAD t = 3600 sec* [cm]	*extracted water t = 3600 sec* [cm³]
spherical	- 85	150	4.5	12	42
spherical	- 158	300	4.5	11	36
spherical	- 294	500	4.5	10	19
cylindrical	- 158	300	6	20	36

$^\dagger log(K) = -0.961 log(\psi)^2 + 2.678 log(\psi) - 6.906$ *with $R^2 = 0.985$*
$log(\psi) = 0.0003\theta^2 - 0.1619\theta + 7.983$ *with $R^2 = 0.904$*

In general, the simulations showed an increase in the suction cup activity domain (SCAD) with time and a decrease with lower ambient water contents and/or higher applied suctions. The amount of extracted water also decreases with lower ambient water contents and/or higher applied suctions. The increase of the suction cup activity domain with time might be a result of non stationary conditions during water extraction.

Van der Ploeg and Beese (1977) developed a numerical method to calculate soil water flow towards a suction cup in an unsaturated soil based on *Richards'* equation (Equation 3.3). To describe the unsaturated soil water flow in the vicinity of a suction cup *Richards'* equation is rewitten in cylindrical coordinates (r and z). If the origin of the coordinate system is taken at the soil surface on the extended axis of the ceramic cup and if radial flow can be assumed Richards equation can be rewritten as:

$$\frac{\partial \theta}{\partial t} = \frac{\frac{1}{r} \partial \frac{K \partial h}{\partial r}}{\partial r} + \frac{\partial \frac{K \partial h}{\partial z}}{\partial z} \tag{6.6}$$

where θ is the volumetric water content of the soil [L³ L⁻³] , t is the time [T], K is the unsaturated hydraulic conductivity [L T⁻¹], and h is the total hydraulic head [L].

After some simplifications, Equation 6.6 has been solved analytically (*Richards and Richards*, 1962; *Klute et al.*, 1964) or numerically for radial flow toward a suction cup. However, for natural conditions in heterogeneous soils, only numerical techniques can provide adequate solutions. *Van der Ploeg and Beese* (1977) showed that the cumulative amounts of extracted water were always higher than the corresponding calculation for the undisturbed percolation, which they assumed to be an indicator for an extraction domain

of the suction cup. They also observed that the amount of extracted water increased with higher applied suctions, and that the relationship between applied suction and the amount of extracted water was not linear. Finally, the authors conclude, that no general valid conclusions for the suction cups activity domain can be given from the few model calculations.

Table 6.4: Boundary, initial conditions, and results of the numerical simulation for a gravel and loamy clay soil after *Grossmann* **(1988). The extraction domain (here in length units as a radius of the SCED) of the suction cup is calculated in analogy to the 50-day-line of drinking-water-sources for an amount of 200 ml of extracted water.**

Material	*pressure head* ψ *[cm]*	*applied suction [cm]*	*irrigation [mm d^{-1}]*	*extracted water [ml d^{-1}]*	*SCSA [cm]*	*SCED [cm]*
gravel	-20	100	5.00	3221	20	13
	-20	400	5.00	5029	25	16
	-100	100	0.05	13.5	25	16
	-100	400	0.05	41.2	45	20
loamy clay	-40	100	5.10	1394	15	7
	-40	400	5.10	2759	20	9
	-400	100	0.10	12.6	25	10
	-400	400	0.10	31.6	40	12

Grossmann (1988) used a numerical model adapted from *Kölling* (1987) to simulate the suction cup extraction domain, sampling area and the dividing streamline under stationary conditions. The boundary, initial condition, and results for two different materials (gravel and loamy clay) are shown in Table 6.4. The results indicate that the sampling area depends on the matric potential in the soil, and thus on the water content, whereby lower water contents result in larger sampling areas for both soils. A larger suction cup extraction domain was simulated for the gravel due to the lower water content. *Grossmann* (1988) also pointed out that the influx of water to the suction cup is derived from the overlying areas of the cup.

Chapter 7

Results

7.1 Numerical simulation of suction cup behaviour

For the simulation of the soil water fluxes the finite element code HYDRUS-2D (*Simunek et al.*, 1999) was used (see Chapter 4.7), which numerically solves the *Richards'* equation (Equation 3.3) for saturated-unsaturated water flow. Various simulations with changing boundary conditions were conducted to define the boundary conditions affecting the suction cup influence. A first set of simulations assumed stationary conditions, a constant *Darcy* flux, J_w, and applied suction in the cup. The second set assumed differences in hydraulic properties of the surrounding soil, while the third set pertained a random distribution of the hydraulic properties within the soil column. Finally, simulations with an atmospheric upper boundary (rainfall and evaporation) were performed. Water flow and solute transport are simulated in a two-dimensional field 200 cm wide and 200 cm deep. The discretization is non-equidistant with a smaller nodal distance in the vicinity of the suction cup (total number of nodes = 40158). The suction cup had an outer radius of 2.4 cm and was implemented in the center of the flow domain. A cross-section of the flow domain is shown schematically in Figure 7.1. The boundary condition of the suction cup was represented as a prescribed head. Infiltration was uniform and constant in time through the upper boundary. The lower boundary was chosen to be a seepage face which is typical for zero-tension lysimeters. No-flow boundary condition were imposed on the remaining boundary nodes. For the simulation three different soils - a clay loam, a sandy clay, and a sand were chosen from the HYDRUS soil cataloque. The hydraulic properties of the soils and the suction cup are listed in Table 7.1 and are shown in Figure 7.2.

Table 7.1: Hydraulic properties of the soil and suction cup.

Soil type	θ_r $[cm^3 cm^{-3}]$	θ_s $[cm^3 cm^{-3}]$	α $[cm^{-1}]$	n $[-]$	Ks $[cm\ h^{-1}]$
clay loam	0.095	0.41	0.0190	1.31	2.600×10^{-1}
sand	0.045	0.43	0.1450	2.68	29.7×10^{-0}
sandy clay	0.100	0.38	0.0270	1.23	2.000×10^{-1}
suction cup	0.001	0.50	0.0005	2.80	2.394×10^{-3}
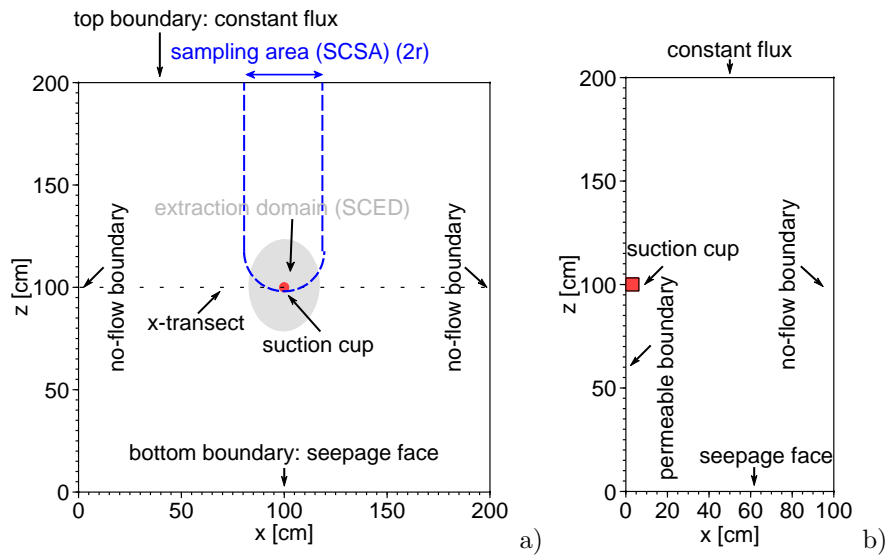
Figure 7.1: Cross-section of the flow domain with a suction cup. a) horizontal plane with graphical definitions of the suction cup extraction domain (SCED), and suction cup sampling area (SCSA). b) axisymmetrical flow domain.
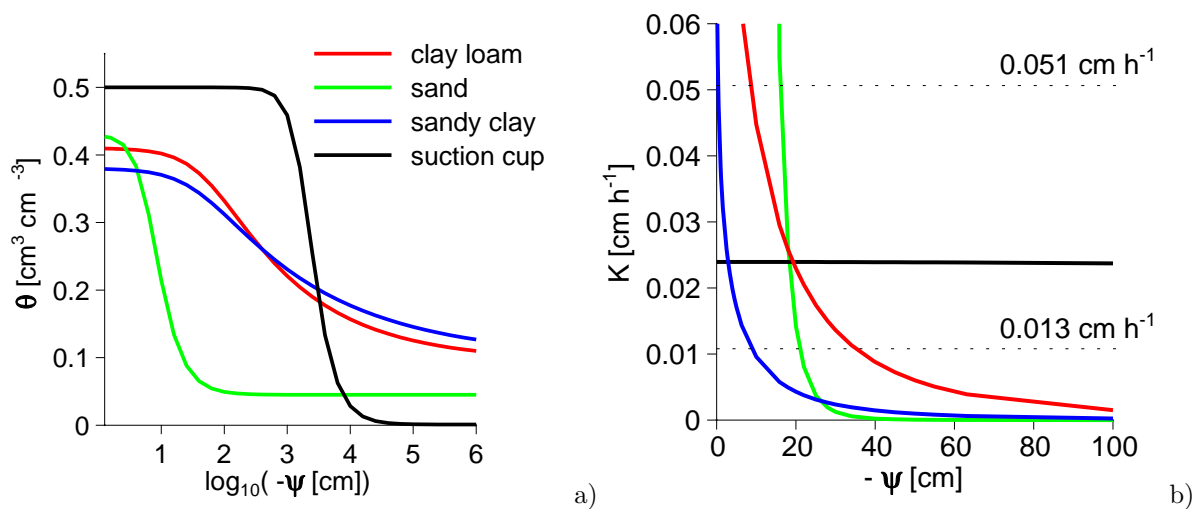
Figure 7.2: Hydraulic properties of the soils and suction cup. a) water retention function and b) hydraulic conductivity function.

The applied suction inside the cups as well as the potential differences (picked at the border of the flow field at the depth of the suction cup) of the matric potentials between a simulation with and without applied suction are listed in Table 7.2. The initial condition

Table 7.2: Applied suction in the suction cups and potential differences in [cm].

	applied suction [cm]	potential difference [cm]	
		infiltration rate = 0.013 cm h^{-1}	infiltration rate = 0.051 cm h^{-1}
clay loam	30[†] , 50, 100, 300, 600, and 1000	20, 70, 270, 570, and 970	22, 42, 92, 292, 592, and 992
sand	30, 50, 100, 300, 600, and 1000	10, 30, 80, 280, 580, and 980	14, 34, 84, 284, 584, and 984
sandy clay	30, 50, 100, 300, 600, and 1000	21, 41, 91, 291, 591, and 991	29, 49, 99, 299, 599, and 999
clay loam[‡]	30, 50, 100, 300, 600, and 1000		
sand[‡]	30, 50, 100, 300, 600, and 1000		
sandy clay[‡]	30, 50, 100, 300, 600, and 1000		

[†] for infiltration rate = 0.051 cm h^{-1}

[‡] Miller-Miller-similar medium with standard deviation = 0.025 and correlation length λ = 10 cm

was a hydrostatic equilibrium with the groundwater table at the lower boundary. The simulation period was chosen to be 9000 hours, which was sufficiently long to reach a stationary flow field for all cases. The global water mass balance error was always less than one percent for all time-steps.

The sampling area and the extraction domain of the suction cup were calculated by tracking the streamlines using particles. In total 2000 particles were uniformly applied at the soil surface.

The sampling area was determined by assigning the initial start position at the soil surface to each particle. This procedure backtraced the initial position of particles trapped in the suction cup. To determine the suction cup extraction domain (SCED), the water flow field was inverted and 2000 particles were released from the suction cup outer surface. The end positions of the particles then delineate the extraction domain as a function of the extraction time.

Local scale heterogeneity in hydraulic properties was generated using Miller-Miller scaling theory (*Miller and Miller*, 1956). The soil is homogeneous on a macroscopic scale but heterogeneous at a microscopic scale (*Miller and Miller*, 1956). This medium is characterized by a reference state $[\psi_m^*(\theta), K^*(\theta)]$ and a single scaling relation for the hydraulic functions. For a Miller-similar medium the scaling relation between a point with characteristic length, χ, and the reference state, χ^*, is given by *Sposito and Jury* (1990).

$$\psi_m\left(\theta\right)\chi = \psi_m^*\left(\theta\right)\chi^*, \qquad K\left(\theta\right)/\chi^2 = K^*\left(\theta\right)/\chi^* \qquad (7.1)$$

Describing the variability in hydraulic properties in soil is thus reduced to define the reference state and specifying spatial correlation structure of χ, which is determined by an autocovariance function. A detailed description of the implementation of the Miller-similar medium in a numerical model is given e.g. by *Roth* (1995). The scaling factors were log normal distributed. The logarithm of the scaling factor, f, had variance, σ_f^2,

and correlation length, λ_f, which is the characteristic length at the microscopic scale. For the autocovariance model, $C_{(x)}$, an exponential model was used.

$$C_{(x)} = \sigma_f^2 \exp\left(-\frac{|x|}{\lambda_f}\right) \tag{7.2}$$

Two scaling parameters may be used to define a linear model of the actual spatial variability in the soil hydraulic properties as follows *Vogel et al.* (1991).

$$K_{(\psi)} = \alpha_K K_{(\psi^*)}^* \tag{7.3}$$

$$\psi = \alpha_\psi \psi^* \tag{7.4}$$

For the most general case α_h and α_K are mutually independent scaling factors for the pressure head and the hydraulic conductivity, respectively. The correlation length λ_f in x and y direction was set either to 5 or 10 cm, and $\sigma_f^2 = 0.0625$, respectively.

Note that the applied suction in the cup is defined as the absolute value of the pressure head, $|h|$.

Suction cup activity domain (SCAD)

The suction cup activity domain (SCAD) for the clay loam, sandy clay and sandy soil with various applied suctions (see Tabel 7.2) and a constant infiltration rate $J_w = 0.013$ cm h^{-1} is shown in Figure 7.3. As expected, the highest matric potential differences occur in the direct vicinity of the suction cup and decline to the periphery. Increasing the applied suctions results in larger differences in matric potential. Suctions larger than 300 cm result in only small changes in matric potential differences. Therefore, the SCAD does not change much. In case of the sandy soil changes in matric potential differences are hardly notable for all applied suctions. The matric potential differences for the sandy soil are somewhat smaller than for the sandy clay and largest for the clay loam. If we look at the hydraulic conductivity function (Figure 7.2 b) and compare the hydraulic conductivities for the applied suction higher than 30 cm a ranking of the three soils occurs with the lowest conductivities for the sandy soil, and highest for the clay loam. If these results are compared with the activity domain of the three soil types, a dependency is obvious. The activity domain is the smallest for sandy soil, slightly larger for sandy clay, and largest for clay loam. It becomes clear that the maximum activity domain of the suction cup is primarily determined by the hydraulic conductivity of the soils. In general, the maximum of the activity domain will be reached for an applied suction where the first derivative of the hydraulic conductivity function converges to zero. This is reached at matric potentials less than 30 cm, 60 cm, and 100 cm for sand, sandy clay, and clay loam, respectively. The limiting factor for the activity domain of the suction cup is, therefore, the hydraulic conductivity at ambient matric potentials. Higher hydraulic conductivities result in larger activity domains for a suction cup. The convergence of the SCAD up to the maximum SCAD also depends on the hydraulic conductivity for ambient matric potentials. Larger changes of the SCAD occur with higher changes in hydraulic conductivity. The SCAD for a higher infiltration rate ($J_w = 0.051$ cm h^{-1}) are plotted in Figure 7.4. As expected the same ranking is observed for the various soils
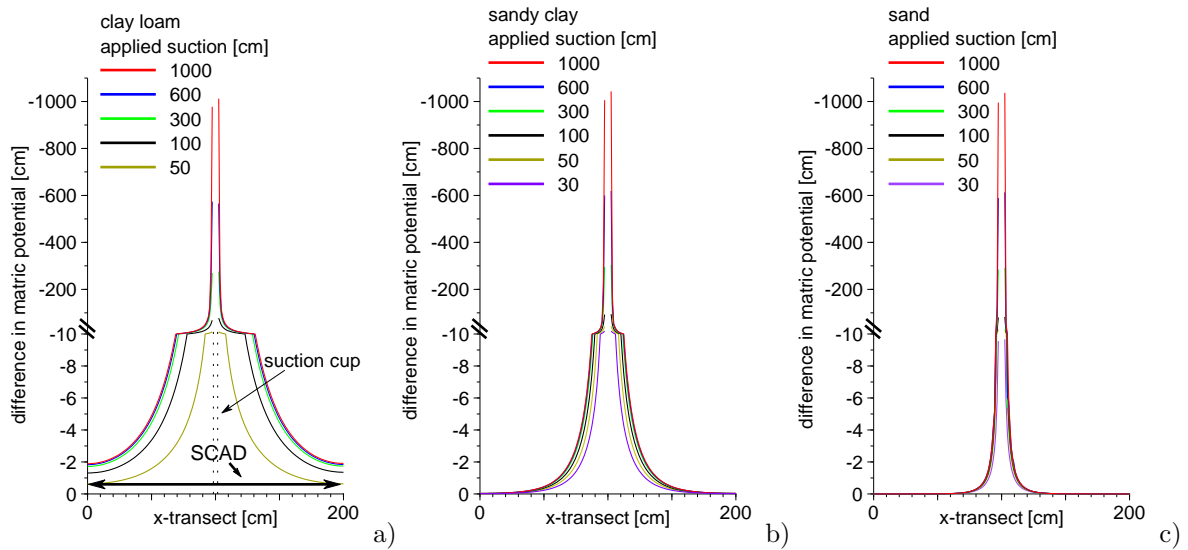
Figure 7.3: Suction cup activity domain (SCAD) on a horizontal transect through the suction cup plotted as matric potential differences for all applied suctions. Upper boundary constant flux $J_w = 0.013$ cm h^{-1}. a) clay loam, b) sandy clay, and c) sand. Note that the ordinate has been split to visualize small differences in the periphery of the cup.

(largest for the clay loam, slightly smaller for the sandy clay, and smallest for the sandy soil). In comparison to the lower infiltration rate ($J_w = 0.013$ cm h^{-1}) smaller absolute changes are observed. It seems that higher infiltration rates and higher matric potential gradients between undisturbed soil and applied suction lead to smaller changes in matric potential differences due to a better additional supply of water to the cup.
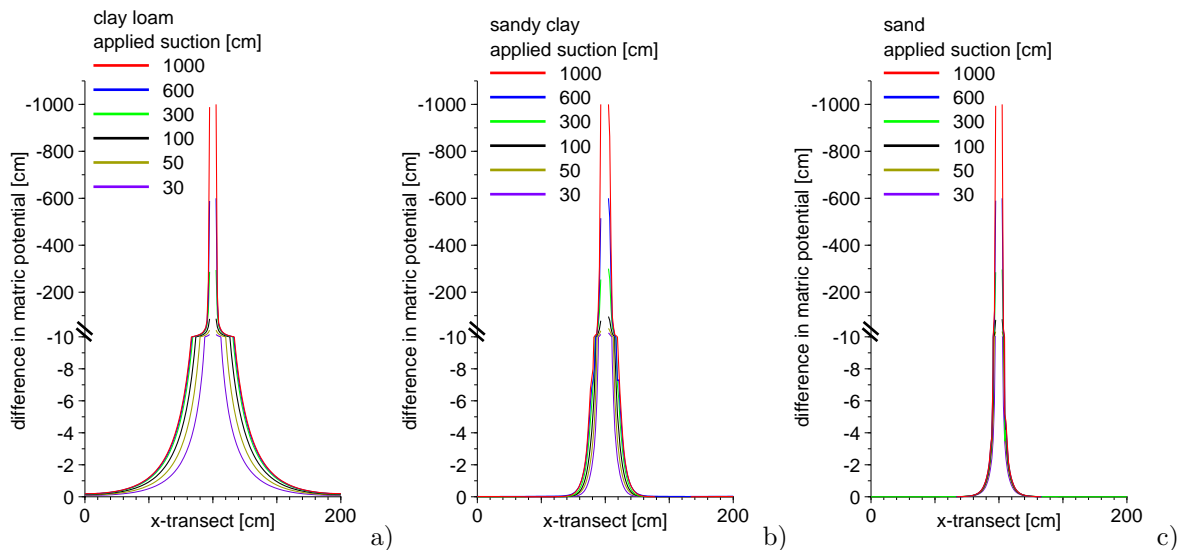
Figure 7.4: Same as for Figure 7.3 but with a constant flux $J_w = 0.051$ cm h^{-1}.

If we compare the activity domain of the homogeneous medium to that of the simu-
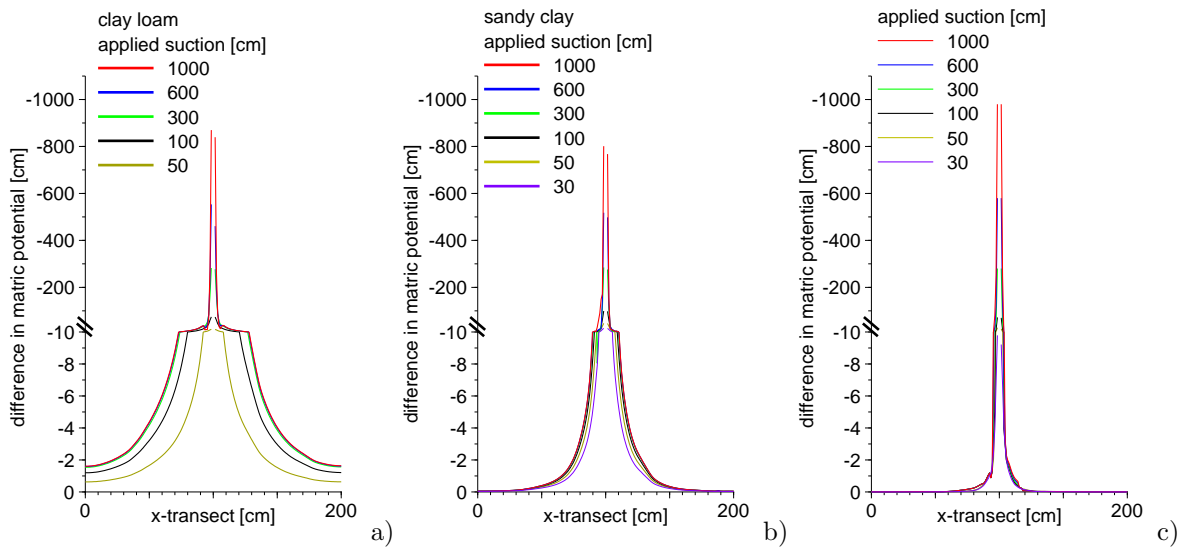
Figure 7.5: Same as for Figure 7.3 but with a constant flux $J_w = 0.013$ cm h^{-1} in a heterogeneous Miller-Miller-similar medium ($\lambda_f = 10$ cm and $\sigma_f^2 = 0.0625$).

lated heterogeneous Miller-Miller-similar medium (see Figure 7.5 and 7.6), only slightly smaller activity domains were found for the heterogeneous cases for all soils and applied suctions. In general, the underlying heterogeneous hydraulic structure seems to play a minor role in the differences in matric potential due to the fact that the gradient of the total head is the driving force for water flow which will be minimized. Therefore, heterogeneity does not directly represent matric potential distribution, in comparison to the water content.

Suction cup sampling area (SCSA)

Figure 7.8 shows the suction cup sampling area ($2r$) as a function of applied suction for the three soils under stationary conditions with varying applied suctions (from 30 to 1000 cm), both for a homogeneous and heterogeneous medium. In general, the sampling area increases with increasing suction in the cup and reaches a maximum value for suctions larger than 300 cm. If we compare the sampling area for each set of simulations, the clay loam shows the largest SCSA, and the sand the smallest. These results confirm the findings of *Warrick and Amoozegar-Fard* (1977), who found the same ranking (see Figure 6.3). For suction smaller than 50 cm this ranking is not valid (Figure 7.8 a and b), because differences in ambient matric potential for the three soils are not negligble for the cases without suction. The hydraulic gradient of the sandy soil, sandy clay and clay loam are 30, 41, and 20 cm, respectively. Simulations with the same hydraulic gradient showed comparable results in ranking even for low applied suctions.

Comparison of the two infiltration rates indicated that the sampling area decreases for increasing fluxes. This decrease can be ascribed to the smaller suction cup activity domains shown in Figure 7.3 and 7.4. The simulated soil heterogeneity does not influence the sampling area and this for all soils.

To confirm these results the sampling area is plotted against the normalized matric flux potential (NMFP), which is the integral of the hydraulic conductivity (K) function
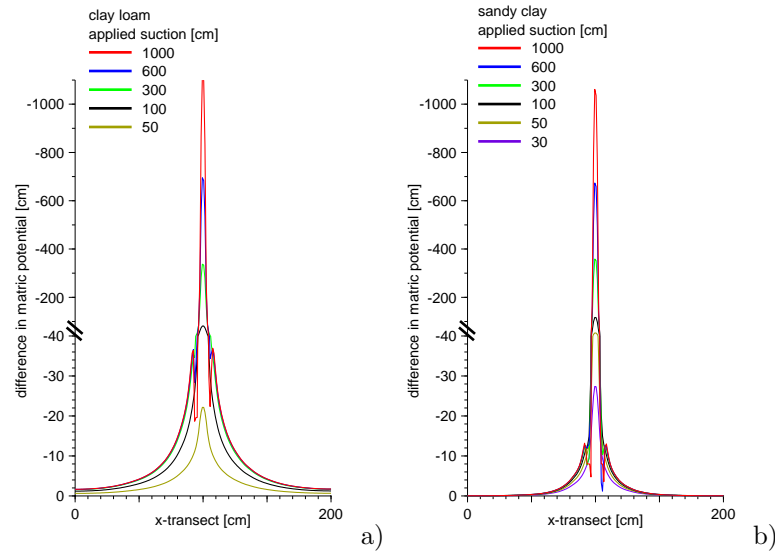
Figure 7.6: Same as for Figure 7.3 but with a constant flux $J_w = 0.013$ cm h^{-1} in a heterogeneous Miller-Miller-similar medium ($\lambda_f = 5$ cm and $\sigma_f^2 = 0.0625$).

from matric potential at the given infiltration rate to applied suction divided by the flux rate (Figure 7.7).

$$NMFP = \int_{\psi_{J_w} \, cm \, d^{-1}}^{\psi = applied \, suction} K_{(h)} dh / J_w \qquad (7.5)$$

The normalized matric flux potential combines the hydraulic properties of the soil, the applied suction in the cup, and the given infiltration rate at the upper boundary. In Figure 7.7 the normalized matric flux potential is plotted versus the sampling area. The plot shows that no unique characteristic for all soils is deducible, but for each soil and flow rate we find an estimation of the SCSA by changes of applied suction in the cup.

In Figure 7.9 the breakthrough of the particles in the suction cups (travel time) indicates a faster arrival of the particles directly applied above the cup and a slower breakthrough for particles trapped at the bottom of the cup compared to the undisturbed flow field (no suction applied within the cup). As a result, an earlier arrival and a pronounced tailing occurs compared to an undisturbed fictive point at the same depth. As shown in Figure 7.10, the arrival time in the cup, as well as the amount of trapped particles depends on the applied suction in the cup, because higher potential gradients induced by applied suction increase the pore-water velocities. The pronounced tailing of the particle breakthrough is a result of a longer travel distance of the particles trapped at the bottom of the cup.

Apart from the activity domain in the direct vicinity of the cup, the extraction of soil water influences also the arrival of particles deeper down in the profile. As shown in Figure 7.9 the arrival of particles at the lower boundary of the flow domain is decelerated if water was extracted. Particles trapped at the lower boundary directly below the suction cup are slower (by a factor of two) than the undisturbed particle flow (see Figure 7.9) due to deflection of streamlines in the flow domain by water extraction of the suction cup. The magnitude of deceleration at the bottom of the flow field depends on the
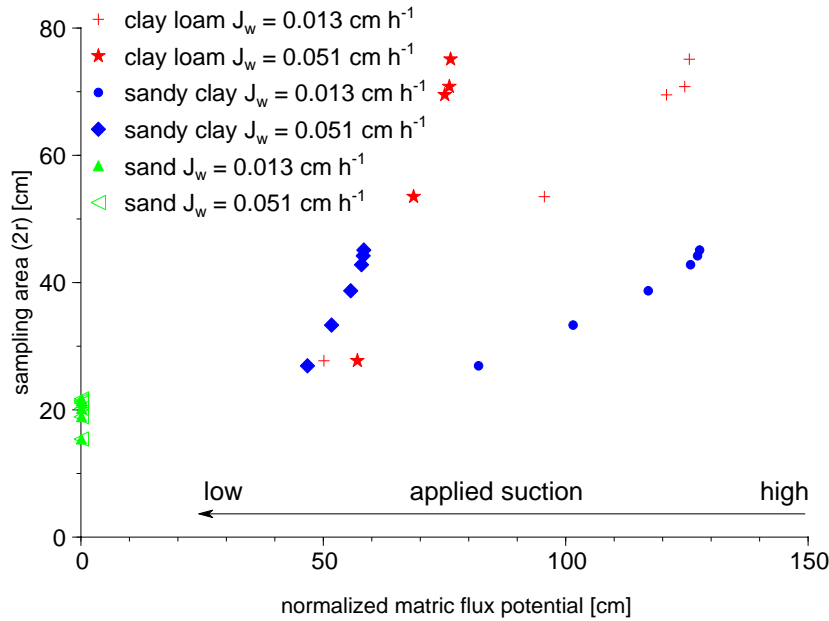
Figure 7.7: Normalized matric flux potential (NMFP) for two infiltration rates J_w = 0.013 cm h^{-1} and 0.051 cm h^{-1} in correlation with the SCSA for a clay loam, sandy clay and sandy soil. NMFP calculated using Equation 7.5.

infiltration rate and the applied suction, whereby higher applied suctions result in a larger deceleration and a more pronounced tailing in the arrival time. This fact has to be taken into account when lysimeter or column experiments were equipped with suction cups operating in a continuous mode.

Suction cup extraction domain (SCED)

The suction cup extraction domain (SCED) is plotted in Figure 7.11 and 7.12 as a function of extraction time for two applied suctions, 100 and 1000 cm, respectively. The infiltration rate for both cases was set to $J_w = 0.013$ cm h^{-1}. The activity domain is also shown as differences in matric potential with smallest changes for an applied suction of 100 cm than for the higher applied suction of 1000 cm. Both figures clearly show that the SCED increases with increasing extraction time. If the time will be set to infinity the SCED will eventually reach the soil surface and than delinieates the SCSA. The geometry of the SCED differs between both cases. The case with larger suction leads to more pronounced water extraction from below the cup.

The SCED for water flow to the cup predicted by the simulations has not a static geometry and, therefore, a comparison with the analytical solutions of the normalized Stokes stream function (*Warrick and Amoozegar-Fard*, 1977) (see Figure 6.3) and other suction cup extraction domains (e.g. Equations after *Hart and Lowery* (1997)) are not applicable. It should also be noted that the source region for water extracted by the cup will be smaller and out of a different region than the activity domain delinated by the deformation of the water content field (see Figure 7.11 and 7.12).
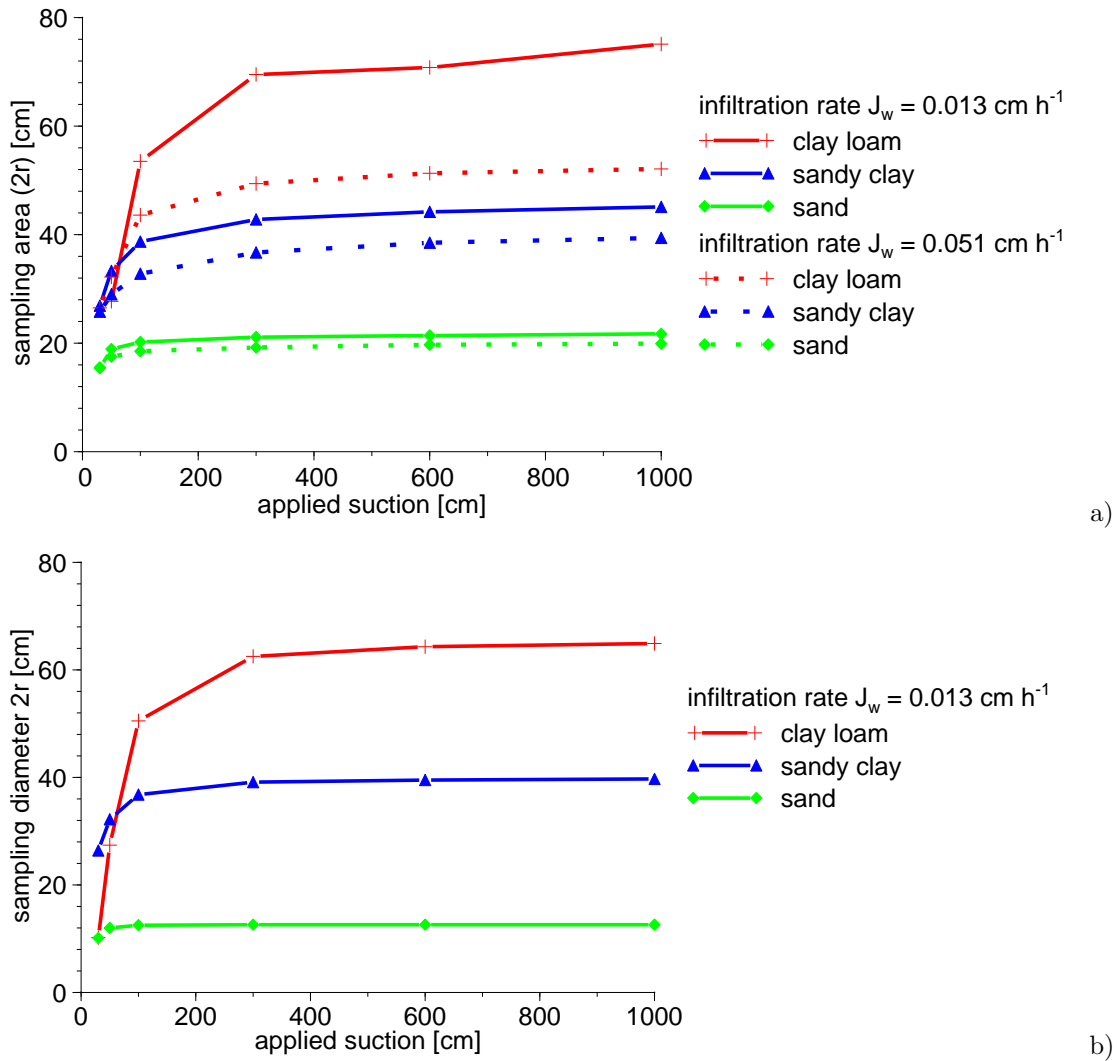
Figure 7.8: Suction cup sampling area (SCSA) (2r) for stationary conditions for a clay loam, sandy clay, and sand for all applied suctions. a) for a homogeneous medium and a constant flux $J_w = 0.013$ cm h^{-1}, and a constant flux $J_w = 0.051$ cm h^{-1} and b) a heterogeneous Miller-Miller-similar medium ($\lambda_f = 10$ cm and $\sigma_f^2 = 0.0625$) and a constant flux $J_w = 0.013$ cm h^{-1}.
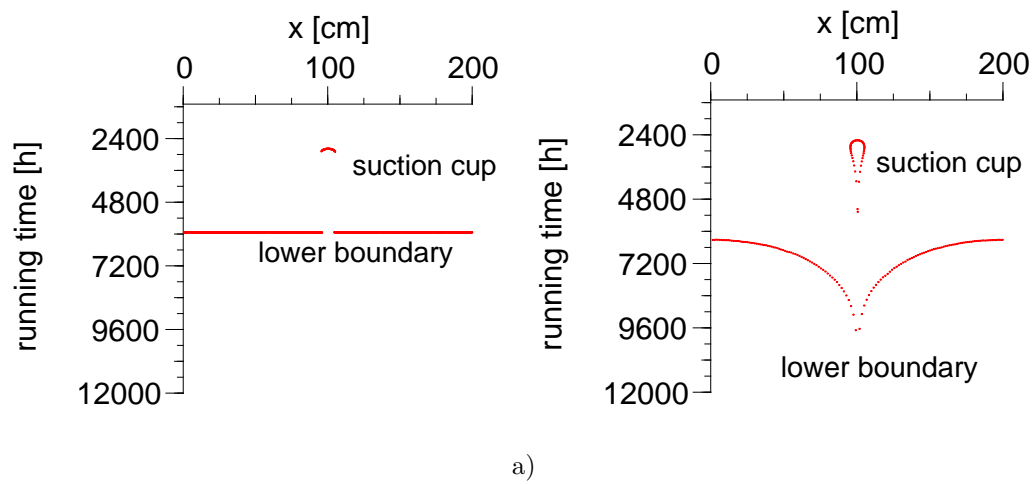
Figure 7.9: Travel time of all particles trapped either in the suction cup or at the lower boundary for a simulation in a clay loam with constant flux $J_w = 0.013$ cm h^{-1} for a) no applied suction in the cup and b) an applied suction of 100 cm in the cup.
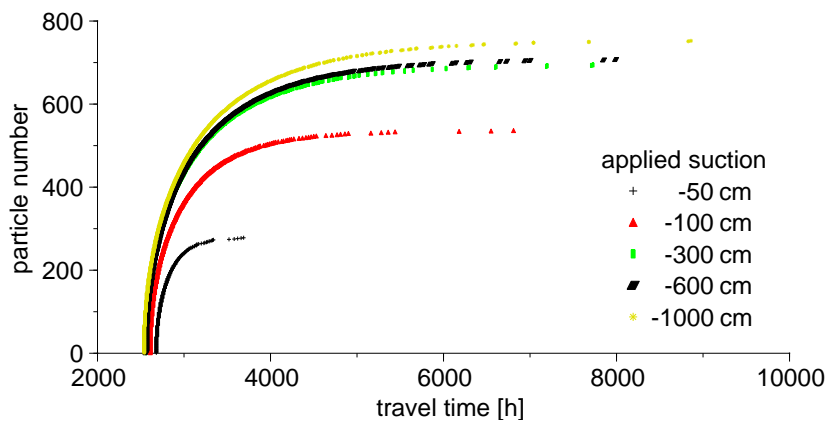
Figure 7.10: Travel time for all particles trapped in the suction cup for a simulation in a clay loam with constant flux $J_w = 0.013$ cm h^{-1} and applied suctions of 50, 100, 300, 600, and 1000 cm in the cup.
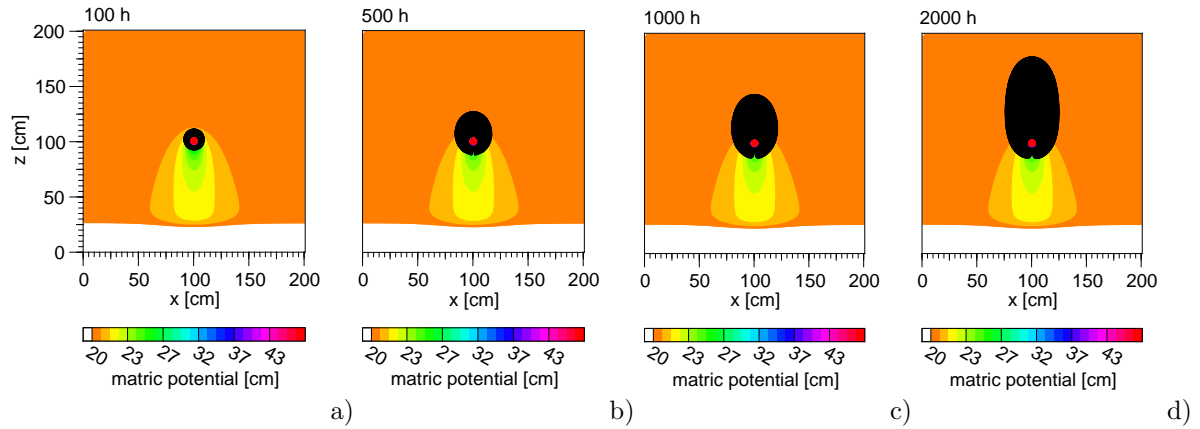
Figure 7.11: Suction cup activity domain (SCAD) (background) and suction cup extraction domain SCED (black contour) for a clay loam with constant flux $J_w = 0.013$ cm h^{-1} and an applied suction of 100 cm for a travel time of a) 100, b) 500, c) 1000, and d) 2000 hours.

7.1.1 Amount of extracted water

For comparison of the amount of extracted soil water by suction cups an axisymmetrical simulation in a homogeneous two-dimensional field 100 cm wide and 200 cm deep was conducted. A cross-section of the axisymmetrical flow domain is shown schematically in Figure 7.1 b). The suction cup with a diameter $r_o = 2$ cm was installed on the left side of the cylinder at a depth of 100 cm. Due to the axisymmetrical simulation mode, the left boundary conditions was changed to be a flux boundary condition. This allows a 3-dimensional simulation by rotation of the 2-D results on the permeable axis. The discretization is non-equidistant with smaller nodal distance in the vicinity of the cup (total number of nodes = 12411). A uniform and constant infiltration was imposed with $J_w = 0.013$ cm h^{-1}. At the lower boundary a seepage face was imposed. Simulations
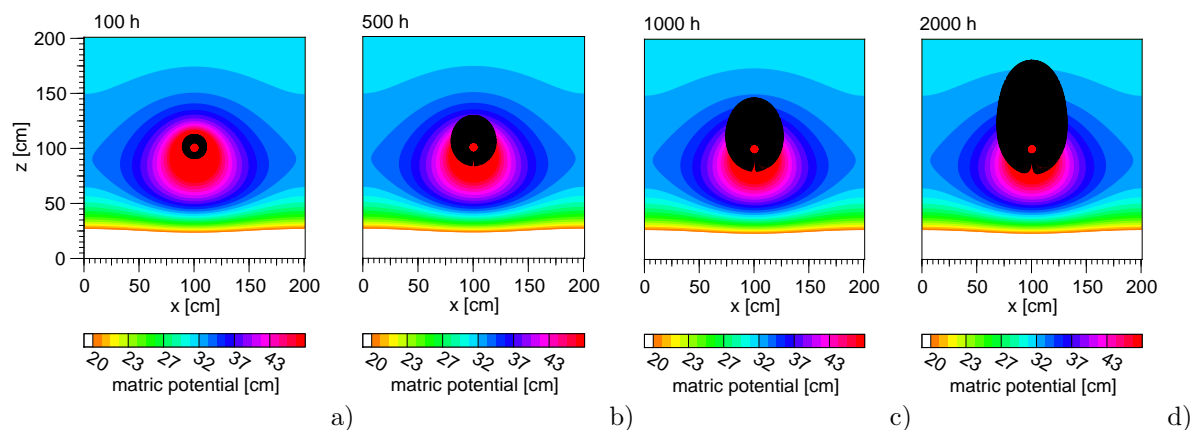
Figure 7.12: Suction cup activity domain (SCAD) (background) and suction cup extraction domain SCED (black contour) for a clay loam with constant flux $J_w = 0.013$ cm h^{-1} and an applied suction of 1000 cm for a travel time of a) 100, b) 500, c) 1000, and d) 2000 hours.

were performed for the clay loamy, the sandy clay, and the sandy soil. Soil and suction cup properties are listed in Table 7.1. Initial conditions in matric potential were set to be 30 cm at the upper boundary and water saturation at the lower boundary and a linear increase inbetween. The boundary condition of the suction cup was represented as a prescribed head with 30, 50, 100, 300, 600 and 1000 cm, respectively. The axisymmetrical simulations were performed to compare the results with the analytical solutions (see Chapter 6.1) as well as to determine the extracted water in dependency of the applied suction.
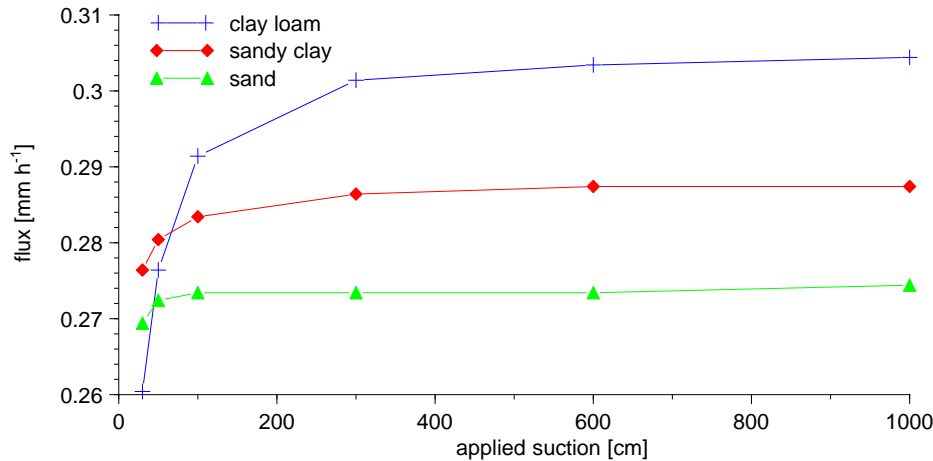
Figure 7.13: Time dependent extraction rates $[\mathrm{mm\ h^{-1}}]$ of the suction cup for a constant flux of $J_w = 0.013$ cm $\mathrm{h^{-1}}$ in different soils (clay loam, sandy clay and sand soil) and various applied suctions (30, 50, 100, 300, 600 and 1000 cm). Note that steady state is reached after $\sim$ 300 h for all cases.

Annex A.9 shows the extraction rates of the suction cup with time for various soils. In all cases the stationary conditions are reached after 300 h of simulation. The changes of the extraction rate before this stage are due to changes in water content and matric potential within the soil column before steady-state. It is noticeable that the highest extraction rates occur with highest applied suctions in the suction cups due to the higher imposed pressure head gradients (Figure 7.13). The smaller increase of the extraction rate with higher pressure head gradients (300 to 1000 cm) are due to the reduction in hydraulic conductivity for the ambient matric potential. Highest fluxes are detectable for the clay loam due to the higher water content for the applied flux of $J_w = 0.013$ cm $\mathrm{h^{-1}}$. Lowest fluxes occur in the sandy soil due to the lower water content for the same flux.

7.1.2   Changes of cup material properties

To get information on the influence of the hydraulic properties of the suction cup on the amount of extracted water and sampled solute concentrations, steady-state simulations were conducted with changing the saturated hydraulic conductivity of the suction cup. A cross-section of the flow domain is shown schematically in Figure 7.1 a). The

discretization is non-equidistant with smaller nodal distance in the vicinity of the cup (total number of nodes = 8921). Infiltration was uniform and constant in time through the upper boundary with $J_w = 0.013$ cm h^{-1}. At the lower boundary a seepage face was imposed. As the surrounding soil a clay loam was chosen (hydraulic properties listed in Table 7.1). The suction cup saturated hydraulic conductivity was set to $K_s = 0.01$, 0.02394, 0.04, 0.2394, 0.26 and 0.52 cm h^{-1}, resprectively. θ_r, θ_s, α, and n are listed in Table 7.1. Initial conditions in matric potential were set to be -30 cm at the upper boundary and water saturation at the lower boundary and a linear increase inbetween. The flow domain was initially void of tracer. The boundary condition of the suction cup was represented as a prescribed head of 50 cm. A conservative tracer pulse of 9.1 g was applied in 1 hour after 996 h at the soil surface, which was sufficiently long to reach a stationary flow field in all cases. The dispersivity was set to 5 cm in longitudinal and 1 cm in transversal direction. The diffusion coefficient was set to 0.00074 cm^2 h^{-1}. The water extraction rate and the sampled solute in mass per length of suction cup [g cm^{-1}] were plotted in Figure 7.14. The results reflect the influence of the suction cup hydraulic properties on the extraction rates and sampled masses, whereby lower saturated hydraulic conductivities of the suction cup led to smaller amounts of extracted water and sampled masses. If the hydraulic conductivity of the cup is set to the hydraulic conductivity of the surrounding soil, or even higher, just small changes are observable. For this case, the hydraulic properties of the surrounding soil limits the extraction rates of the suction cup. The variability of extracted soil water and the solute masses in dependance of the hydraulic conductivity of the suction cup has to be taken into account if suction cups were used in field and lysimeter studies. But, it is also questionable whether these rather small effects are detectable in field soils where other sources of error, like defects in suction cups, measurement errors, and breakdown of the suction supply occurs. Also soil heterogeneity will influenece the amount of extracted masses and water (see Chapter 7.1.3).
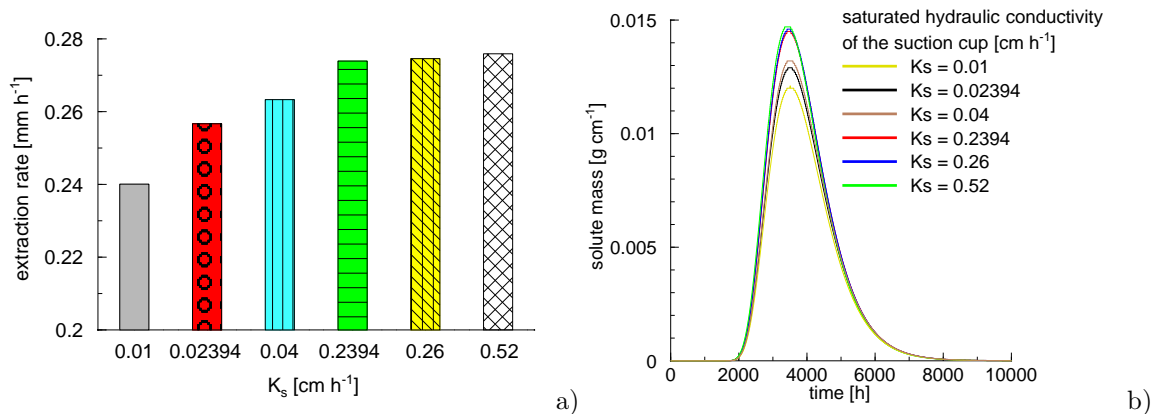
Figure 7.14: a) Water extraction rates mmh^{-1} for different K_s-values of the cup and b) solute masses per length of suction cup extracted by a cup under stationary conditions for different K_s-values of the cup. Note: All simulations in a clay loam.

7.1.3   Solute extraction in a heterogeneous medium

Simulations in a heterogeneous soil were conducted to characterize the influence of the soil heterogeneity on the amount of extracted soil water and the solute breakthrough in the suction cup. Water flow is simulated in a two-dimensional field 100 cm wide and 100 cm deep with a suction cup (outer radius $r_o = 2.4$ cm) implemented in 40 cm depth. The discretization is non-equidistant with smaller nodal distances in the vicinity of the suction cup (total number ~ 20000). Infiltration was uniform and constant in time through the upper boundary ($J_w = 0.4$ cm h^{-1}). The lower boundary was chosen to be a free drainage unit gradient. No-flow boundary conditions were imposed on the remaining boundary nodes. To obtain informations about the matric potential in a depth of 40 cm, ten observation nodes were picked out which reflect different positions of the tensiometers. The boundary condition of the suction cup was represented as a prescribed head with an applied suction of 60 cm. For the soil a clay loam was chosen. The clay loam and suction cup hydraulic parameters are listed in Table 7.3.

Table 7.3: Hydraulic parameters for the soil and suction cup.

	θ_r $[cm^3 cm^{-3}]$	θ_s $[cm^3 cm^{-3}]$	α cm^{-1}	n $[-]$	K_s $cm\,h^{-1}$
clay loam	0.095	0.436	0.0064	1.353	1.8629
suction cup	0.001	0.500	0.0005	2.800	0.0133

Table 7.4: Scaling parameters (variance, σ_f^2, and correlation length, λ_f, for the Miller-Miller-similar soils and applied suction in the cup [cm] for the various sets of simulations.

set	σ_f^2 $[cm]$	λ_f $[cm]$	*applied suction* $[cm]$
1-1	-	-	-
1-2	-	-	60
2-1	0.09	20	-
2-2	0.09	20	60
3-1	0.09	20	-
3-2	0.09	20	60
4-1	0.09	20	-
4-2	0.09	20	60

At the initial stage the matric potential was set to -28 cm for all nodes. The simulation period was chosen to be 1000 h, which was sufficiently long to reach a stationary flow field in all cases. A bromide tracer was applied for one hour after 200 h with a total amount of 152 g m^{-2}. The global water and solute mass balance error was always less than one percent. Local scale heterogeneity in hydraulic properties was generated using

Miller-Miller scaling theory (*Miller and Miller*, 1956). The scaling parameters were set to $\sigma_f^2 = 0.9$ and $\lambda_f = 20$ cm and the applied suction in the cup. The input paremeters for the different sets of simulations are listed in Table 7.4.

To visualize the water flow channels in the flow domain for each set of simulation the absolute water flux $|J_w|$ was calculated and is plotted in Figure 7.15. The underlying heterogeneous structure results in regions with pronounced percolation and in regions with less percolation. As a result the suction cup is located either in a preferred flow channel or outside one of these structures. Single spots with high water fluxes in direct vicinity of the suction cup can be backtraced to uncertainties in the gridding procedure. As a result of the soil homogeneity no flow channels can be detected in simulation 1-1. In contrast to simulation 1-1 the suction cup in simulation 2-1 and 3-1 is located in a region with higher absolute water fluxes. The suction cup in simulation 4-1 is located in a region with the lowest fluxes. In general, the differences between the simulations are rather low due to the limits of the input of scaling parameters in the Hydrus-2D implemented random field generator (no variance, σ_f^2, and correlation length, λ_f, larger 0.09 and 20 cm, can be specified in the code). The bromide breakthrough of one realization (3-2)

Table 7.5: Mass recovery, 1. moment, and σ^2 for the various sets of simulations.

set	*recovery* [%]	τ_1 [T]	σ^2 [T^2]
1-2	357.7	247.7	630.4
2-2	354.7	246.2	624.3
3-2	358.4	246.2	604.1
4-2	357.1	249.1	657.2

and the fit of the CDE using CXTFIT (*Toride et al.*, 1999) is plotted in Figure 7.17. Due to the pronounced tailing of the breakthrough as a result of the deformation of the streamlines, the CDE fit is not in good agreement with the observed data. Therefore, the breakthrough curves were described in the following using the methods of moments, whereby the 1. moment is related to the mean pore water velocity, v, and the σ^2 to the dispersivity, λ. The observed breakthrough curves with the calculated 1. moment and σ^2 are plotted in Figure 7.16 and the parameters are listed in Table 7.5. Mass recoveries, 1. moment, and σ^2 from the samplers in the various flow fields did not differ much due to the small differences in absolute water flux $|J_w|$. However, small variabilities are detectable, depending on the location of the suction cup in the flow field. If we assume that larger σ_f^2 will lead to larger differences in the absolute water flux, $|J_w|$, the variability in the breakthrough curves will become larger too. As stated above, a pronounced tailing of the solute breakthrough via suction cups is visible in Figure 7.17 compared to the fitted breakthrough with CXTFIT (*Toride et al.*, 1999). This result is in accordance with the finding of the particle tracking (Chapter 7.10) due to the deformation of the streamlines and, therefore, a longer travel path of the solute sampled from below the cup.
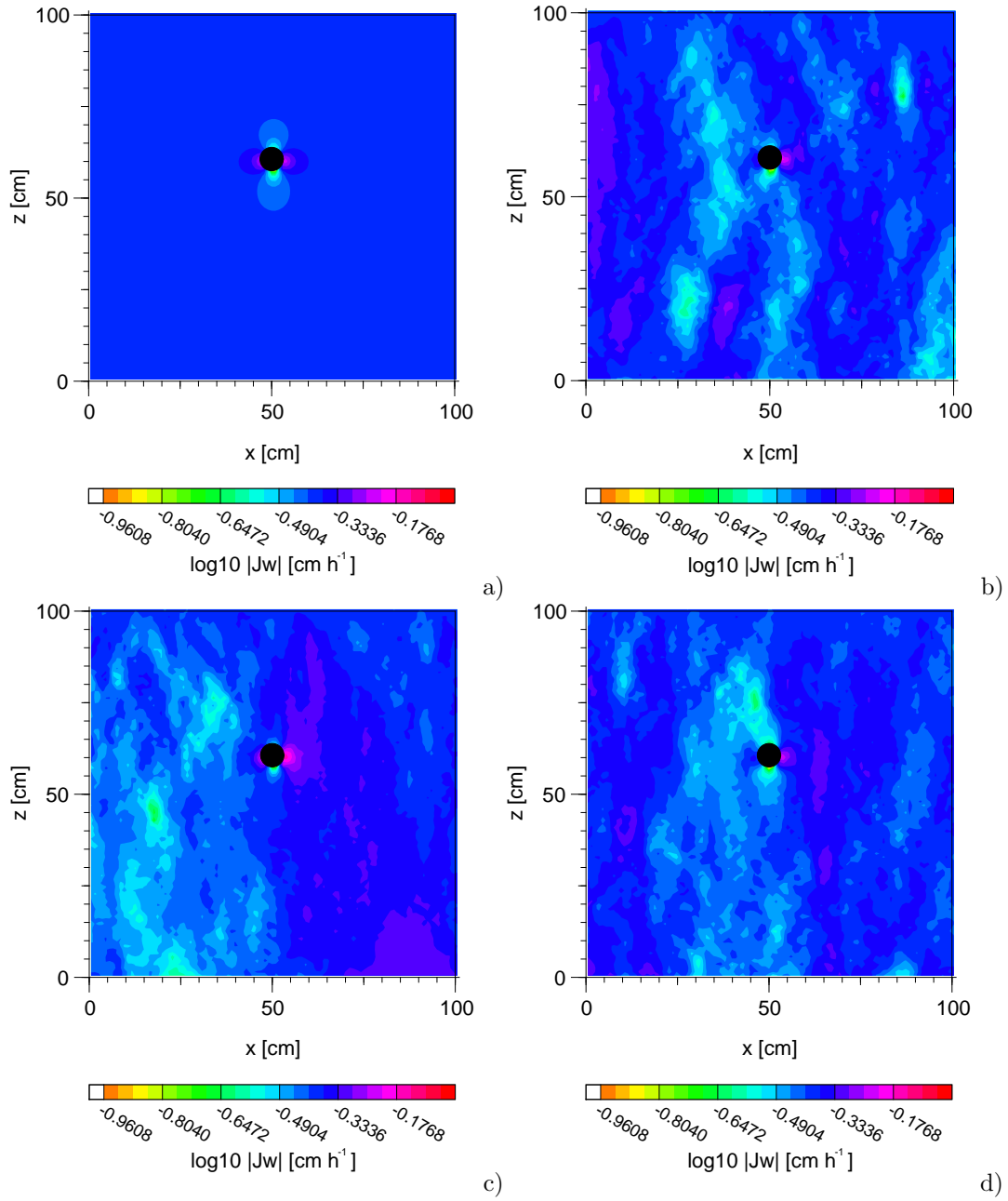
Figure 7.15: Absolute value of the water flux $|J_w|$ [cm h^{-1}] for the various sets of simulation. a) simulation 1-1, homogeneous soil , b) simulation 2-1, heterogeneous soil, c) simulation 3-1, heterogeneous soil, and d) simulation 4-1 heterogeneous soil. All simulations are with $\sigma_f^2 = 0.09$ and $\lambda_f = 20$ cm.

7.1.4   Simulation with transient conditions

For the simulation with transient conditions (atmospheric upper boundary) the vertical flow field was chosen as described in Figure 7.1 a. The soil parameters of the clay loam were listed in Table 7.1. For a better infiltration of the precipitation the saturated hydraulic conductivity, K_s, of the clay loam was set to 1 cm h^{-1}. The atmospheric
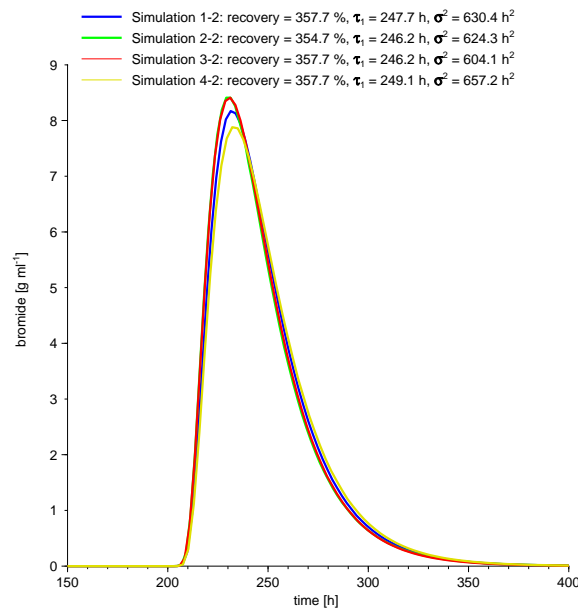
Figure 7.16: Bromide breakthrough in a suction cup for a homogeneous and heterogeneous soils. Simulation 1-2 = homogeneous soil, simulation 2-2, 3-2, and 4-3 heterogeneous soil with $\sigma_f^2 = 0.09$ and $\lambda_f = 20$ cm.
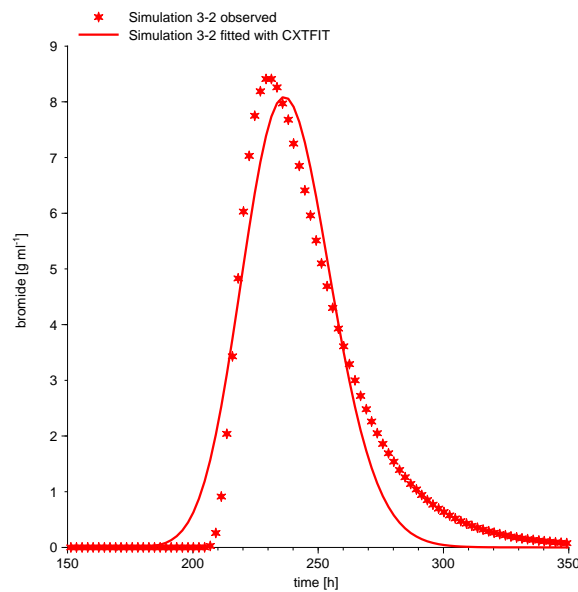
Figure 7.17: Bromide breakthrough in a suction cup for a heterogeneous soil with $\sigma_f^2 = 0.09$ and $\lambda_f = 20$ cm.

boundary conditions are shown in Figure 7.18, whereby a simulation period of 800 days
(two times the input data of 400 days) was chosen for a complete tracer breakthrough.
A conservative tracer puls of 75 g m^{-2} was applied at the upper surface at day zero. Two

a)

b)
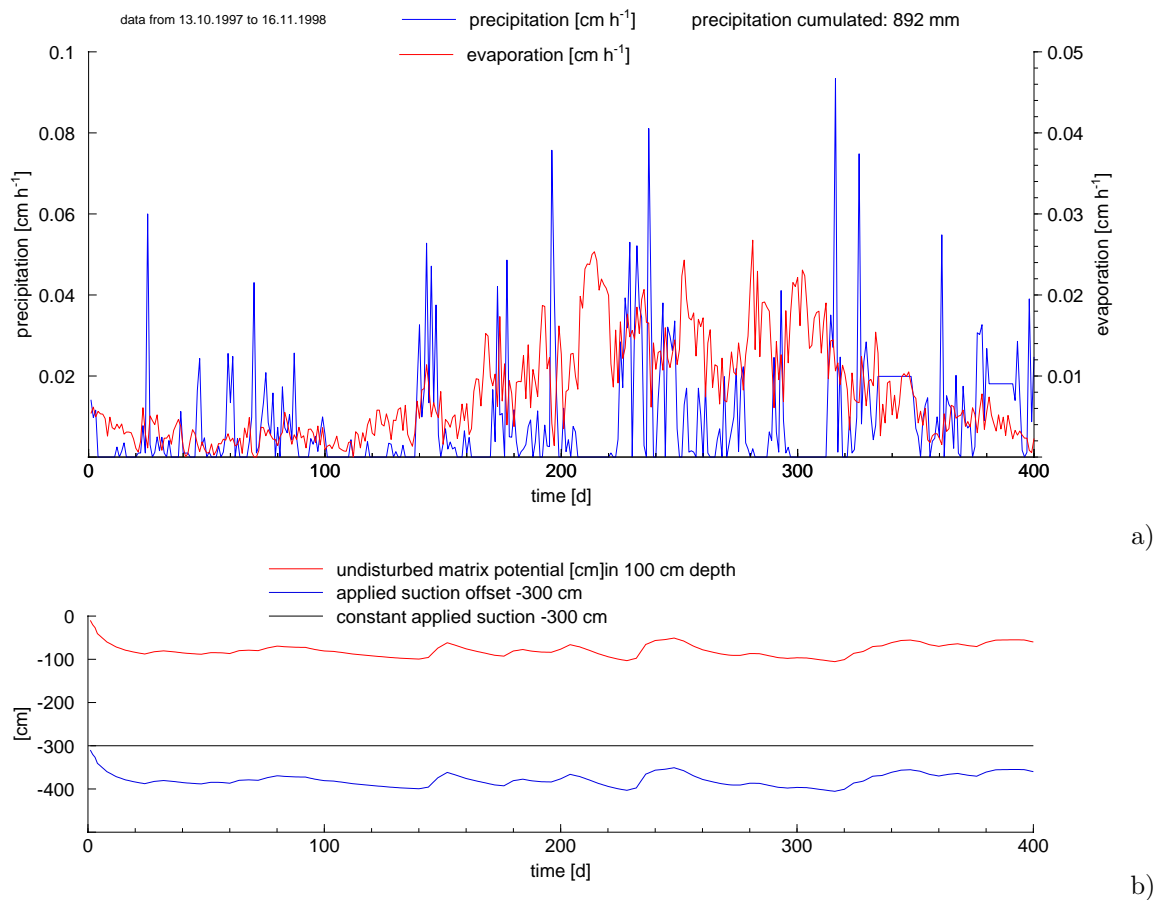
**Figure 7.18: a) Atmospheric upper boundary conditions and b) undisturbed matric
potential in 100 cm depth, applied suction offset of 300 cm and constant applied
suction of 300 cm. Data Merzenhausen from 13.10.1997 to 16.11.1998.**

different modes of operation for the suction cup were assumed - a continuous operation
with a constant applied suction of 300 cm in the suction cup and an an operation mode
with an offset of 300 cm added to the ambient matric potential. The results of the
extracted bromide concentrations (for a two-dimensional case [g cm^{-2}]) are plotted in
Figure 7.19. Just small differences in the bromide breakthrough are detectable for the
diffent operation modes.

   To visualize the two dimensional suction cup activity domain (in cm^2) the matric
potential differences larger than 5 cm of the two operation modes were calculated and
plotted in Figure 7.20. In general the SCAD show just small differences between the two
operation modes depending on the potential gradient between suction cup and actual
matric potential in the soil. Even when the boundary value for the matric potential
differences was set to 5 cm, the whole flow field is temporarily influenced by the suction
cup. Changes are also noticable during simulation time due to changes in water content
as a result of the atmospheric boundary conditions.
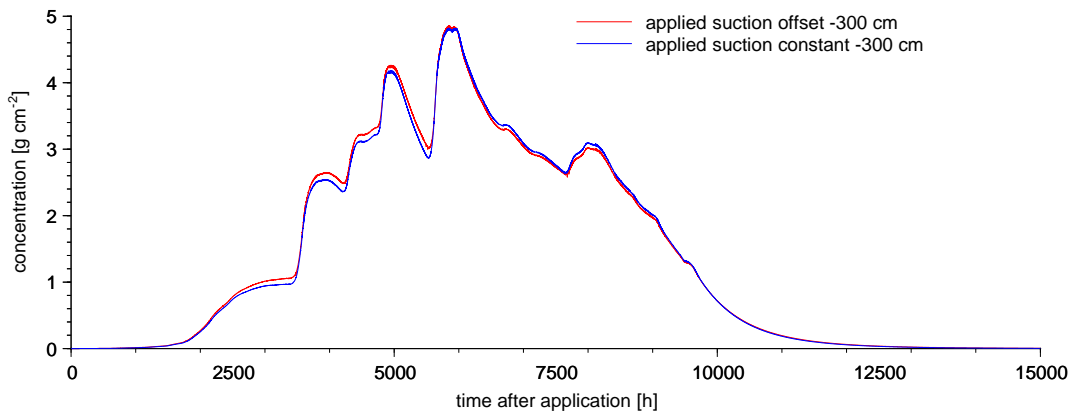
Figure 7.19: **Extracted tracer concentrations** $[gcm^{-2}]$ **in the suction cup for atmospheric boundary conditions and two different suction cup operation modes (continuously applied suction 300 cm and continuously applied offset 300 cm).**
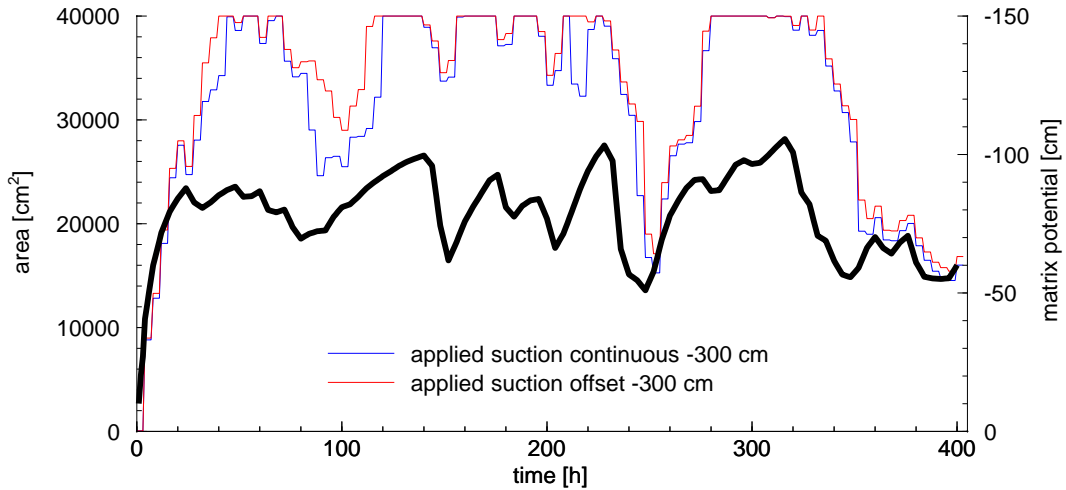
Figure 7.20: **Two-dimensional suction cup activity domain (SCAD)** $[cm^2]$ **for atmospheric boundary conditions and two different suction cup operation modes (continuously applied suction 300 cm and continuously applied offset 300 cm) and a boundary value of 5 cm in matric potential differences. Note that the black curve indicates the undisturbed matric potential [cm] in the same depth of the suction cup.**

7.2 Field- and lysimeter experiment

Soil water extracted by suction cups and ceramic plates as well as the percolate at the bottom of the lysimeters were sampled from the date of application on the 3rd of May, 2003, until the 22nd of June, 2004, in a two week interval. However, in case of transient infiltration, time must be replaced by cumulated leachate to obtain the transport parameters. For the comparison of the different sampling systems the total amount of water was normalized by the surface area of the devices (see Chapter 4.3.2). In a first step the breakthrough curves were plotted and, if possible (total bromide breakthrough), analyzed by the method of moments (see Chapter 4.8). The calculated moments were used to derive the effective transport parameters, i.e. pore water velocity, v (cm translocation for cm precipitation), and dispersivity, λ, using the relations shown in Annex A.15. These transport parameters were used to calculate the breakthrough curve using the convection-dispersion-equation (CDE) by Equation Annex A.6.

In a second step a direct fit of the CDE (see Chapter 3.2) using the code CXTFIT (*Toride et al.*, 1999) was conducted to obtain v and D ($D = \lambda v$). For both cases the effective water content, θ_e, was calculated by setting $\theta_e = \frac{1}{v}$. For all sampling devices with no complete bromide breakthrough a qualitative description was chosen using the first arrival time determined from the breakthrough plots. The arrival time was defined as the sample where the bomide concentration exceeds 0.001 g l^{-1}. High single values in advance of the inclining branch of the BTC were not considered for the arrival time due to the fact that these values are ascribed to preferential flow events. The breakthrough of the test substances MBT and ETD was also described in qualitative terms, because no complete breakthrough was observed.

7.2.1 Field experiment

The climatic variables precipitation and potential evaporation for the test site Merzenhausen are plotted in Figure 7.21. The total amount of precipitation (precipitation and irrigation) was 841.8 mm, and the calculated total potential evaporation was 1203.9 mm. A clear annual trend is detectable in the potential evaporation data, with high daily evaporation rates during the summer and low rates during the winter season. The low daily potential evaporation in the second half of the experimental time might be a result of low summer temperatures and net radiation. This trend is also visible in the tensiometer data, where the extreme values of the first half of the experiment were not reached in the last half (see Figure 7.22). Also problems in data acquisition (weak database for net radiation) may cause the differences between the two years.

Tensiometers

The matric potential, ψ [cm], measured with tensiometers in 40 cm and 120 cm depth for the two sampling pits at the test site Merzenhausen are plotted as the average of three tensiometers for each depth in Figure 7.22. The data show a clear annual trend with low matric potentials during summer times and higher matric potential during the wetter winter season. The extremely low matric potentials at the beginning of the experiment to the end of the summer 2003, reflect the extreme low rainfall in summer 2003. As
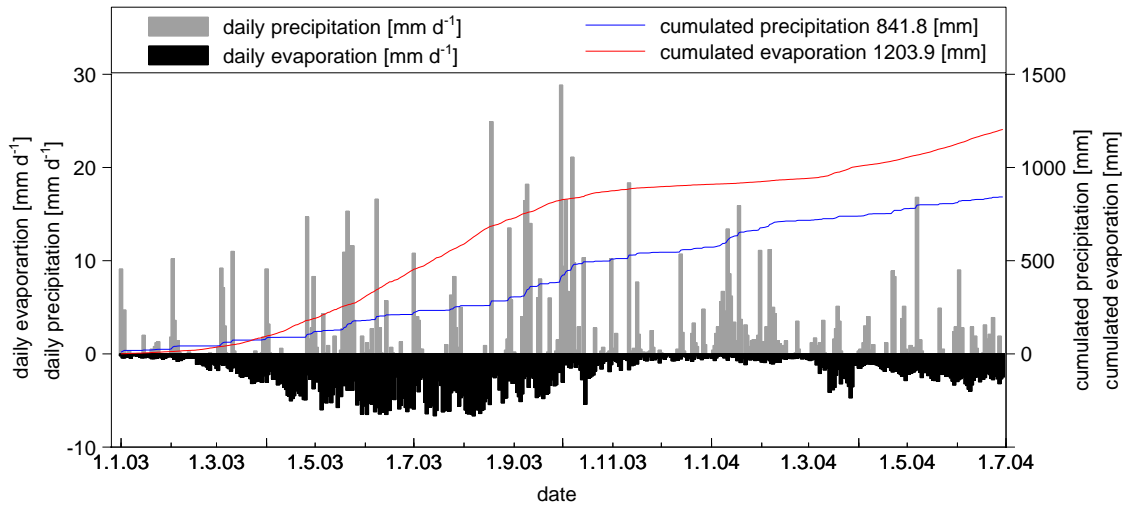
Figure 7.21: Daily precipitation (sum of precipitation and irrigation) and daily evaporation (calculated with Equation 4.6) [mm d^{-1}], and cumulated precipitation and evaporation [mm] for the test site Merzenhausen.

expected, the amplitude of the matric potential is more pronounced in the tenisometers installed close to the surface. With beginning of rainfall and irrigation in September 2003 matric potential increases and nearly reached saturation. In general, sampling pit 4 showed lower matric potentials at 40 cm depth for the whole sampling period, but nearly comparable potentials at 120 cm depth.

Extracted amount of water

The cumulative normalized leachate for the ceramic plates at the test site Merzenhausen is plotted in Figure 7.23. Plate 1 and 6 at 40 cm depth in sampling pit 4 were not considered due to sampling problems. Overall the ceramic plates in 40 cm depth in sampling pit 2 extracted slighly higher amounts of water compared to sampling pit 4. This behaviour reflects the tensiometer measurements in both sampling pits (Figure 7.22) for the depth of 40 cm with lower matric potentials in pit 4 and, therefore, lower water contents compared to sampling pit 2. At a depth of 120 cm the differences between the sampling pits are minimal. The rapid increase of extracted water for plate 11 (sampling pit 4) at sampling date 24/06/2003 might be a result of higher ambient water contents and, therefore, higher potential gradients next to the plate, or a measurement error. The variability of extracted soil water for the single plates at 40 and 120 cm depth shown in Figure 7.23 influences the time of the tracer plume arrival in the plates, but not the mass recovery. Assuming that each single suction plate is connected to a stream tube with a specific water flux, each plate would get a mass recovery of 100 %. This is not the case (see Table 7.6), and therefore, the process of lateral mixing is also detectable.
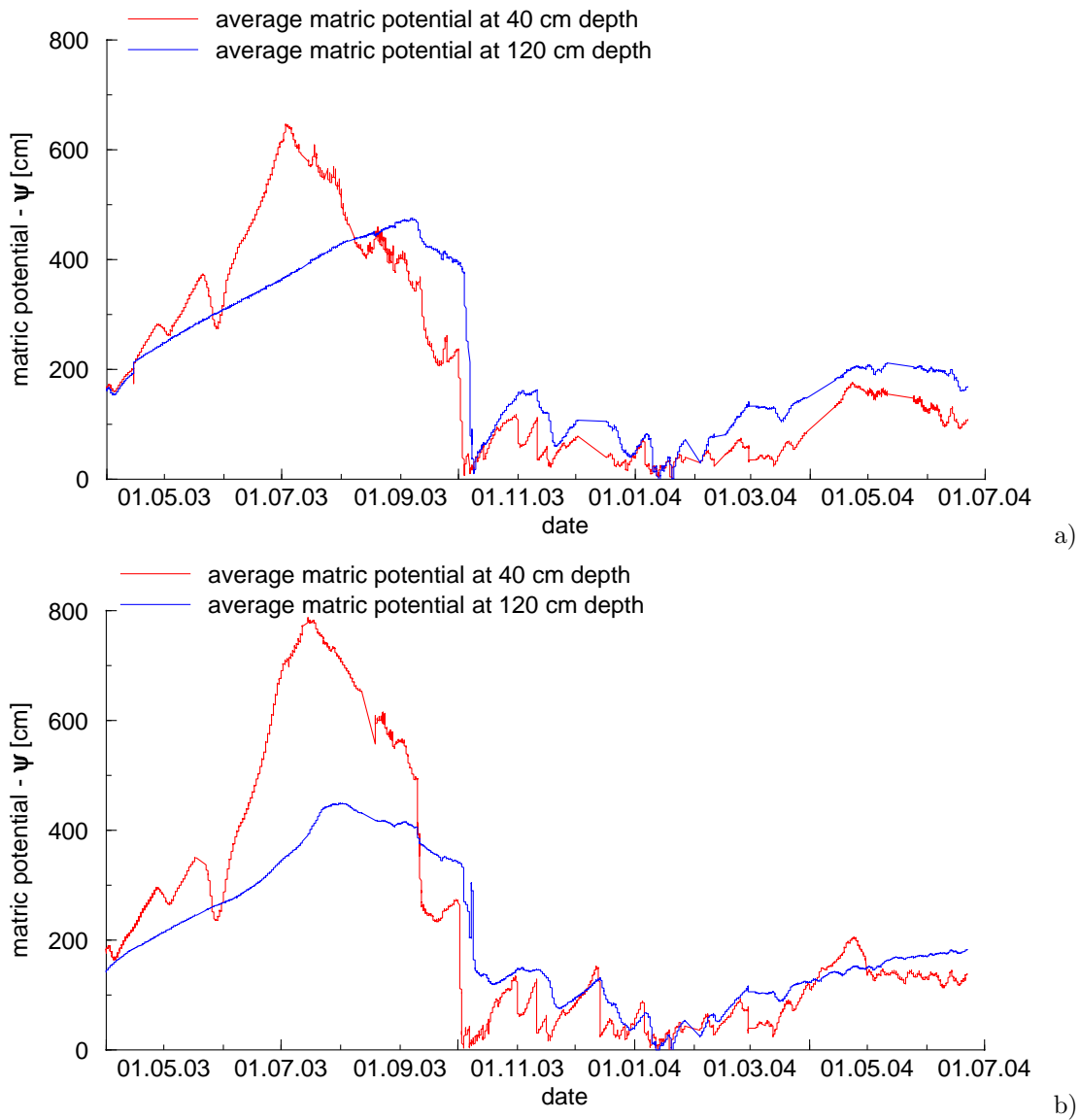
Figure 7.22: Average matric potential, -ψ [cm], measured by three tensiometers in 40 cm and 120 cm depth for the two sampling pits at the test site Merzenhausen for a) sampling pit 2 and b) sampling pit 4.
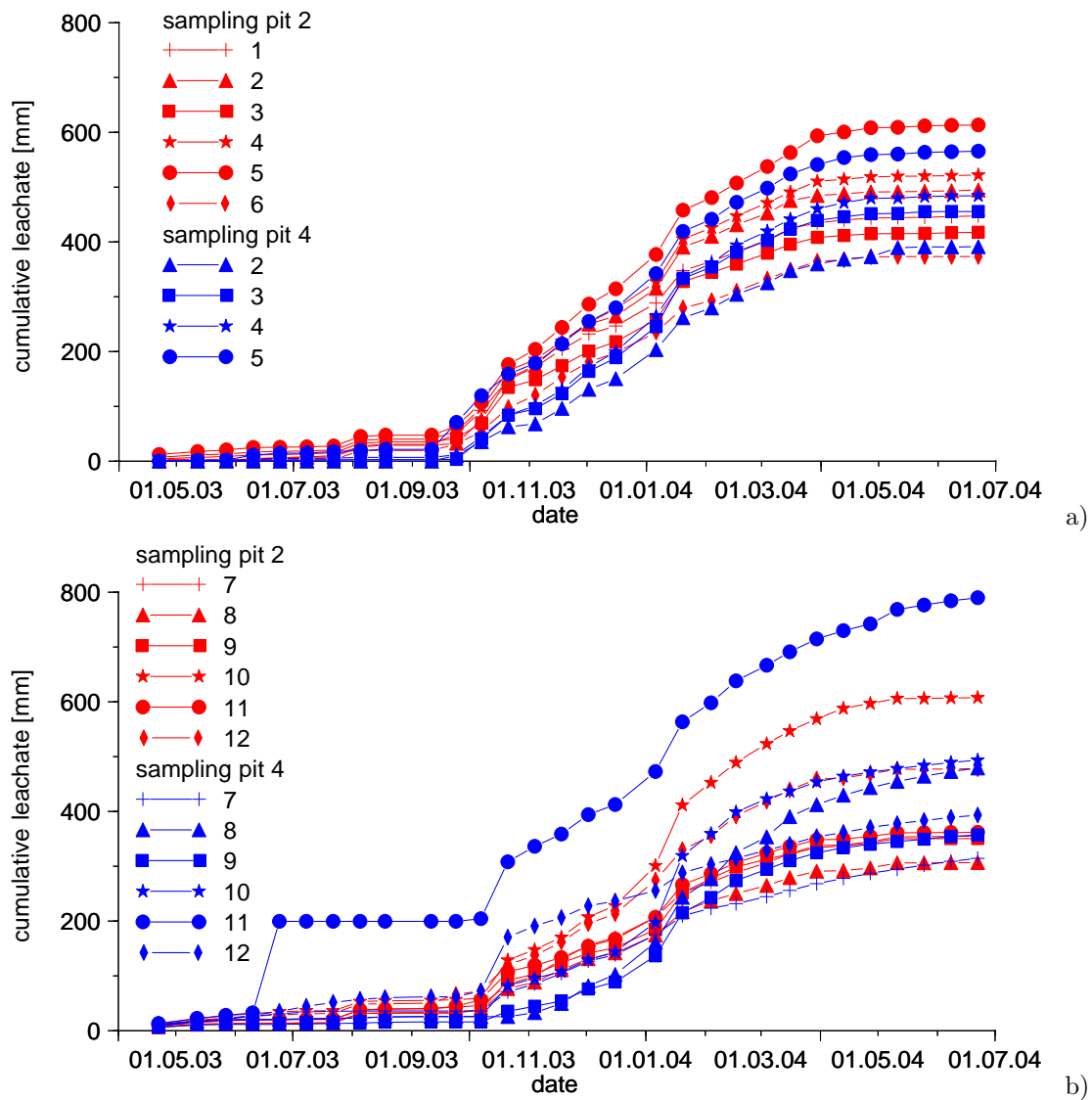
Figure 7.23: Cumulative leachate for the ceramic plates in sampling pit 2 and 4 at the test site Merzenhausen for a) 40 cm depth and b) 120 cm depth.

Bromide breakthrough

Ceramic plates

The bromide breakthrough for all ceramic plates at 40 and 120 cm depth at the test site Merzenhausen are listed in Table 7.6 and the BTC for each single plate is shown in Annex A.16. If we look at the arrival time of the tracer plume in the sampling pits at a depth of 40 cm it varies from 3 mm in plate 4-3 to 71 mm in plate 4-5. The bromide recovery derived from the measured concentrations is always smaller compared to the recovery calculated by methods of moments and fitted CDE. These differences can be backtraced to the procedure of integration (numerical evaluation using the trapezoidal rule) of the breakthrough curve for the methods of moments. The methods of moments and the fitted CDE show comparable values for the recovery. The bromide recovery (calculated by measured concentrations) also varies with smallest values for plate 4-2 to largest for plate 2-4 by a factor of 6.5 (see Table 7.6). The analyzed total mass recovery of 27.0 % in plate 2 is exceptional low compared to all other samplers. The pore water velocities range by a factor of 3, whereby plate 2-5 shows the lowest velocities. For all plates the calculated pore water velocity, v, based on the method of moments and fitted CDE, is in close agreement. The dispersivity, λ, indicates higher discrepancies between the methods. It seems that the method of moments has lower dispersivities for all cases compared to the fitted results. The highest calculated values of λ were observed for plate 4-2, and 4-4 with 11.43, and 9.77, respectively. Plate 2-5 shows the lowest disperisvity with a value of 2.87 for the fitted CDE. Overall the dispersivity ranges by a factor of 2.5 for all plates. For the various samplers λ varies by a factor of 3. High bromide concentrations with low extracted amounts of water indicate preferential flow in plate 4-4.

The arithmetic mean and the standard deviation of the recovery, pore water velocity, dispersivity, mean water content, and arrival time are also listed in Table 7.6. The range in dispersivity and pore-water velocity values shows a higher variability in the observed BTCs of sampling pit 2 compared to the values of sampling pit 4. However, it has to be taken into account that only four samplers were analyzed in sampling pit 4, compared to six samplers for sampling pit 2.

For the samplers installed at 120 cm depth no complete bromide breakthrough was observed during the experiment (Annex A.14 and A.16). The total mass recovery calculated by measured concentration varies from 34.6 % in sampler 2-7 to 125.5 % in sampler 4-11. Based on the visual inspection of the bromide BTC, the arrival time was determined. The arrival time in sampling nest 2 varies from 38 mm in plate 2-9 to 129 mm in plate 2-10, and between 35 mm in plate 4-9 to 308 mm in plate 4-11.

Figure 7.24 shows the mean BTC for sampling pit 2 and 4 derived from the individual ceramic plate data. From this BTC λ and v were estimated using the methods of moments and the fitted CDE. The bromide recovery (calculated by measured concentration) derived from the mean BTC at 40 cm depth is smaller for sampling pit 4 compared to sampling pit 2. On the other hand, sampling pit 4 indicates a slightly higher pore water velocities and dispersivities as well as a 2 times faster arrival time. Differences between the method of moments and the direct fit of the CDE become evident with a lower dispersivity for the methods of moments. The pore water velocity shows nearly

Figure 7.24: Mean bromide breakthrough for the ceramic plates at 40 cm depth in (a) sampling pit 2 and (b) sampling pit 4 as well as the plates in 120 cm depth in (c) sampling pit 2 and (d) sampling pit 4 at the test site Merzenhausen. Mass recovery was calculated using the measured concentration.

same results for both methods.

The breakthrough curves at 120 cm depth with mass recoveries of 57 % in sampling pit 2 and 64 % in sampling pit 4 indicate that the breakthrough is not complete. Compared to the mean arrival time of 101.5 mm in sampling pit 2 the mean arrival times of 63.3 mm in sampling pit 4 is somewhat smaller, whereby sampling pit 2 shows larger variabilities (STD = 96 mm). The high concentrations detected in sampling pit 4 at an arrival time of ~ 10 mm, indicates preferential flow.

Suction cups

The bromide breakthrough for the suction cups at 40 cm depth at the test site Merzenhausen are depicted in Annex A.17 and A.19. Note that the amount of extracted water and, therefore, the mass recovery are normalized by the surface of the sampling devices. Due to the weak database for some of the samplers only two of the BTCs were analyzed using methods of moments and fitted CDE, namely cup 2-2, and cup 4-1 (see Table 7.8). Figure 7.25 shows the mean BTC for sampling pit 2 and 4 derived from the individual suction cup data. From this BTC λ and v were estimated using CDE and methods of moments, whereby the weak database does not allow any comparison between the samplers or locations. The bromide breakthrough at 120 cm depth could not be described either by the methods of moments or fitted CDE. The arrival times are in good agreement for both sampling pits but a slightly higher recovery is detected in sampling pit 2. The advanced peak concentration of 0.04 g l^{-1} indicates preferential flow detected in all single suction cups in sampling pit 4. A direct comparison with the findings of the ceramic plate is not valid due to the fact that the SCSA and the SCED are not known for the transient conditions.
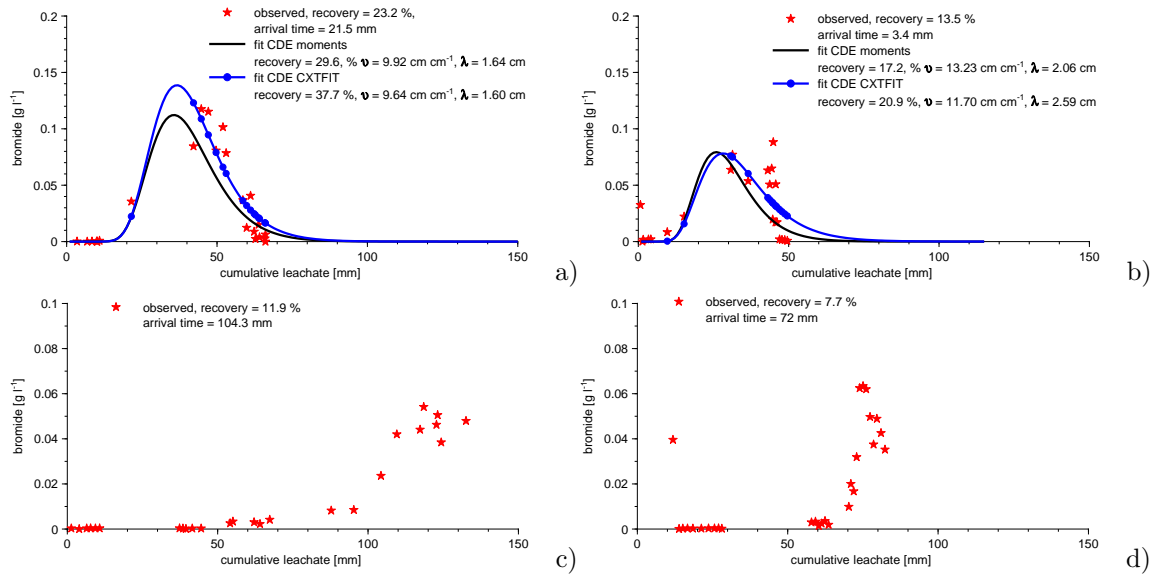
Figure 7.25: **Mean bromide breakthrough for the suction cups at 40 cm depth in (a) sampling pit 2 and (b) sampling pit 4 as well as the plates in 120 cm depth in (c) sampling pit 2 and (d) sampling pit 4 at the test site Merzenhausen. Mass recovery was calculated using the measured concentration.**

Table 7.6: Bromide recovery, mean pore water velocity, v, dispersivity, λ, effective water content, Θ, and arrival time (AT) for the ceramic plates at 40 cm depth at the test site Merzenhausen. Note that sampling pit 2 = location 2 and sampling pit 4 = location 4. The number identifies the samplers in the sampling pits. MOM = methods of moments - CDE is fitted with **CXTFIT** (*Toride et al.*, **1999**).

| *location* | *recovery [%]* | | | v [cm cm^{-1}] | | λ [cm] | | Θ [%] | | AT |
Nr.	*mass* [†]	*MOM*	*CDE*	*MOM*	*CDE*	*MOM*	*CDE*	*MOM*	*CDE*	[mm]
2-1	114	165	168	2.05	1.95	4.20	6.00	49	51	50
2-2	108	165	171	2.51	2.52	5.93	6.98	40	39	32
2-3	87	129	134	2.25	2.18	3.47	4.90	45	46	42
2-4	178	265	277	2.05	1.98	3.26	4.09	49	51	55
2-5	144	260	251	1.31	0.13	2.87	2.87	72	76	64
2-6	104	161	169	2.79	2.55	4.27	7.44	36	39	32
mean BTC [‡]	123	183	193	2.11	2.01	4.08	5.70	47	50	46
mean [§]	123	190	195	2.16	2.07	4.01	5.53	48	50	46
STD [§]	33	52	51	0.44	0.42	0.99	1.43	12	13	12
4-2	27	42	42	3.56	3.24	7.38	11.43	28	31	11
4-3	129	194	191	3.32	3.24	7.70	8.20	30	31	3
4-4	94	149	144	2.33	2.00	5.55	9.77	43	50	12
4-5	176	271	258	1.66	1.56	3.27	3.51	60	64	71
mean BTC [‡]	106	167	162	2.44	2.28	5.41	6.93	44	41	24
mean [§]	106	164	159	2.72	2.51	5.98	8.23	40	44	24
STD [§]	63	96	91	0.88	0.86	2.04	3.41	15	16	31
mean all [¶]	116	177	180	2.25	2.11	4.63	6.40	45	47	37

[†] *calculated by amount of analyzed bromide in relation to the applied bromide for the surface of the ceramic plates*

[‡] *BTC calculated by mean of all single devices in one sampling pit*

[§] *arithmetic mean and standard deviation (STD) calculated by parameters for all single devices in one sampling pit*

[¶] *BTC calculated by mean of all single devices in both sampling pits*

Table 7.7: **Bromide recovery, and arrival time (AT) for the ceramic plates at 120 cm depth at the test site Merzenhausen. Note that sampling pit 2 = location 2 and sampling pit 4 = location 4. The number identifies the samplers in the sampling pits.**

location *Nr.*	*recovery [%]* *mass* [†]	AT [mm]
2-7	35	85
2-8	38	88
2-9	47	38
2-10	105	129
2-11	42	107
2-12	76	120
mean BTC [‡]	57	102
mean [§]	57	96
STD [§]	28	30
4-7	43	138
4-8	50	102
4-9	50	35
4-10	79	82
4-11	126	308
4-12	37	73
mean BTC [‡]	64	63
mean [§]	64	115
STD [§]	33	91
mean all [¶]	61	58

[†] *calculated by amount of analyzed bromide in relation to the applied bromide for the surface of the ceramic plates*

[‡] *BTC calculated by mean of all single devices in one sampling pit*

[§] *arithmetic mean and standard deviation (STD) calculated by parameters for all single devices in one sampling pit*

[¶] *BTC calculated by mean of all single devices in both sampling pits*

Table 7.8: Bromide recovery, mean pore water velocity, v, dispersivity, λ, effective water saturation, Θ, and arrival time, (AT), for the suction cups at 40 cm depth at the test site Merzenhausen. Note that sampling pit **2** = location **2** and sampling pit **4** = location **4**. The number identifies the samplers in the sampling pits. **MOM** = methods of moments - **CDE** is fitted with **CXTFIT** (*Toride et al.*, **1999**).

| *location* | *recovery [%]* | | | v *[cm cm^{-1}]* | | λ *[cm]* | | Θ [%] | | AT |
Nr.	*mass* [†]	*MOM*	*CDE*	*MOM*	*CDE*	*MOM*	*CDE*	*MOM*	*CDE*	[mm]
2-1	4									50
2-2	36	58	59	6.65	6.65	1.96	2.55	15	15	31
2-3	29									27
2-4	24									18
mean BTC [‡]	23	30	38	9.92	9.64	1.64	1.59	10	10	22
4-1	18	24	26	9.76	8.42	2.52	2.97	10	12	14
4-2	2									1
4-3	27									11
4-4	7									32
mean BTC [‡]	14	17	21	13.23	11.70	2.06	2.59	8	9	3
mean all [§]	18	24	29	11.39	10.90	1.83	1.87	9	9	7

[†] *calculated by amount of analyzed bromide in relation to the applied bromide for the surface of the ceramic plates*

[‡] *BTC calculated by mean of all single devices in one sampling pit*

[§] *BTC calculated by mean of all single devices in both sampling pits*

Table 7.9: Bromide recovery and arrival time (AT) for the suction cups at 120 cm depth at the test site Merzenhausen. Note that sampling pit 2 = location 2 and sampling pit 4 = location 4. The number identifies the samplers in the sampling pits.

location *Nr.*	*recovery [%]* *mass* [†]	AT [mm]
2-5	5	14
2-6	22	104
2-7	20	40
2-8	9	71
2-9	14	64
2-10	1	51
mean BTC [‡]	12	104
4-5	8	83
4-6	5	14
4-7	1	2
4-8	8	27
4-9	8	83
4-10	16	164
mean BTC [‡]	8	72
mean all [§]	10	56

[†] *calculated by amount of analyzed bromide in relation to the applied bromide for the surface of the ceramic plates*

[‡] *BTC calculated by mean of all single devices in one sampling pit*

[§] *BTC calculated by mean of all single devices in both sampling pits*

MBT/ETD breakthrough

Ceramic plates

The MBT/ETD breakthrough for the ceramic plates at 40 and 120 cm depth are plotted in Figure 7.26. No typical breakthrough was observed for MBT and ETD at both depths. Therefore, no transport parameters can be determined for these samplers. The mass recoveries calculated by the measured concentrations as well as the highest analyzed concentration (peak concentration) are listed in Table 7.10 and 7.11. In general, larger ETD recoveries were measured compared to the MBT, which is in good accordance to the phyiscal properties of the pesticides - which characterize ETD as a "leacher" and MBT as a "non-leacher". But still the total amount of leached pesticides is low. ETD peak concentrations exceeding 1 μg l^{-1} were measured for all samplers at both locations at a depth of 40 cm. The highest peak concentration was measured in sampler 4-3 with 146.45 μg l^{-1} for the MBT at the 27th of May, 2003. These high concentrations can be traced back to a single event. The measured MBT/ETD breakthrough at a depth of 120 cm shows lower recoveries compared to installation at 40 cm depth. The peak concentrations are also less variable and the absolute values are smaller due to more spreading at larger depths.

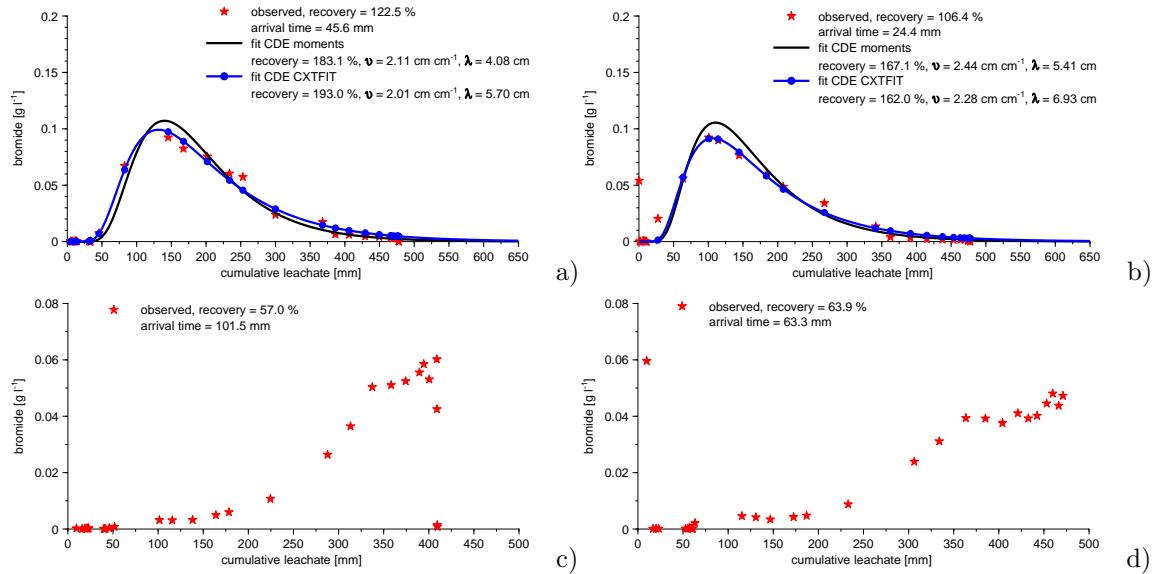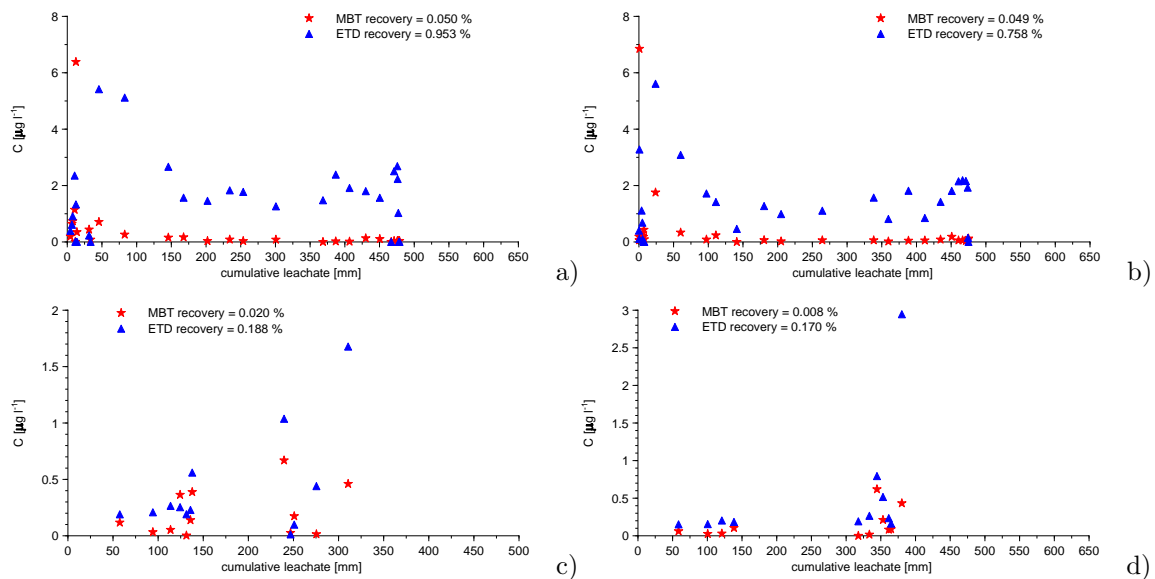**Figure 7.26: Mean MBT/ETD breakthrough for the ceramic plates at 40 cm depth in (a) sampling pit 2 and (b) sampling pit 4 as well as in 120 cm depth in (c) sampling pit 2 and (d) sampling pit 4 at the test site Merzenhausen. Mass recovery was calculated using the measured concentration. Note the different scaling of the ordinates.**

Suction cups

The MBT/ETD breakthrough for the suction cups at 40 and 120 cm depth are plotted in Figure 7.27. Again, no total breakthrough was observed for the samplers at both depths.

Table 7.10: MBT/ETD recovery and peak concentration for the ceramic plates at 40 cm depth in sampling pit 2 and 4 at the test site Merzenhausen. Mass recovery was calculated using the measured concentration.

location	ETD		MBT	
Nr.	recovery [%]	highest $C^{\dagger}[\mu g\ l^{-1}]$	recovery [%]	highest $C^{\dagger}[\mu g\ l^{-1}]$
2-1	1.12	10.93	0.09	9.28
2-2	1.35	15.71	0.09	2.00
2-3	0.89	15.98	0.05	2.74
2-4	0.71	2.28	0.02	2.67
2-5	0.81	10.79	0.03	43.35
2-6	0.84	4.24	0.01	0.15
mean BTC‡	0.95	5.41	0.05	6.38
4-2	0.41	2.03	0.01	0.16
4-3	0.55	56.67	0.01	146.45
4-4	0.41	1.49	0.02	0.60
4-5	1.67	7.21	0.15	2.26
mean BTC‡	0.76	5.61	0.05	6.85

† *highest measured concentration*

‡ *BTC calculated by mean of all single devices in one sampling pit*

Table 7.11: MBT/ETD recovery and peak concentration for the ceramic plates at 120 cm depth in sampling pit 2 and 4 at the test site Merzenhausen. Mass recovery was calculated using the measured concentration.

location	ETD		MBT	
Nr.	recovery [%]	highest $C^{\dagger}[\mu g\ l^{-1}]$	recovery [%]	highest $C^{\dagger}[\mu g\ l^{-1}]$
2-7	0.10	1.58	0.01	1.19
2-8	0.17	1.31	0.00	0.56
2-9	0.30	6.00	0.03	1.21
2-10	0.06	0.31	0.01	0.36
2-11	0.14	5.68	0.04	3.22
2-12	0.35	1.89	0.03	0.19
mean BTC‡	0.19	1.68	0.02	0.67
4-7	0.02	0.27	0.00	0.20
4-8	0.05	0.31	0.00	0.23
4-9	0.10	0.63	0.01	0.25
4-10	0.07	0.32	0.00	0.46
4-11	0.25	0.76	0.01	0.21
4-12	0.45	4.12	0.03	0.59
mean BTC‡	0.16	2.95	0.01	0.62

† *highest measured concentration*

‡ *BTC calculated by mean of all single devices in one sampling pit*

Therefore, no transport parameters were determined. The mass recoveries calculated by the measured concentrations as well as the highest analyzed concentration (peak concentration) are listed in Table 7.12 and 7.13. Like in the ceramic plates, larger ETD recoveries were measured compared to the MBT in the suction cups. The ETD peak concentrations were higher in sampling pit 4 compared to pit 2 which can be traced back to the single event in sampler 4-4.
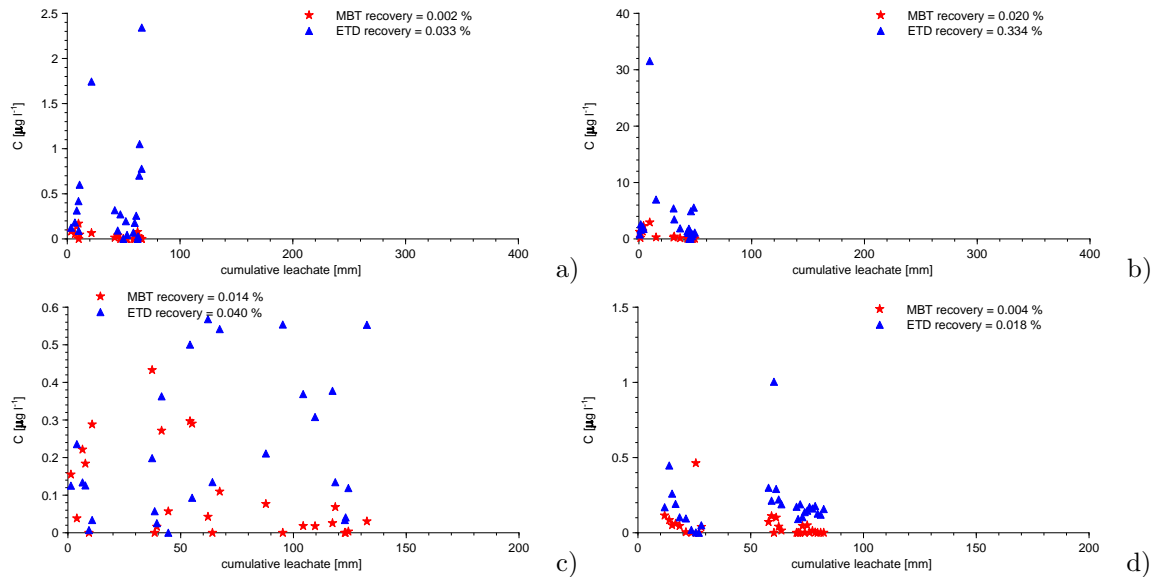
Figure 7.27: Mean MBT/ETD breakthrough for the suction cups at 40 cm depth in (a) sampling pit 2, (b) sampling pit 4, and at 120 cm depth in (c) sampling pit 2 and (d) sampling pit 4 at the test site Merzenhausen. Mass recovery was calculated using the measured concentration. Note the different scaling of the ordinates.

Field lysimeter

The tracer breakthrough at the bottom of the field lysimeter at the test site Merzenhausen demonstrated that no complete breakthrough occured at a depth of 120 cm (see Figure 7.28). In contrast to the normalized extracted amount of soil water in the ceramic plates, a two times lower percolation was measured ($\sim$ 180 mm), resulting in a lower bromide recovery (38.3 %) compared to over 50 % in the ceramic plates. At the same time a peak concentration was measured at the beginning of the sample period, which also indicates preferential flow.

Table 7.12: MBT/ETD recovery and peak concentration for the suction cups at 40 cm depth in sampling pit 2 sampling pit 4 at the test site Merzenhausen. Mass recovery was calculated using the measured concentration.

location	ETD		MBT	
Nr.	recovery [%]	highest $C^{\dagger}[\mu g\ l^{-1}]$	recovery [%]	highest $C^{\dagger}[\mu g\ l^{-1}]$
2-1	0.03	3.91	0.00	2.81
2-2	0.28	2.64	0.00	0.08
2-3	0.06	2.61	0.00	0.25
2-4	0.01	0.27	0.00	0.27
mean BTC‡	0.03	2.34	0.00	0.17
4-1	0.23	10.78	0.01	4.58
4-2	0.01	4.71	0.00	1.22
4-3	0.02	1.49	0.00	0.61
4-4	1.08	31.53	0.07	3.21
mean BTC‡	0.33	31.50	0.02	2.92

† *highest measured concentration*

‡ *BTC calculated by mean of all single devices in one sampling pit*

Table 7.13: MBT/ETD recovery and peak concentration for the suction cups at 120 cm depth in sampling pit 2 sampling pit 4 at the test site Merzenhausen. Mass recovery was calculated using the measured concentration.

location	ETD		MBT	
Nr.	recovery [%]	highest $C^{\dagger}[\mu g\ l^{-1}]$	recovery [%]	highest $C^{\dagger}[\mu g\ l^{-1}]$
2-5	0.00	0.26	0.00	1.72
2-6	0.02	0.84	0.02	0.61
2-7	0.17	1.20	0.02	1.82
2-8	0.01	0.52	0.01	0.38
2-9	0.01	0.20	0.02	0.55
2-10	0.03	0.80	0.01	0.41
mean BTC‡	0.04	0.57	0.01	0.43
4-5	0.01	1.80	0.01	0.53
4-6	0.00	0.22	0.00	0.15
4-7	0.00	0.74	0.00	0.19
4-8	0.01	0.74	0.01	1.52
4-9	0.07	0.81	0.01	0.45
4-10	0.01	0.16	0.01	0.46
mean BTC‡	0.02	1.00	0.00	0.46

† *highest measured concentration*

‡ *BTC calculated by mean of all single devices in one sampling pit*
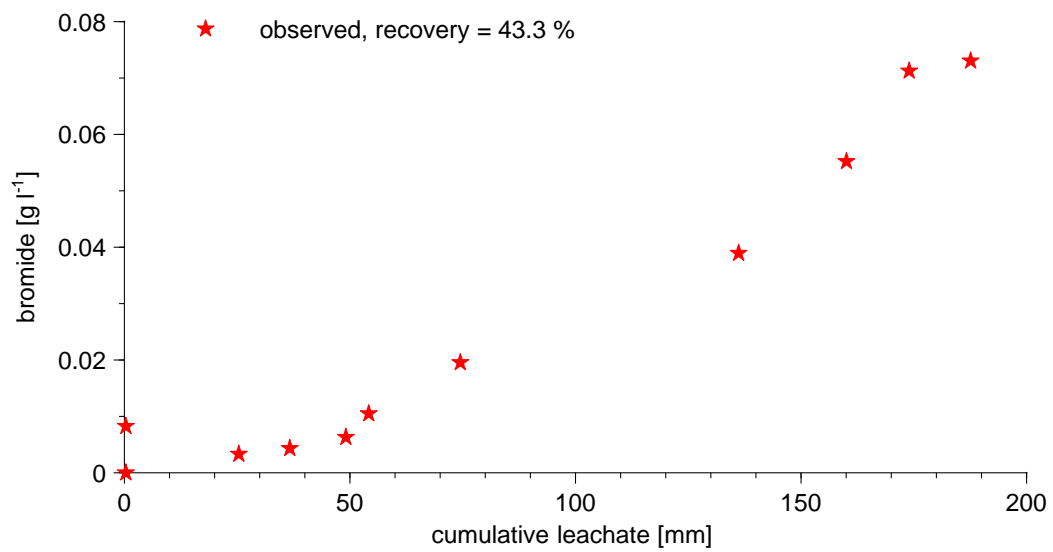
Figure 7.28: Bromide breakthrough [g l^{-1}] at the bottom of the field lysimeter (120 cm depth) at the test site Merzenhausen. Mass recovery was calculated using measured concentration.

7.2.2   Lysimeter experiment

The climatic variables precipitation and potential evaporation for the lysimeter station at the Agrosphere Institute are plotted in Figure 7.29. The total amount of precipitation (precipitation and irrigation) is 968.5 mm, with a calculated total potential evaporation of 1213.3 mm. Again a clear annual trend is detectable in the data. The low daily evaporation in the second half of the experimental time might be a result of low summer temperatures and net radiation and again in problems in data acquisition to calculate net radiation. The slightly higher amount of total precipitation compared to the test site Merzenhausen indicates the influence of the microclimate at the two locations. The potential evaporation was assumed to be comparable to the test site Merzenhausen due to the weak database for evaporation calculation at the lysimeter station.
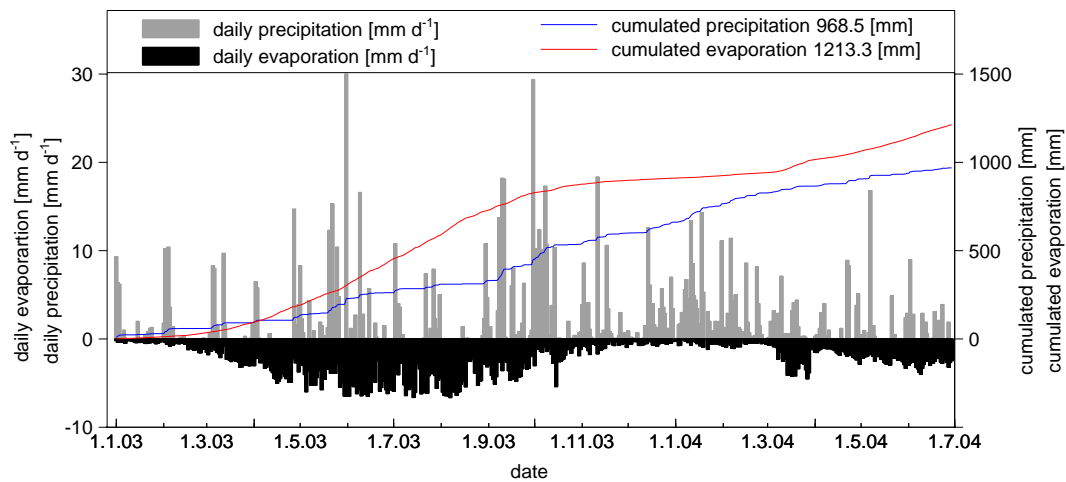
Figure 7.29: Daily precipitation (sum of precipitation and irrigation) and daily evaporation (calculated with Equation 4.6) [mm d^{-1}], and cumulated precipitation and evaporation [mm] for the lysimeter at the Agrosphere Institute.

The daily mean weight of the lysimeters plotted in Figure 7.30 shows also a clear annual trend with low masses, and as a result low water contents during the dry summer period. With the beginning of the rainfalls in autumn 2003 and irrigation, a constant increase of the water content was observed. The smaller absolute weights of lysimeter 2 can be traced back to a lower level of soil filled in the cylinder or higher water contents prior to the installation. The annual evolution is almost identical without this effect. The well-defined masses over the course of the experiment allowed the calculation of a water balace and the calculation of the actual evaporation, E_A, during the experiment:

$$E_A = P - D_r - \Delta S \tag{7.6}$$

where ΔS as the storage term of the lysimeter [L] (amount of stored water in the period of the experiment), P is the precipitation [L] and D_r is the extracted and drained amount of water [L].

The values for the storage term, drainage, precipitation, potential evaporation, and actual evaporation are depicted in Table 7.14. Under consideration of all known sinks

Table 7.14: Water storage term, ΔS, drainage, and extracted water by suction cups, D_r, precipitation, P, calculated potential evaporation, E_{pot}, and calculated actual evaporation, E_A, for the lysimeters at the lysimeter station at the Agrosphere Institute during the experiment from 04/04/2003 to the 22/06/2004.

	ΔS	D_r	P	E_A	E_{pot}	E_A in % of E_{pot}
	$[mm^2]$	$[mm^2]$	[mm]	[mm]	[mm]	
lysimeter 1	$34.0 * 10^4$	543.9	968.5	679.5	1213.3	56.0
lysimeter 2	$32.6 * 10^4$	530.7	968.5	686.8	1213.3	56.6

(mass of water extraction by the porous cups and percolated water at the lower boundary) and sources (precipitation and irrigation) the actual evaporation in the sampling period between 03/04/2003 and 22/06/2004 was calculated to be 679.5 and 686.8 mm in lysimeter 1 and 2, respectively. For both lysimeters the actual evaporation is about half of the potential evaporation. Microclimatic influences can be considered as a hypothesis for the high actual evaporation on a bare soil in the lysimeters compared to field conditions. A fundamental weakness is the soil surface which is below the lysimeter casting (about 15 cm). This can lead to minimal turbulences and a reduced exchange of the air packages resulting in the formation of a stable boundary layer overlying the soil surface. If this boundary layer is water saturated, just minimal evaporation will take place. A factor for the differences between the lysimeters can be seen in the reduction of the evaporation during dry periods which depends on the local heterogeneity in soil properties at the soil surface.
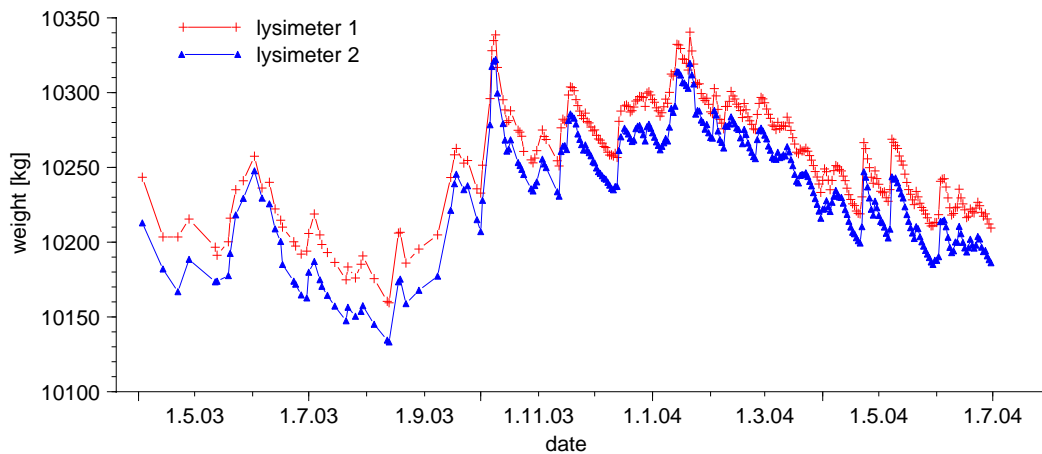
Figure 7.30: Daily mean weight of the lysimeter 1 and 2 (lysimeter station at the Agrosphere Institute).

Tensiometers

The matric potential, ψ, measured with tensiometers at 40 and 120 cm depth for the two lysimeters is plotted as the average of three tensiometers for each depth in Figure

7.31. In general, the two lysimeters show nearly identical matric potential characteristic during the whole period. As stated before, the tensiometer values are depth depending and time-shifted. In comparison to the field site Merzenhausen higher matric potentials were observed resulting in higher water contents.
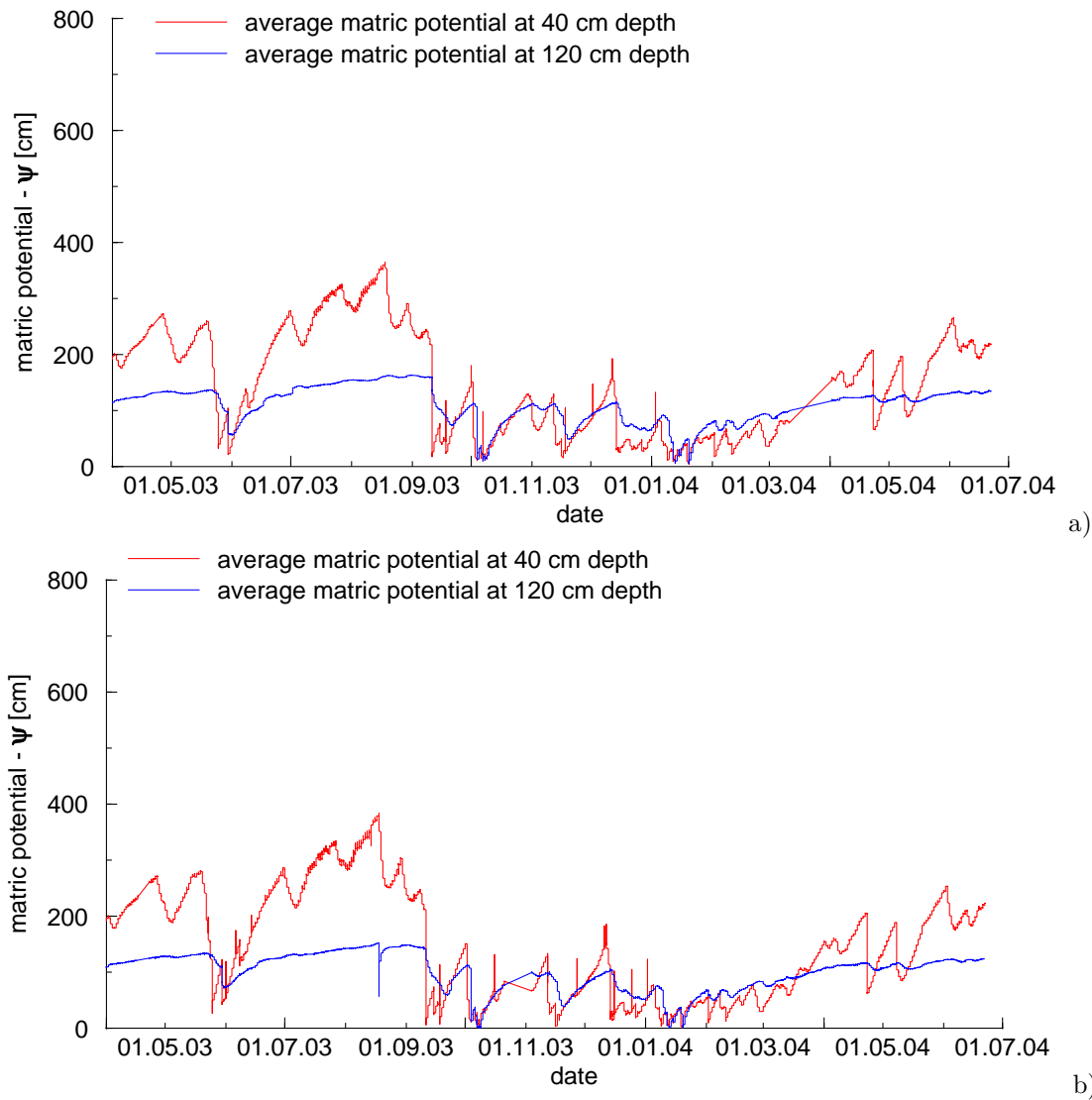
Figure 7.31: Average matric potential, $-\psi$, measured by tensiometers at 40 and 120 cm depth for the two lysimeters a) 1 and b) 2.

Soil temperature

The soil temperatures in the lysimeters depicted in Figure 7.32 indicate a typical horizontal distribution for a field soil with high temperatures at the soil surface and lower temperatures with depth and smooth temperature changes for temperatures at depth lower than 90 cm. An annual trend is also detectable. In contrast to the measured soil temperatures, measured closely to the lysimeter walls, numerical simulations exhibit

a different soil temperature distribution for the inner regions of the lysimeter (A.13) ascribed to the air conditioning of the lysimeter cellar.
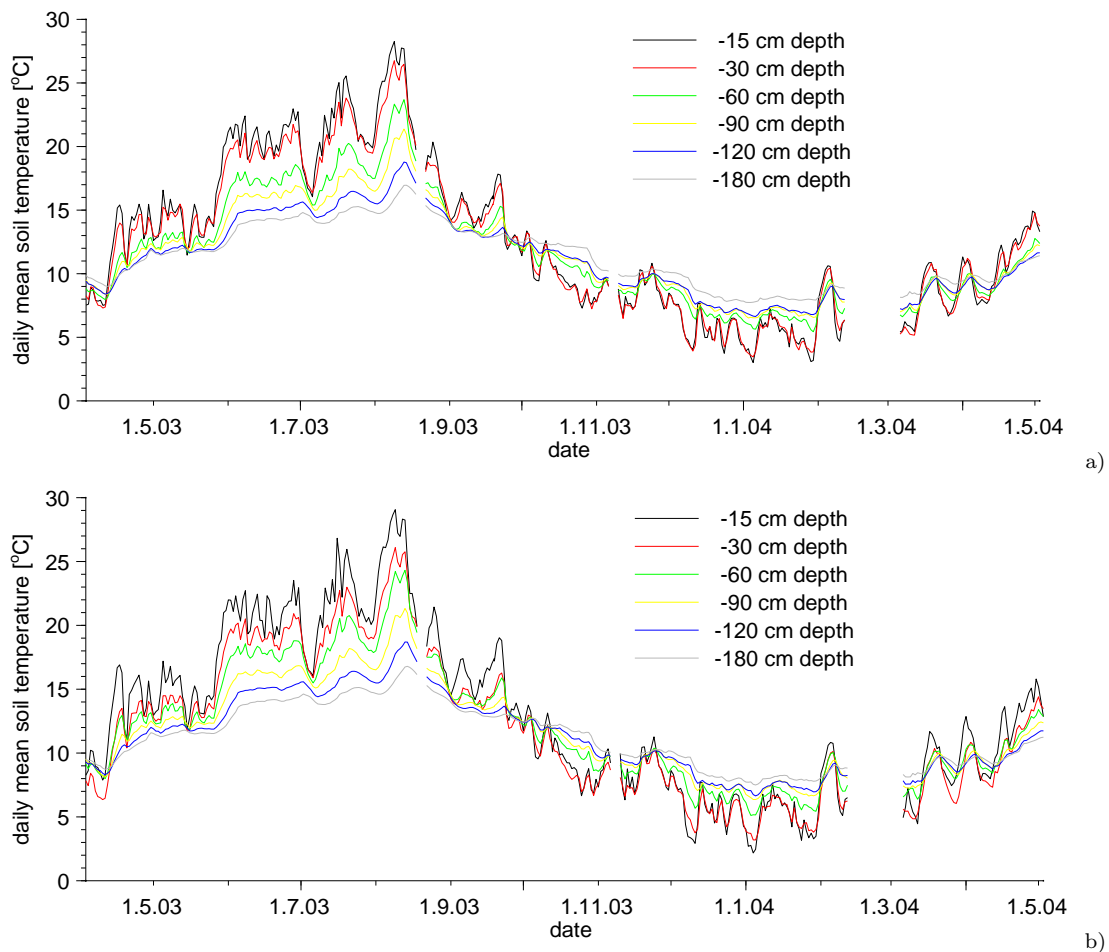
Figure 7.32: Daily mean soil temperature at 15, 30, 60, 90, 120, and 180 cm depth for the lysimeters a) 1 and b) 2 (lysimeter station at the Agrosphere Institute).

TDR-measurements

In this study TDR probes were used to determine the water content in the lysimeters. The volumetric water content was calculated as an average of 2 replications for each depth. The volumetric water content of the two lysimeters depicted in Figure 7.33 shows an annual variation in the top layer and just small changes in the deeper horizons. The lower water contents at a depth of 175 to 195 cm for both soils is visible within the first year of the measurement period. Due to the dramatic and sudden change of the water content the results may be related to problems in the TDR signal, which leads to erroneous θ data. The higher water content at 40 cm depth of lysimeter 1 θ (40 cm) = >20 % compared to lysimeter 2 θ (40 cm) = $\sim$ 10 % correlates with higher matric potentials measured by tensiometry in lysimeter 1 (Figure 7.31). If the hydraulic function plotted in Figure 4.2 will be compared with the tensiometer measurements and

the TDR results in lysimeter 2, it will be obvious that a measurement error occured in the TDR-signal.
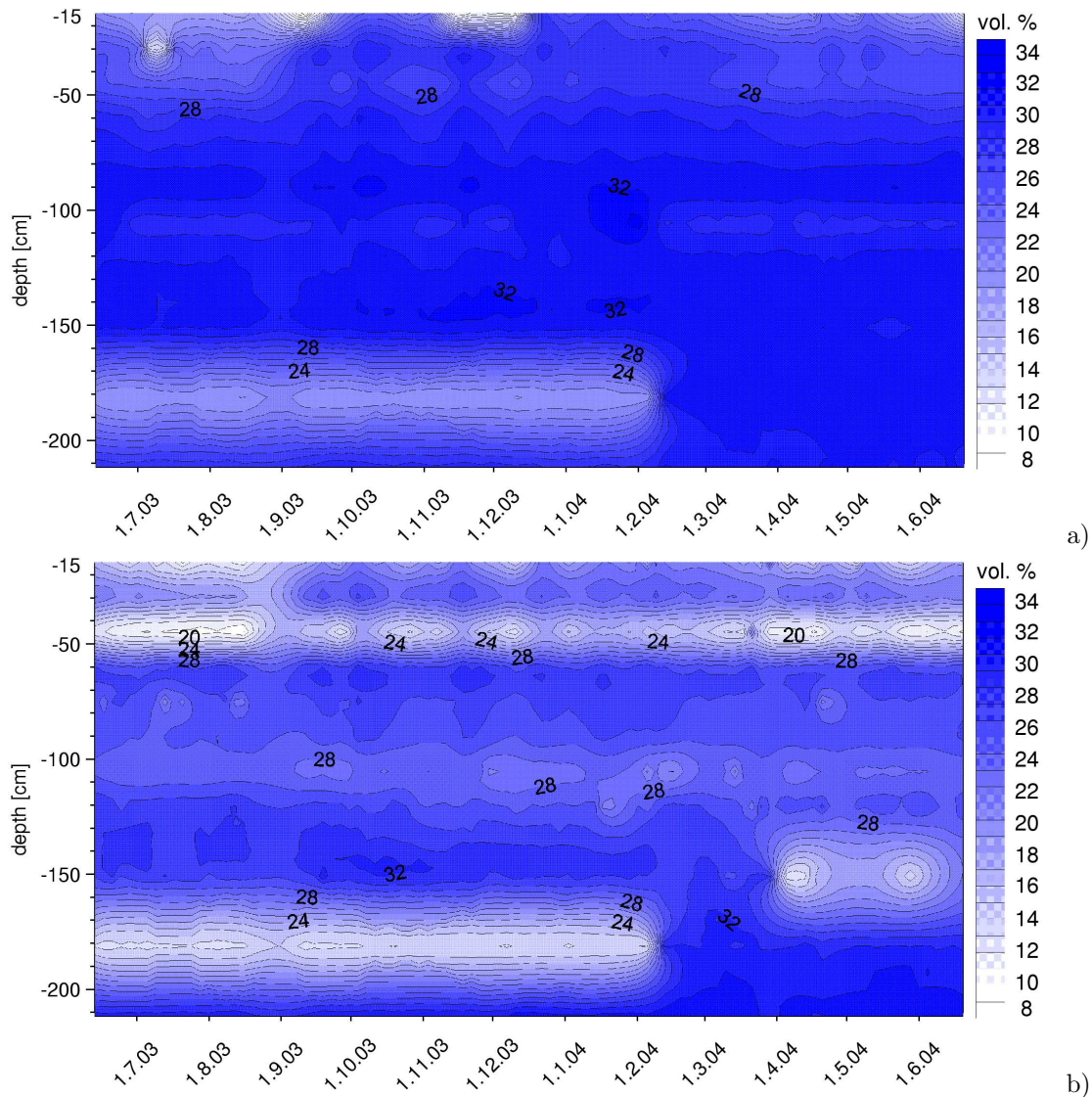
Figure 7.33: Temporal change of the volumetric water content in the lysimeters at the lysimeter station at the Agrosphere Institute measured by TDR for lysimeter a) 1 and b) 2. Note that the TDR installation depths are 15, 30, 45, 60, 75, 90, 120, 150, 180, and 210 cm, respectively

Extracted amount of water

The cumulative leachate at the bottom of the two lysimeters shown in Annex A.10 and Figure 7.34 shows a clear annual trend with high leaching rates during the winter months. The spatial variability between the single segments with larger amounts of drainage water in the inner segments of both lysimeters is in contrast to the assumption that preferential flow along the lysimeter casting occurs during certain specific boundary

conditions. At least the amounts are not too large compared to what is leached in the inner segments. This might lead to the conclusion that a preferred percolation in the inner area of the soil column occured. It seems to be more reasonable that the leaching behaviour might be an artifact of the system, due to the low applied suction of 10 cm at the lower boundary, resulting in water saturation above the sintered steel-plate and percolation to the deepest point which is in the center of the plate.
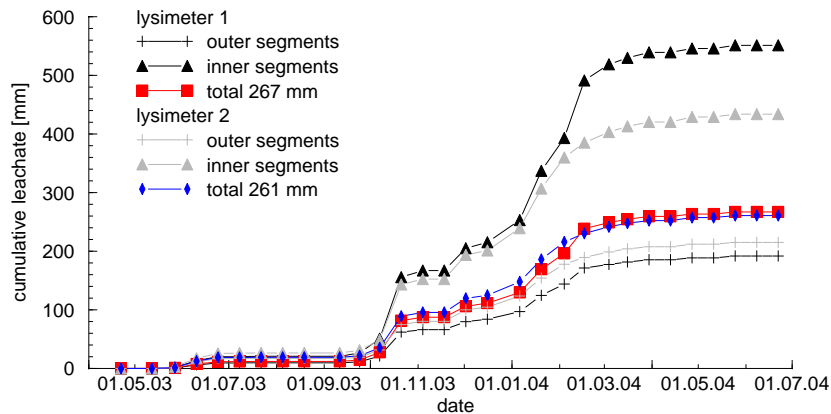
Figure 7.34: Cumulative leachate at the bottom of the lysimeters at the lysimeter station Agrosphere Institute.

In contrast to the spatial varibility just small differences are detectable for the total amount of leachate in the two lysimeters with slightly higher percolation in lysimeter 1 (267 mm) compared to lysimeter 2 (261 mm). Regardless of the spatial differences the total drainage of the lysimeters indicates a comparable leaching behaviour over time which were confirmed by the tensiometer and TDR measurements (Figure 7.31) and 7.33).
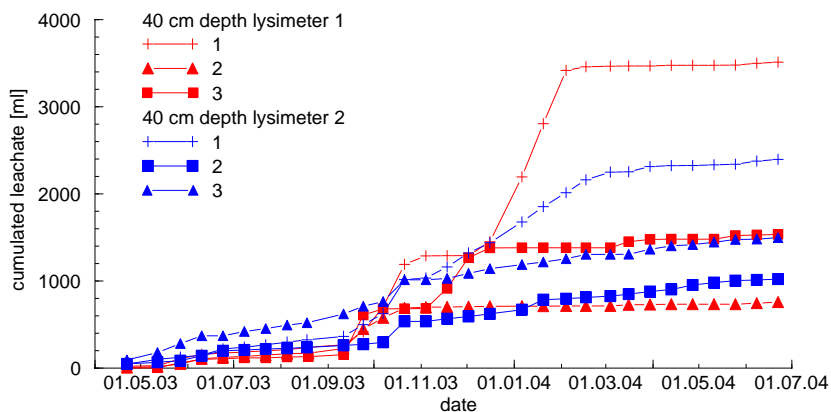
Figure 7.35: Cumulative leachate of the suction cups at 40 cm depth in the lysimeters 1 and 2.

Bromide breakthrough in suction cups   The bromide BTCs for the suction cups installed at 40 cm depth in the lysimeters at the lysimeter station demonstrate the variability of extracted soil water from 170 mm in cup 2 to 600 mm in cup 1 in lysimeter 1 (see Figure Annex A.11). The mass recovery calculated by measured concentration also varies by a factor of over 37 between cup 1 and cup 2 in lysimeter 1 and by a factor of 7 in lysimeter 2. Except for cup 1 in lysimeter 1 and cup 1 and 2 in lysimeter 2, no transport parameters could be determined by methods of moments or direct fit of the CDE. The tracer plume arrival times in the suction cups range from 19 mm in cup 1-2 to 73 mm in cup 1-1 (see Table 7.15). The mean BTCs of the two lysimeters depicted in Figure 7.36 indicate a two times higher mass recovery, slightly higher pore water velocities and dispersivities in lysimeter 2. The method of moments seems not to describe the measurements in lysimeter 1. The bromide breakthrough in the suction cups at 120 cm depth is not complete for all samplers (see Annex A.12) and, therefore, no transport parameters were estimated. The bromide mass recovery varies again from 1 % in cup 2-2 to 26.7 % in cup 1-4. The mean arrival time ranges between 19 mm in cup 1-3 to 236 mm in cup 2-1. No transport parameters could be calculated for the mean BTC for each single lysimeter, but mass recovery is comparable with about 11 %, with a two times higher arrival time in lysimeter 2.
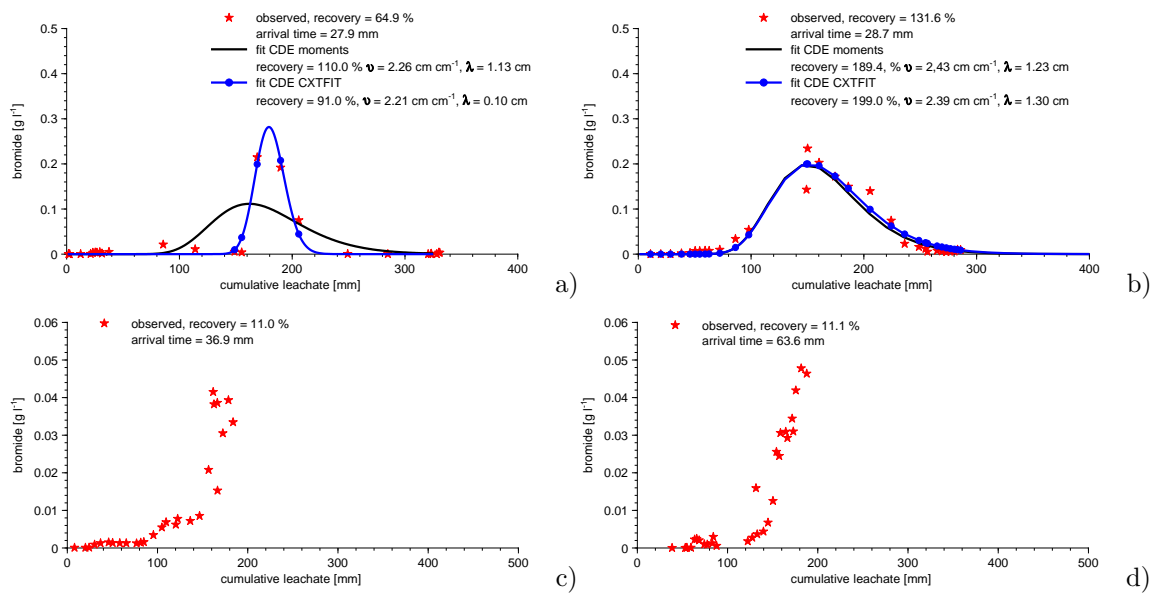
Figure 7.36: Mean bromide breakthrough for the suction cups at 40 cm depth in the lysimeters (a) 1 and (b) 2 and 120 cm depth in the lysimeter (c) 1 and (d) 2 at the station at the Agrosphere Institute. Mass recovery was calculated using the measured concentration.

Table 7.15: Bromide recovery, mean pore water velocity, *v*, dispersivity, λ, effective water saturation, Θ, and arrival time (AT) for the suction cups at 40 cm depth at the lysimeter station at the Agrosphere Institute. Note that lysimeter 1 = location 1 and lysimeter 2 = location 2. MOM = methods of moments - CDE is fitted with CXTFIT (*Toride et al.*, 1999).

| *location* | *recovery [%]* | | | v *[cm cm^{-1}]* | | λ *[cm]* | | Θ [%] | | AT |
Nr.	*mass* [†]	*MOM*	*CDE*	*MOM*	*CDE*	*MOM*	*CDE*	*MOM*	*CDE*	[mm]
1-1	493	751	822	1.10	1.105	2.05	2.72	91	95	73
1-2	11									19
1-3	183									21
mean BTC [‡]	65	110	91	2.26	2.21	1.13	0.10	44	45	37
2-1	284	412	399	1.80	1.70	1.90	2.02	55	59	26
2-2	71	88	69	4.19	3.83	1.29	0.54	24	26	35
2-3	39									177
mean BTC [‡]	132	189	199	2.43	2.39	1.23	1.30	41	42	29
mean all [§]	180	267	240	2.08	2.00	1.33	1.11	48	50	30

[†] *calculated by amount of analyzed bromide in relation to the applied bromide for the surface of the ceramic plates*

[‡] *BTC calculated by mean of all single devices in one sampling pit*

[§] *BTC calculated by mean of all single devices in both sampling pits*

Table 7.16: Bromide recovery and arrival time (AT) for the suction cups at 120 cm depth in the lysimeters at the lysimeter station at the Agrosphere Institute. Note that lysimeter 1 = location 1 and lysimeter 2 = location 2.

| *location* | *recovery [%]* | AT |
Nr.	*mass* [†]	[mm]
1-4	9	98
1-5	5	52
1-6	4	19
1-7	27	63
mean BTC [‡]	11	37
2-4	34	236
2-5	1	20
2-6	2	98
2-7	7	79
mean BTC [‡]	11	64
mean all [§]	11	50

[†] *calculated by amount of analyzed bromide in relation to the applied bromide for the surface of the ceramic plates*

[‡] *BTC calculated by mean of all single devices in one sampling pit*

[§] *BTC calculated by mean of all single devices in both sampling pits*

MBT/ETD breakthrough in the suction cups　The MBT/ETD breakthrough for the suction cups at 40 and 120 cm depth are plotted in Figure 7.37. No typical breakthrough was observed for MBT and ETD at both depths. Again, no transport parameters were determined. The mass recoveries calculated by the measured concentrations as well as the highest analyzed concentration (peak concentration) are listed in Table 7.17 and 7.18. In general, larger ETD recoveries were measured compared to the MBT. The high recovery in sampler 1-1 (0.824 %) can be traced back to the high concentrations measured over the whole sampling period, with peak concentrations up to 6.43 μg l^{-1}.
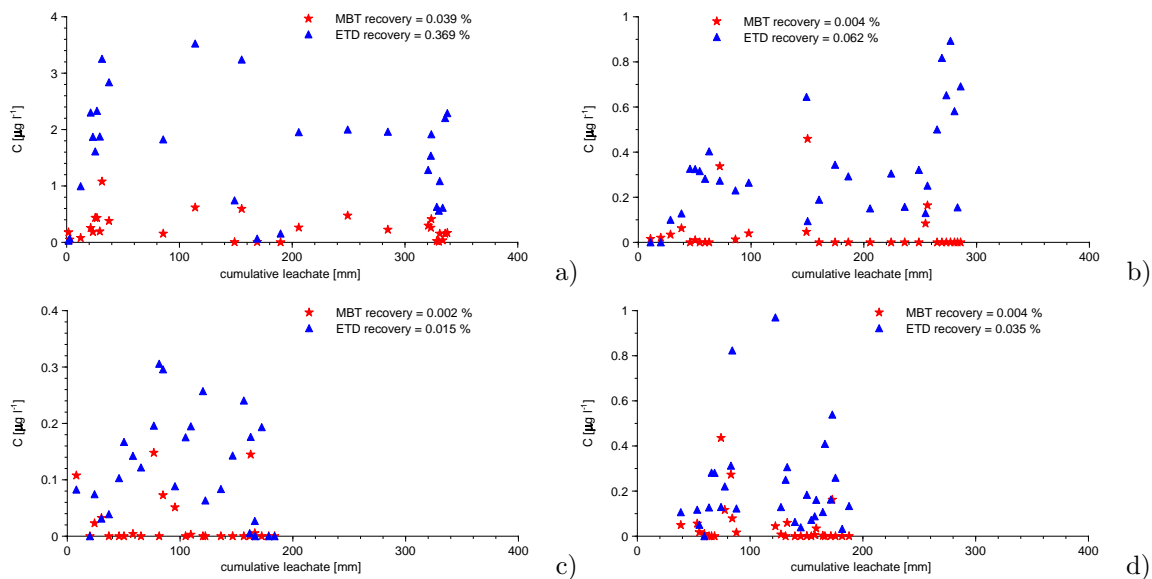
Figure 7.37: Mean MBT/ETD breakthrough for the suction cups at 40 cm depth in the lysimeters (a) 1 and (b) 2 and at 120 cm depth in the lysimeter (c) 1 and (d) 2 at the lysimeter station at the Agrosphere Institute. Mass recovery was calculated using the measured concentration.

Comparison of the samplers　Since the bromide BTCs of the various soil extraction devices as well as the mean BTC derived from the individual sampler data at the single locations indicated high variabilities, an average BTC for the three different samplers is plotted in Figure 7.38 and 7.40. The large differences in mass recovery by a factor of 10 are remarkable between the suction cups in the lysimeter and at the test site Merzenhausen. This can be regarded as an artifact of extremely high single recoveries in suction cup 1 in lysimeter 1 and 2 of 492.6 % and 284.2 %, respectively. The total amount of extracted water is also several times lower in the suction cups at the test site Merzenhausen, which might be caused by higher water contents in the lysimeters, confirmed by a four times smaller mean pore water velocity. Thus, less water transported the tracer to the same depth, resulting in a larger pore water velocity. The faster arrival time of the bromide in the suction cups in the sampling pits should be relativated due to the small total amount of extracted water. Dispersivities are less variable between the two locations compared to the pore water velocity. For the comparison of the suction

Table 7.17: MBT/ETD recovery and peak concentration for the suction cups at 40 cm depth at the lysimeter station at the Agrosphere Institute. Note that lysimeter 1 = location 1 and lysimeter 2 = location 2.

location	*ETD*		*MBT*	
Nr.	*recovery* [%]	*highest $C^{\dagger}[\mu g \ l^{-1}]$*	*recovery* [%]	*highest $C^{\dagger}[\mu g \ l^{-1}]$*
1-1	0.84	6.43	0.11	1.34
1-2	0.25	4.82	0.01	0.31
1-3	0.02	0.61	0.00	0.00
mean BTC‡	0.37	3.52	0.04	1.08
2-1	0.01	0.24	0.01	1.02
2-2	0.08	1.34	0.00	0.68
2-3	0.10	1.58	0.00	0.00
mean BTC‡	0.06	0.89	0.00	0.46

† *highest measured concentration*

‡ *BTC calculated by mean of all single devices in one sampling pit*

Table 7.18: MBT/ETD recovery and peak concentration for the suction cups at 120 cm depth at the lysimeter station at the Agrosphere Institute. Note that lysimeter 1 = location 1 and lysimeter 2 = location 2.

location	*ETD*		*MBT*	
Nr.	*recovery* [%]	*highest $C^{\dagger}[\mu g \ l^{-1}]$*	*recovery* [%]	*highest $C^{\dagger}[\mu g \ l^{-1}]$*
1-4	0.00	0.18	0.00	0.18
1-5	0.01	1.28	0.00	0.23
1-6	0.04	1.85	0.00	0.84
1-7	0.01	0.27	0.00	0.17
mean BTC‡	0.02	0.31	0.00	0.15
2-4	0.01	0.15	0.00	0.27
2-5	0.00	0.64	0.00	3.14
2-6	0.03	1.10	0.01	0.49
2-7	0.10	2.34	0.01	1.20
mean BTC‡	0.04	0.97	0.00	0.44

† *highest measured concentration*

‡ *BTC calculated by mean of all single devices in one sampling pit*

cups with the ceramic plates it has to be taken into account, that the amount of extracted water and, therefore, the mass recovery are normalized by the surface of the sampling devices. The bromide mass recovery of the ceramic plates is about 6 times higher than in the suction cups at the same location but smaller than in the lysimeters. On the other hand, the total normalized amount of extracted water is largest for the ceramic plates and 5 times lower in the suction cups in the sampling pits. Dispersivity for the different samplers in the same location are more than 2 times larger for the ceramic plates, by a 4 times smaller mean pore water velocity. The consequence of the larger dispersivity in the ceramic plates is more solute spreading and, therefore, a lower peak concentration. Due to the normalization of the extracted amount of water a direct
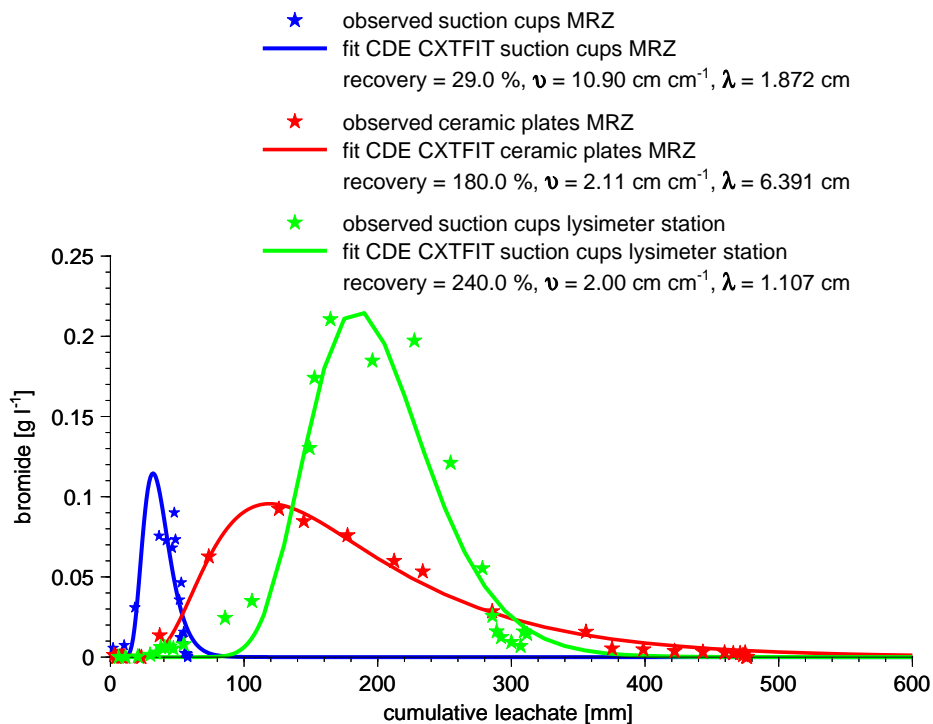
Figure 7.38: Mean bromide breakthrough at 40 cm depth for the suction cups and ceramic plates at the test site Merzenhausen and the suction cups in the lysimeters.

temporal comparison between the sampler is not directly possible. To get information of the temporal breakthrough of the tracer the bromide concentration is plotted against the time after application in Figure 7.39. As expected the time variability is less than the variability in cumulative leachate.

As expected, no total bromide breakthrough was found for the mean of all samplers at 120 cm depth. Except for the suction cups at the test site Merzenhausen, no transport parameters could be calculated. Contrary to the samplers at 40 cm depth, the bromide mass recovery is highest in the ceramic plates and about 6 times lower in the suction cups at both locations. The arrival time of the tracer plume is less variable between the location and samplers compared to the installations at 40 cm depth. The pesticide BTCs showed no total breakthrough for all samplers and locations. Therefore, no transport parameters could be determined. In general, only small recoveries < 2 % were measured.
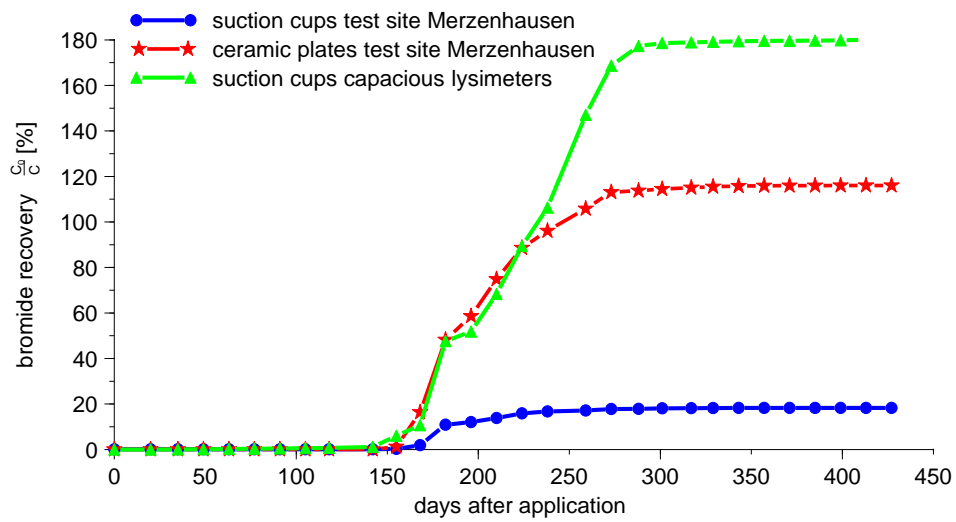
Figure 7.39: Bromide recovery at 40 cm depth for the suction cups and ceramic plates at the test site Merzenhausen and the suction cups in the lysimeters.
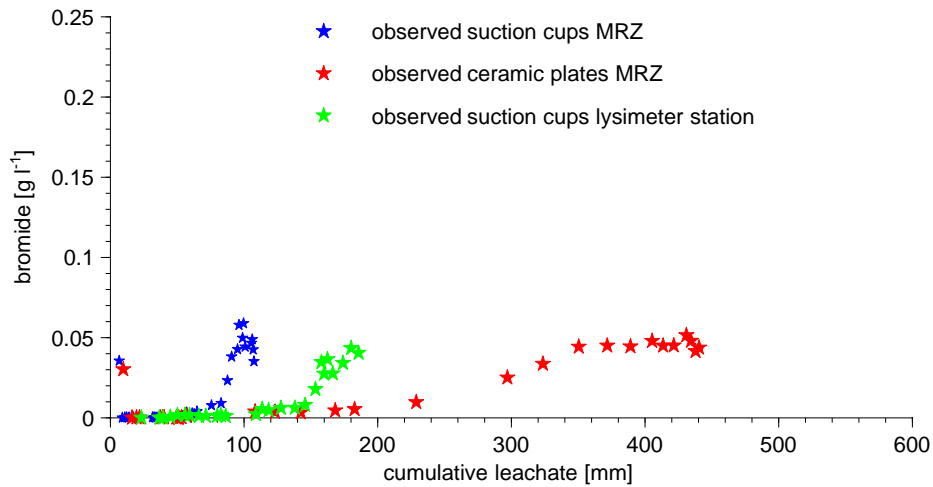
Figure 7.40: Mean bromide breakthrough at 120 cm depth for the suction cups and ceramic plates at the test site Merzenhausen and the suction cups in the lysimeters.

Summarizing the main experimental findings, a large variability in bromide breakthrough curves between the various samplers and between the locations was measured, resulting in differences in mass recovery, tracer arrival time, mean pore water velocity, and dispersivity. On the other hand no transport parameters could be determined for the pesticide breakthrough at all locations. *Kasteel et al.* (2004) used numerical sim-
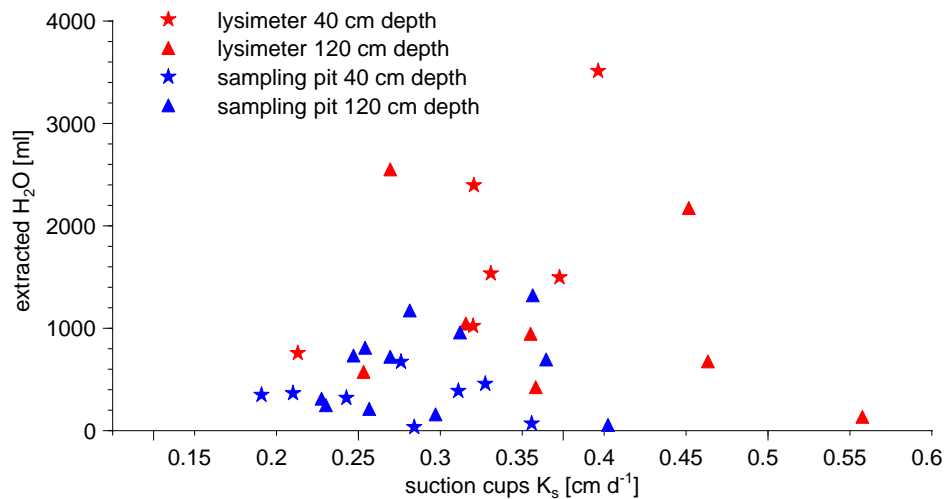
Figure 7.41: Correlation of the total amount of extracted soil water [ml] of the suction cups in field and lysimeter experiments with the saturated hydraulic conductivity [cm d^{-1}] of the cups.

ulations in a heterogeneous soil profile to explain the variability of extracted amount

of water and mass recovery of a conservative tracer in the ceramic plates at the test site Merzenhausen. They stated that the lower mass recovery and amount of extracted water cannot necessarily be explained by occasional breakdowns of the suction system due to the obligatory technical defects, but by the fact that part of the water apparently circumvented the suction plates. On the other hand, high recoveries and amounts of extracted water might be described to channeled water flow to the suction plates and/or by partially upward flow of water due to evaporation during the summer time, resulting in an ascending or stagnation of the tracer plume and, therefore pronounced bromide sampling. They also showed that the material hydraulic properties (K_s) of the ceramic plates might influence the results. This means that the amount of water collected by the ceramic plates directly depends on the flow resistance of the suction plates in combination with the hydraulic properties of the soil. If we take into account that some of the ceramic plates were replaced during the latest experiment and that the saturated hydraulic conductivity differs for the plates the detected variabilities can be explained. The same sensitivity of the material properties for the suction cups was shown in Chapter 7.1.2. A correlation of the saturated hydraulic conductivity K_s of the suction cups with the total amount of extracted water shows no coherence (Figure 7.41). In general, the extracted bulk water is larger for the lysimeters compared to the field plot due to higher water contens in the lysimeters (see Figure 7.22 and 7.31). In contrast to the results of the numerical simulations (Chapter 7.1.2) the hydraulic conductivity of the suction cups seems to play a minor role for the amount of extracted soil water compared to the local heterogeneity of the surrounding soil (see Chapter 7.1.3).

The main result of the experimental part was the perception that the installation of only few suction cups (6 at a depth of 40 cm in the lysimeters and 8 at a depth of 40 cm at the test site Merzenhausen), especially if only half of them hardly sample any solute or water, is not suitable to describe effective mass flow in field-scale experiments and to compare the transport measured with suction cups and ceramic plates. Therefore, the main disadvantage of the suction cups can be seen in the fact that more samplers are necessary to define a field average breakthrough behaviour.

Chapter 8

Summary and Conclusion

In the first part of this thesis, the impact of suction cups was analyzed on the state variables of water flow and solute transport using numerical simulations in homogeneous and heterogeneous soils. The numerical simulations were performed for three soil types and two infiltration rates. As a result three typical characteristics have been defined to describe the effect of the suction cups on the flow field:

1. suction cup activity domain (SCAD)

2. suction cup extraction domain (SCED)

3. suction cup sampling area (SCSA)

The suction cup activity domain depends on the soil hydraulic properties, the infiltration rate, and the applied suction in the cup. In general, the SCAD is detectable within decimetres from the suction cup, with lower SCAD values for the coarser soils. The spatial extent of the activity domain showed a pronounced propagation of the matric potential differences below the suction cup. A decrease of the SCAD occurred with an increase of the infiltration. The results also indicated that the SCAD is not a static region for non-stationary conditions. The numerical experiments showed good agreement with the analytical results presented by *Warrick and Amoozegar-Fard* (1977) who also found a pronounced propagation of the matric potential differences below the suction cup. The results for the non-stationary conditions were also in good accordance to the findings of the numerical experiments of *Germann* (1972).

Also the suction cup sampling area depends on the soil hydraulic properties, the infiltration rate, and the applied suction in the cup. Again, lowest SCSA values were found for the coarser soils. A decrease in the SCSA was observed with an increase of the infiltration. The analyses of the sampling area resulted in qualitative estimations that correspond to those derived using the analytical solutions of *Warrick and Amoozegar-Fard* (1977) with a dependency of the SCAD on the soil hydraulic properties and smallest SCAD for the coarser soils. The numerical model used by *Grossmann* (1988) indicated that the water content of the soil influences the SCSA which was confirmed by the numerical simulations.

The suction cup extraction domain reflects the region where water is extracted from. Therefore, it is not useful to interpret changes in matric potential (SCAD) as the extraction domain. Furthermore, the extraction domain is a function of time, and therefore,

not a static region. For prolonged sampling times, soil water will also be sampled which is not in the direct vicinity of the cup. Thus, soil water sampled from the profile will not necessarily represent the solute concentration at the depth of the suction cup and it might even be extracted from below the cup. The analytical solutions of the SCED derived by *Warrick and Amoozegar-Fard* (1977) and *Hart and Lowery* (1997) did not fit to the data of this study due to problems in parameter estimation of the α-parameter in the *Gardner* Equation. Also, no time dependent extraction domain could be deduced by the authors.

The detected arrival time of a tracer pulse in the suction cup was shorter compared to the undisturbed case. Also the tailing of the breakthrough was more pronounced using suction cups compared to the undisturbed case, because of the deflection of the streamlines towards the cup. This resulted in longer percolation distances before reaching the cup. As a consequence, enhanced spreading of the breakthrough curve will occur compared to solute transport in the undisturbed case. The mean travel time of the tracer pulse at the lower boundary (seepage face) will be delayed if extraction of soil water is performed by suction cups under continuous applied suction. This effect should be taken into account if suction cups are used to predict solute transport in lysimeters.

The numerical simulations showed that the amount of extracted water increased with the increase in applied suction, finally approaching an asymptotic value. At the same time, differences were detected between the three soils, with largest extraction rates for the clay loam and the lowest for the sandy soil. These findings match the results of the numerical approach of *Van der Ploeg and Beese* (1977) who observed that the amount of water increased with higher applied suctions. Furthermore, they observed that the relation between applied suction and the amount of extracted water was not linear.

The hydraulic properties of the suction cup also influence the amount of extracted water and solute mass besides the infiltration rate, applied suction in the cup and soil hydraulic properties. Therefore, it is necessary to define the saturated hydraulic conductivity for each single sampler, and if possible, to choose suction cups with saturated conductivities larger than the surrounding soil. The measurement of the saturated hydraulic conductivity is also fundamental to eliminate suction cups with manufactoring defects.

In the second part of the thesis different solute sampling devices, namely suction cups and porous plates, were studied in a field and lysimeter experiment over a 427 day period. As test compounds a conservative tracer (bromide) and two pesticides, namely Methabenzthiazuron (MBT) and Ethidimuron (ETD), were applied. In general, the two lysimeters at the lysimeter station at the *Agrosphere Institute* showed comparable leaching behaviour over time, reflected by tensiometer, TDR and drainage measurements. In comparison to the lysimeters, the sampling pits at the test site Merzenhausen showed lower water contents and amounts of extracted water over the whole sampling period. These differences can be explained by the presence of variability in the climatic data (e.g. precipitation and evaporation) caused by microclimatic distinctions at the two locations or by much higher initial water contents in the lysimeters prior to installation.

The variability in the breakthrough behaviour of bromide at 40 cm depth for the different samplers at the two locations is reflected in the variability of the mass recovery, mean pore water velocity, v, and dispersivity, λ. The large differences in mass recovery by a factor of 10 are remarkable between the suction cups in the lysimeters and at the

test site Merzenhausen. This can be regarded as an artifact of extremely high single recoveries in two suction cups. The total amount of extracted water is also several times lower in the suction cups at the test site Merzenhausen, which might be caused by higher water contents in the lysimeters, confirmed by a four times smaller mean pore water velocity. Dispersivities are less variable between the two locations compared to the pore water velocity. The bromide mass recovery of the ceramic plates is about 6 times higher than in the suction cups at the same location but smaller than in the lysimeters. On the other hand, the total normalized amount of extracted water is largest for the ceramic plates and 5 times lower in the suction cups in the sampling pits. Dispersivity for the different samplers in the same location are more than 2 times larger for the ceramic plates, by a 4 times smaller mean pore water velocity. The consequence of the larger disperisvity in the ceramic plates is more solute spreading and, therefore, a lower peak concentration. The results of the field and lysimeter experiments show that no complete tracer breakthrough was observed at the depth of 120 cm for the sampling pits and the lysimeters as a consequence of the short sampling time and the very dry summer in 2003. A comparison between the suction cups, ceramic plates and the lysimeter is not possible due to the total length of 240 cm for the lysimeter. Contrary to the samplers at 40 cm depth, the bromide mass recovery is highest in the ceramic plates and about 6 times lower in the suction cups at both locations. The arrival time of the tracer plume is less variable between the locations and samplers compared to the installation at 40 cm depth. As a result of redardation, the breakthrough of the test substances MBT and ETD is far from being complete even for the samplers at 40 cm depth. Therefore, no transport parameters could be determined for the pesticide breakthrough at all locations, and the MBT/ETD breakthrough for all locations were just described qualitatively. In general, only small recoveries <2 % were measured. In general, larger ETD recoveries were measured compared to the MBT for all samplers, whereby high peak concentrations in the samplers can be traced back to single events.

Kasteel et al. (2004) showed that the differences in the amount of extracted water, bromide masses, and, as a result, variations in transport parameters in the ceramic plates were closely related to the heterogeneity of the surrounding soil. The numerical simulations presented in this study indicated that the variability in bromide breakthrough measured by suction cups can also be explained by the local heterogeneity in the hydraulic properties of the surrounding soil. The larger variability of the suction cups compared to the ceramic plates can be explained by the smaller surface area of the suction cups and, therefore, smaller integration over the sampling area and larger influence of local heterogeneity. Especially bypass flow is likely to be missed using suction cups (*England*, 1974; *Shaffer et al.*, 1979; *Roth et al.*, 1990a; *Flury et al.*, 1994). The comparison of the breakthrough in the suction cups and the ceramic plates is not directly possible due to uncertainties in the normalization of the amount of extracted water and the lack of knowledge of the SCED and SCSA for transient conditions for the suction plates as well as for the suction cups.

The main result of the experimental part was the perception that the installation of only few suction cups (6 at a depth of 40 cm in the lysimeters and 8 at a depth of 40 cm at the test site Merzenhausen), especially if only half of them hardly sample any solute or water, is not suitable to describe effective mass flow in field-scale experiments and to compare the transport measured with suction cups and ceramic plates. Therefore, the

main disadvantage of the suction cups can be seen in the fact that more samplers are necessary to define a field average breakthrough behaviour.

Bibliography

AGBoden, *Bodenkundliche Kartieranleitung*, 4. Auflage, E. Schweizbart'sche Verlags-buchhandlung, Stuttgart, 1994.

Alberts, E., R. Burwell, and G. Schuman, Soil nitrate-nitrogen determined by coring and soil solution extraction techniques, *Soil Science Society of America Journal*, *41*, 90 – 92, 1977.

Altfelder, S., T. Streck, and J. Richter, Nonsingular sorption of organic compounds in soil: The role of slow kinetics, *Journal of Environmental Quality*, *29*, 917 – 925, 2000.

Altfelder, S., T. Streck, M. Maraqa, and T. Voice, Nonequilibrium sorption of dimethylphthalate - Compatibility of batch and column techniques, *Soil Science Society of America Journal*, *65*, 102 – 111, 2001.

Andersen, B., Dissolved inorganic and organic phosphorus in soil water from an acid forest soil collected by ceramic and PTFE soil water samplers, *Bulletin Environmental Contamination and Toxicology*, *53*, 361 – 367, 1994.

Barbarick, K., B. Sabey, and A. Klute, Comparison of various methods of sampling soil water for determining ionic salts, sodium, and calcium content in soil columns, *Soil Science Society of America Journal*, *43*, 1053 – 1055, 1979.

Barbee, G., and K. Brown, Comparison between suction and free drainage soil solution samplers, *Soil Science*, *141*(2), 149 – 154, 1986.

Barcelona, M., J. Helfich, and E. Garske, Verification of sampling methods and selection of materials for ground-water contamination studies, *Ground-Water Contamination - Field Methods, ASTM STP 963, A.G Collins and A.I Johnson, Eds., American Society for Testing and Materials, Philadelphia*, pp. 221 – 231, 1988.

Bayer, Ustilan - Technische Informationen, *Bayer AG Leverkusen*, 1975.

Bayer, Tribunil - Technische Informationen, *Bayer AG Leverkusen*, 1982.

Beese, F., Gesetzmäßigkeiten beim Transport gelöster Stoffe im Boden, *Beiträge zur Hydrologie, Sonderheft 4*, 267 – 300, 1982.

Beier, C., and K. Hansen, Evaluation of porous cup soil-water samplers under controlled field conditions: Comparison of ceramic and PTFE cups, *Journal of Soil Science*, *43*, 261 – 271, 1992.

Beier, C., K. Hansen, P. Gundersen, B. Andersen, and L. Rasmussen, Long-term field comparison of ceramic and poly(terafluorethene) porous cup soil water samplers, *Environmental Science and Technology*, *26*, 2005 – 2011, 1992.

Bell, R., Porous ceramic soil moisture samplers, an application in lysimeters studies on effluent spray irrigation, *New Zealand Journal of Experimental Agriculture*, *2*, 173 – 175, 1974.

Bottcher, A., L. Miller, and K. Campbell, Phosphorous adsorption on various soil water extraction cup materials: Effect of acid wash, *Soil Science*, *137*(4), 239 – 245, 1984.

Brandi-Dohrn, F., R. Dick, M. Hess, and J. Selker, Suction cup sampler bias in leaching characterization of an undisturbed field soil, *Water Resources Research*, *32*(5), 1173 – 1182, 1996.

Bredemeier, M., N. Lamersdorf, and G. Wiedey, A new mobile and easy to handle suction lysimeter for soil water sampling, *Fresenius Journal of Analytical Chemistry*, *336*, 1 – 4, 1990.

Briggs, L., and A. McCall, An artifical root for including capillary movement of soil moisture, *Science*, *20*(513), 566 – 569, 1904.

Brooks, R., and A. Corey, Hydraulic properties of porous media, *Hydrology Paper No.3, Civil Engineering Department, Colorado State University, Fort Collins; Colorado*, 1964.

Brumhard, B., Lysimeterversuche zum Langzeitverhalten der herbizide Matamitron (GOLTIX) und Methabenzthiazuron (TRIBUNIL) in einer Parabraunerde mit besonderer Berücksichtigung der Transport- und Verlagerungsprozesse unter Einbeziehung von Detailuntersuchungen, *Dissertation an der Rheinischen Friedrich-Wilhelms-Universität zu Bonn, Berichte des Forschungszentrums Jülich GmbH; Jülich 2465*, pp. 1 – 235, 1991.

Brumhard, B., F. Führ, and W. Mittelstaedt, Leaching behaviour of aged pesticides: Standardized soil column experiments with 14C-metamitron and 14C-methabenzthiazuron, *In: Proc. British Crop Protection Conf. - Weeds, BCPC; Surrey; UK*, *2*, 585 – 592, 1987.

Buckingham, E., Studies on the movement of soil moisture, *Bulletin 38, U.S. Department of Agriculture, Bureau of Soils*, *Washington, DC*, 1907.

Caron, J., S. B. Jemia, J. Gallichand, and L. Trepanier, Field bromide transport under transient state: Monitoring with Time Domain Reflectrometry and porous cup, *Soil Science Society of America Journal*, *63*, 1544 – 1553, 1999.

Cole, D., Alundum tension lysimeters, *Soil Science*, *85*, 293 – 296, 1958.

Creasey, C., and S. Dreiss, Porous cup samplers: Cleaning procedures and potential sampling bias from trace element concentration, *Soil Science*, *145*, 93 – 101, 1988.

Czeratzki, W., Saugvorrichtung für kapillar gebundenes Bodenwasser, *Landbauforschung Völkenrode*, *21*(1), 13 – 14, 1971.

Dahiya, J., J. Richter, and R. Malik, Soil spatial variability: A review, *International Journal of Tropical Agriculture*, *2*(1), 1 – 102, 1984.

Dahiya, J., R. Anlauf, K. Kersebaum, and J. Richter, Spatial variability of some nutrient constituents of an Alfisol from loess: 2 geostatistical analysis, *Zeitschrift für Pflanzenernährung und Bodenkunde*, *148*, 268 – 277, 1985.

Darcy, H., Les fontaines de la ville de dijon, *Dalmont, Paris*, 1856.

Dazzo, F., and D. Rothwell, Evaluation of porcelain cup water samplers for bacteriological sampling, *Applied Microbiology*, *27*(6), 1172 – 1174, 1974.

Debyle, N., R. Hennes, and G. Hart, Evaluation of ceramic cups for determining soil solution chemistry, *Soil Science*, *146*(1), 30 – 36, 1988.

Djurhuus, J., and O. Jacobsen, Comparison of ceramic suction cups and KCl extraction for the determination of nitrate in soil, *European Journal of Soil Science*, *46*, 387 – 395, 1995.

Dressel, J., Transport von Ethidimuron und Methabenzthiazuron in einer Parabraunerde - Experimente und Modellierung, *Dissertation an der Rheinischen Friedrich-Wilhelms-Universität zu Bonn*, pp. 1– 181, 2003.

Duke, H., and H. Haise, Vacuum extractors to assess deep percolation losses and chemical constituents of soil water, *Soil Science Society of America Proceedings*, *37*, 963 – 964, 1973.

DVWK, *Gewinnung von Bodenwasserproben mit Hilfe der Saugkerzen-Methode*, DVWK-Merkblätter zur Wasserwirtschaft; DK 628.112.1 Wassergewinnung; DK 556.322.2 Bodenwasser 217/1990, Kommissionsvertrieb Verlag Paul Parey, Hamburg und Berlin, 1990.

ecoTech, Bodenkunde, *Produktkatalog, ecoTech Umweltmesssysteme GmbH, Bonn*, 2001.

England, C., Comments on a technique using porous cups for water sampling at any depth in the unsaturated zone by warren w. wood, *Water Resources Research*, *10*(5), 1049, 1974.

Flemming, J., and G. Butters, Bromide transport detection in tilled and nontilled soil: Solution samplers vs. soil cores, *Soil Science Society of America Journal*, *59*(5), 1207 – 1216, 1995.

Flury, M., H. Flühler, W. Jury, and J. Leuenberger, Susceptibility of soils to preferential flow of water: A field study, *Water Resources Research*, *30*(7), 1945 – 1954, 1994.

Food and Agricultural Organization of the United Nations, FAO statistical databases, *http://apps.fao.org*, 2001.

Forrer, I., R. Kasteel, M. Flury, and H. Flühler, Longitudinal and lateral dispersion in an unsaturated field soil, *Water Resources Research*, *35*(10), 3049 – 3060, 1999.

Fortin, J., M. Flury, W. Jury, and T. Streck, Rate-limited sorption of simazine in saturated soil columns, *Journal of Contaminant Hydrology*, *25*, 219 – 234, 1997.

Franz, R., F. Applegath, F. Morriss, F. Biaocchi, and L. Breed, A new synthesis of ureas. iv. The preparation of unsemetrical ureas from carbon monoxide, sulfur, and amines, *Journal of Organic Chemestry*, *27*, 4341 – 4346, 1962.

Führ, F., R. Hance, J. Plimmer, and J. Nelson, eds., *The lysimeter concept*, ACS Symposium, Series 699, American Chemical Society, Washington D.C., USA, 1998.

Geologisches-Landesamt-Nordrhein-Westfalen, Bodenkarte von Nordrhein-Westfalen 1:25.000, Blatt 5003 Linnich, 1972.

Germann, P., Eine Methode zur Gewinnung von kapillar gebundenem Bodenwasser - Testergebnisse und erste Analysendaten, *Mitteilungen der Deutschen Bodenkundlichen Gesellschaft*, *16*, 146 – 155, 1972.

Grossmann, J., Physikalische und chemische Prozesse bei der Probenahme von Sickerwasser mittels Saugsonden, *Dissertation an der TU München*, *Institut für Wasserchemie und Chemische Balneologie der Technischen Universität München*, 1 – 108, 1988.

Grossmann, J., and P. Udluft, The extraction of soil water by the suction-cup method: A review, *Journal of Soil Science*, *42*, 83 – 93, 1991.

Grossmann, J., G. Freitag, and B. Merkel, Eignung von Nylon- und Polyvinyliden-fluoridmembranfiltern als Materialien zum Bau von Saugkerzen, *Zeitschrift Wasser-Abwasser-Forschung*, *18*, 187 – 190, 1985.

Grossmann, J., M. Bredemeier, and P. Udluft, Sorption of trace metals by suction cup of aluminum oxide, ceramic and plastics, *Zeitschrift für Pflanzenernährung und Bodenkunde*, *153*, 359 – 364, 1990.

Grover, B., and R. Lamborn, Preparation of porous ceramic cups to be used for extraction of soil water having low solute concentrations, *Soil Science Society of America Proceedings*, *34*, 706 – 708, 1970.

Guggenberger, G., and W. Zech, Sorption of dissolved organic carbon by ceramic p80 suction cups, *Zeitschrift für Pflanzenernährung und Bodenkunde*, *155*, 151 – 155, 1992.

Hack, H., Der Einsatz von Methabenzthiazuron zur frühtzeitigen Unkrautbekämpfung in Weizen, *Zeitschrift Pflanzenkrankheiten Pflanzenschutz*, *SH IV*, 251 – 255, 1968.

Hack, H., Tribunil, ein neues breit wirksames Herbizid für den Getreideanbau, *Pflanzenschutz-Nachrichten Bayer*, *22*, 341 – 360, 1969.

Hack, H., L. Eue, and W. Schäfer, Method for selective weed control in barley or wheat cultivation, *GB-Patent 1085430*, 1967.

Hajrasuliha, S., N. Baniabbassi, J. Metthey, and D. Nielsen, Spatial variability of soil sampling for salinity studies in southern iran, *Irrigation Science*, *1*, 197 – 208, 1980.

Hansen, E., and A. Harris, Validity of soil-water samples collected with porous ceramic cups, *Soil Science Society of America Proceedings*, *39*, 528 – 536, 1975.

Hart, G., and B. Lowery, Axial-radial influence of porous cup soil solution samplers in a sand soil, *Soil Science Society of America Journal*, *61*, 1765 – 1773, 1997.

Hendershot, W., and F. Courchesne, Comparison of soil solute chemistry in zero tension and ceramic-cup tension lysimeters, *Journal of Soil Science*, *42*, 577 – 583, 1991.

Hetch, W., F. Beese, and B. Ulrich, Die Beeinflussung der Bodenlösung durch Saugkerzen aus Ni-Sintermetall und Keramik, *Zeitschrift für Pflanzenernährung und Bodenkunde*, *142*, 29 – 38, 1979.

Hillel, D., *Environmental soil physics*, Academic Press, San Diego, London, Boston, New York, Sydney, Tokio, Toronto, 1998.

Hock, B., C. Fedtke, and R. Schmidt, *Herbizide, Entwicklung, Anwendung, Wirkungen, Nebenwirkungen*, Georg Thieme Verlag; Stuttgart, New York, 1995.

Hughes, S., and B. Reynolds, Evaluation of porous ceramic cups for monitoring soil water aluminium in acid soils: Comment on a paper by Raulund-Rasmussen (1989), *Journal of Soil Science*, *41*, 325 – 328, 1990.

IVA, *Wirkstoffe in Pflanzenschutz- und Schädlingsbekämpfungsmitteln*, 2nd ed., Industrieverband Agrar (IVA) e.V., BLV Verlagsgesellschaft mbH, München, 1990.

Jaekel, U., A. Georgescu, and H. Vereecken, Asymtotic analysis of nonlinear equilibrium solute transport in porous media, *Water Resources Research*, *32*(10), 3093 – 3098, 1996.

Jarczyk, H., Method of gas-chromatographic determination of Ustilan residues in soil and water, with an N-specific detector, *Pflanzenschutznachrichten Bayer*, *32*, 186 – 195, 1979.

Joslin, J., P. Mays, M. Wolfe, J. Kelly, R. Garber, and P. Brewer, Chemistry of tension lysimeter water and lateral flow in spruce and hardwood stands, *Journal of Environmental Quality*, *16*(2), 152 – 160, 1987.

Jury, W., and H. Flühler, Transport of chemicals through soils: Mechanisms, models, and field applications, *Advances in Agronomy*, *47*, 141 – 201, 1992.

Jury, W., and K. Roth, *Transfer functions and solute movement through soil: Theory and applications*, Birkhäuser, Basel and Boston, 1990.

Jury, W., and G. Sposito, Field calibration and validation of solute transport models for the unsaturated zone, *Soil Science Society of America Journal*, *49*, 1331 – 1341, 1985.

Kaiser, R., Kleinparzellen- und Feldversuch zur Beschreibung der räumlichen Variabilität des Verlagerungsverhaltens der Wassertracer 2.6-Difluorbenzoesäure und Bromid, sowie des 13/14C-markierten Wirkstoffs Ethidimuron in einer Parabraunerde, *Dissertation an der Rheinischen Friedrich-Wilhelms-Universität zu Bonn*, pp. 1 – 165, 2002.

Kasteel, R., T. Pütz, and H. Vereecken, Bromide transport in a heterogeneous field soil with transient unsaturated flow measured by soil coring, suction plates, and lysimeters, *Vadose Zone Journal*, (in process), 2004.

Kenaga, E., Predicted bioconcentration factors and soil sorption coefficients of pesticides and other chemicals, *Ecotoxicology and Environmental Safey*, *4*, 26 – 38, 1980.

Kidd, H., and D. James, *The Agrochemical Handbook; 3th ed*, Royal Society of Chemistry, Cambridge, UK, 1991.

Kimmerle, G., and E. Löser, Akute und subchronische Toxizität von Tribunil, *Pflanzenschutznachrichten Bayer*, *22*, 361 – 393, 1969.

Klute, A., F. Whisler, and E. Scott, Soil water diffusivity and hysteresis data from radial flow pressure cells, *Soil Science Society America Proceedings*, *28*, 160 – 163, 1964.

Koch, D., and M. Grupe, Schwermetall-Sorptionsverhalten einer Saugkerze aus porösem Borosilikatglas, *Zeitschrift für Pflanzenernährung und Bodenkunde*, *156*, 95 – 96, 1993.

Kolbe, W., Untersuchungen über Sortenverträglichkeit, Ertragsbeeinflussung und Unkrautwirkung von Tribunil im Wintergerstenbau unter Berücksichtigung der Anbauentwicklung, *Pflanzenschutz-Nachrichten Bayer*, *27*, 91 – 112, 1974.

Kolbe, W., and K. Zimmer, Zur Frage der chemischen Unkrautbekämpfung mit Tribunil im Freiland-Gemüsebau unter Berücksichtigung der Arten und Sortenverträglichkeit, *Pflanzenschutznachrichten Bayer*, *22*, 361 – 393, 1969.

Kölling, C., Numerisches Modell zur Berechnung der ungesättigten Wasserströmung in porösen Medien auf der Basis der Finiten Elemente, *Lehrstuhl für Wasserbau, TU München*, *previously unreleased*, 1987.

Kreft, A., and A. Zuber, On the physical meaning of the dispersion equation and its solutions for different initial and boundary conditions, *Chemical Engineering Science*, *33*, 1471 – 1480, 1978.

Krone, R., H. Ludwig, and J. Thomas, Porous tube device for sampling soil solution during water spreading operations, *Soil Science*, *73*, 211 – 219, 1951.

Kubo, H., R. Sato, I. Hamura, and T. Ohi, Herbicidal activity of 1,3,4-thiadiazole derivatives, *Journal of Agricultural and Food Chemistry*, *18*(1), 60 – 65, 1970.

Ledieu, J., P. DeRidder, P. DeClerck, and S. Dautrebande, A method of measuring soil moisture by time-domain reflectrometry, *Journal of Hydrology*, *88*, 319 – 328, 1986.

Levin, M., and D. Jackson, A comparison of in situ extractors for soil water, *Soil Science Society of America Journal*, *41*, 535 – 536, 1977.

Linden, D., Design, installation, and use of porous ceramic cups for measuring nitrate leaching, *Journal of Soil Science*, *44*, 435 – 449, 1977a.

Linden, D., Design, installation, and use of porous ceramic samplers for monitoring soil water quality, *Agricultural Research Service, U.S. Department of Agriculture, Technical Bulletin*, *1562*, 16, 1977b.

Litaor, M., Review of soil solution samplers, *Water Resources Research*, *24*, 727–733, 1988.

Lord, E., and M. Shepherd, Developments in the use of porous ceramic cups for measuring nitrate leaching, *Journal of Soil Science*, *44*, 435 – 449, 1993.

Magid, J., and N. Christensen, Soil solution sampled with and without tension in arable and heathland soils, *Soil Science Society of America Journal*, *57*, 1463 – 1469, 1993.

Magid, J., N. Christensen, and H. Nielsen, Measuring phosphorous fluxes through the root zone of a layered sandy soil: Comparison between lysimeter and suction cell solution, *Journal of Soil Science*, *43*, 739 – 747, 1992.

Maitre, V., G. Bourrie, and P. Curmi, Contamination of collected soil water samples by the dissolution of the mineral constituents of porous P.T.F.E. cups, *Soil Science*, *152*(4), 289 – 293, 1991.

Marques, R., J. Ranger, D. Gelhaye, B. Pollier, Q. Ponette, and O. Goedert, Comparison of chemical composition of soil solutions collected by zero-tension plate lysimeters with those from ceramic-cup lysimeters in a forest soil, *European Journal of Soil Science*, *47*, 407 – 417, 1996.

Marshall, T., and J. Holmes, *Soil Physics*, Cambridge University Press, Cambridge, New York, New Rochelle, Melbourne, Sydney, Second Edition, 1988.

McCall, P., and D. Laskowski, Measurement of sorption coefficient of organic material;test protocols for environmental fate and movement of toxicants, in *A.O.A.C. Symposium Proceedings; 94th annual meeting*, pp. 91 – 112, Washigton DC, 1980.

McGuire, P., and B. Lowery, Monitoring drainage solution concentrations and solute flux in unsaturated soil with porous cup samplers and soil moisture sensors, *Ground Water*, *32*(3), 356 – 362, 1994.

McGuire, P., B. Lowery, and P. Helmke, Potential sampling error: Trace metal adsorption on vacuum porous cup samplers, *Soil Science Society of America Journal*, *56*, 74 – 82, 1992.

Metzger, C., and L. Eue, Thiadiazolyl(5)-harnstoffe, ihre Verwendung als Herbizide und Verfahren zu ihrer Herstellung, *Offenlegungsschrift 1816568*, pp. 1 – 23, 1970.

Miller, E., and R. Miller, Physical theory for capillary flow phenomena, *Journal of Applied Physics*, *27*, 324–332, 1956.

Mitchell, M., G. McGee, P. McHale, and K. Weathers, Experimental design and instumentation for analyzing solute concentrations and fluxes for quantifying biogeochemical processes in watersheds, in *Methodology paper series of the 4th International Conference on ILTER in East Asia and Pacific Region*, pp. 15 – 21, Ulaanbaatar-Hatgal, Mongolia, 2001.

Monteith, J., Evaporation and environment, *Symposium of the Society of Experimental Biology*, *19*, 205 – 234, 1965.

Montgomery, B., L. Prunty, and J. Bauder, Vacuum through extractors for measuring drainage and nitrate flux through sandy soils, *Soil Science Society of America Journal*, *51*(2), 271 – 276, 1987.

Moore, M., A new herbicide for non selective vegetation control, *Proceedings of the 29th N.Z. Weed and Pesticide Control Conference*, pp. 130 – 134, 1976.

Morrison, R., A modified vacuum-pressure lysimeter for soil water sampling, *Soil Science*, *134*(3), 206 – 210, 1982.

Morrison, R., and B. Lowery, Effect of cup properties, sampler geometry, and vacuum on the sampling rate of porous cup samplers, *Soil Science*, *149*(5), 308 – 316, 1990.

Moutonnet, P., and J. Fardeau, Inorganic nitrogen in soil solution collected with tensionic samplers, *Soil Science Society of America Journal*, *61*, 822 – 825, 1997.

Mualem, Y., A new model for predicting the hydraulic conductivity of unsaturated porous media, *Water Resources Research*, *12*(3), 513 – 522, 1976.

Nagpal, N., Comparison among and evaluation of ceramic porous cup soil water samplers for nutrient transport studies, *Canadian Journal of Soil Science*, *62*, 685 – 694, 1982.

Narasimhan, T., and S. Dreiss, A numerical technique for modeling transient flow of water to a soil water sampler, *Soil Science*, *141*(3), 230 – 236, 1986.

Neary, A., and F. Tomassini, Preparation of alundum/ceramic plate tension lysimeters for soil water collection, *Canadian Journal Soil Science*, *65*, 169 – 177, 1985.

Nüsslein, L., and F. Arndt, Thiadiazolylharnstoffe mit herbizider Wirkung, *Offenlegungsschrift 2044442*, pp. 1 – 22, 1972.

O'Conner, K., and C. Dowding, *Geomeasurements by pulsing TDR cables and probes*, CRC Press, Boca Raton, London, New York, Washington D.C., 1999.

Parizek, R., and B. Lane, Soil-water sampling using pan and deep pressure-vacuum lysimeters, *Journal of Hydrology*, *11*, 1 – 21, 1970.

Patterson, B., P. Franzmann, J. Rayner, and G. Davis, Combining coring and suction cup data to improve the monitoring of pesticides in sandy vadose zones: A field-experiment, *Journal of Contaminant Hydrology*, *46*, 187 – 204, 2000.

Penman, H., Natural evaporation from open water, bare soil and grass, *Proceedings of the Royal Society London*, *A193*, 120 – 146, 1948.

Perrin-Garnier, C., M. Schiavon, J. Portal, C. Breuzin, and M. Babut, Porous cups for pesticides monitoring on soil solution - laboratory tests, *Chemosphere*, *26*(12), 2231 – 2239, 1993.

Perrin-Garnier, C., J.-M. Portal, M. Benoit, and M. Schiavon, Monitoring Isoproturon leaching in the field by drainage and porous cup sampling, *Chemosphere*, *32*(10), 2043 – 2048, 1996.

Philip, J., Steady infiltration from buried point sources and spherical cavities, *Water Resources Research*, *4*, 1039 – 1047, 1968.

Potschin, M., Bodenwassergewinnung mittels Saugkerzen an extremen Standorten - Möglichkeiten und Grenzen, *Journal of Plant Nutrition and Soil Science*, *162*, 193 – 199, 1999.

Printz, H., Lysimeter- und begleitende Detailuntersuchungen zum Einfluß einer Maisstrohdüngung auf Abbau und Verlagerung des Herbizidwirkstoffs Methabenzthiazuron im Boden sowie zur Bedeutung des CO-Transports unter Freilandbedingungen, *Dissertation an der Rheinischen Friedrich-Wilhelms-Universität zu Bonn*, pp. 1 – 179, 1995.

Puhl, R., and J. Hurley, Soil adsorption and desorption of Ustilan-thiadiazol-2-14C, *Mobay AG Chem Report*, *No 66596*, 1978.

Pütz, T., Lysimeterversuche zum Verlagerungsverhalten von Methabenzthiazuron und gelöstem organischen Kohlenstoff in einer Parabraunerde, Aufbau von zwei Klimameßstationen und Untersuchungen zur Validierung des Lysimetersystems, *Dissertation an der Rheinischen Friedrich-Wilhelms-Universität zu Bonn, Berichte des Forschungszentrums Jülich GmbH; Jülich 2812*, pp. 1 – 223, 1993.

Raats, P., Steady infiltration from point sources, cavities, and basin, *Soil Science Society America Proceedings*, *36*, 399 – 401, 1971.

Rasmussen, L., P. Jorgensen, and S. Kruse, Soil water samplers in ion balance studies on acidic forest soils, *Bulletin of Environmental Contamination and Toxicology*, *36*, 563 – 570, 1986.

Raulund-Rasmussen, K., Aluminium contamination and other changes of acid soil solution isolated by means of porcelain suction-cups, *Journal of Soil Science*, *40*, 95 – 101, 1989.

Reeve, R., and E. Doering, Sampling soil solution for salinity appraisal, *Soil Science*, *99*(5), 339 – 344, 1965.

Richards, L., Capillary conduction of liquids through porous mediums, *Physics*, *1*, 1931.

Richards, L., and P. Richards, Radial-flow cell for soil-water measurement, *Soil Science Society America Proceedings*, *26*, 515 – 518, 1962.

Roth, K., Steady state flow in an unsaturated, two-dimensional, macroscopically homogeneous, miller-similar medium, *Water Resources Research*, *31*(9), 2127 – 2140, 1995.

Roth, K., *Lecture Notes in Soil Physics*, Version 3.2, Institute of Soil Science University of Hohenheim, 1996.

Roth, K., H. Flühler, and W. Attinger, *Transport of a conservative tracer under field conditions: Qualitative modelling with random walk in a double porous medium*, vol. Field-Scale Water and Solute Flux in Soils, Proceedings of the Centro Stefano Franscini, Monte Verita, Ascona, Birkhäuser, Basel, Switzerland, 1990a.

Roth, K., R. Schulin, H. Flühler, and W. Attinger, Calibration of time domain reflectrometry for water content measurement using a composite dielectric approach, *Water Resources Research*, *26*, 2267 – 2273, 1990b.

Scheffer, F., and P. Schachtschabel, *Lehrbuch der Bodenkunde*, 13th ed., Ferdinand Enke Verlag, Stuttgart, 1992.

Schimmack, W., K. Bunzel, and K. Kreuzer, Sorption von Schwermetallionen aus Bodenlösungen durch Saugkerzen - Einfluss der Huminsäuren, in *Proceedings Symposium 'Wald und Wasser'*, Grafenau, 1984.

Schmidt, H., Die Wirkstoffmeldungen nach Paragraph 19 des Pflanzenschutzgesetztes - Ergebnisse aus dem Meldeverfahren für das Jahr 1994 im Vergleich zum Jahr 1993, *Nachrichtenblatt des Deutschen Pflanzenschutzdienstes*, *48*, 36 – 42, 1996.

Schmidt-Eisenlohr, A., Räumliche und zeitliche Variabilität von Bodenparametern in einer Parabraunerde aus Schwemmlöß in der Jülicher Börde, *Diplomarbeit am Geographischen Institut der Rheinischen Friedrich-Wilhelms-Universität Bonn*, pp. 1 – 80, 2001.

Searle, N., 1-Methyl-3(2-benzothiazolyl)-ureas and their use as herbicides, *U.S.A.-Patent 2756135*, 1956.

Severson, R., and D. Grigal, Soil solution concentrations: Effects of extraction time using porous ceramic cups under constant tension, *Water Resources Bulletin*, *12*(6), 1161 – 1170, 1976.

Shaffer, K., D. Fritton, and D. Baker, Drainage water sampling in a wet, dual-pore system, *Journal of Environmental Quality*, *8*, 241 – 246, 1979.

Shimshi, D., Use of porous ceramic points for the sampling of soil solution, *Soil Science*, *101*(2), 98 – 103, 1966.

Siemens, J., and M. Kaupenjohann, Dissolved organic carbon released from sealings and glues of pore water samplers, *Soil Science Society of America Journal*, *67*, 795 – 797, 2003.

Silkworth, D., and D. Grigal, Field comparison of soil solution samplers, *Soil Science Society of America Journal*, *45*, 440 – 442, 1981.

Simmons, K., and D. Baker, A zero-tension sampler for the collection of soil water in macropore systems, *Journal of Environmental Quality*, *22*, 207 – 212, 1993.

Simunek, J., M. Sejna, and M. van Genuchten, The HYDRUS-2D software package for simulating the two-dimensional movement of water, heat, and multiple solutes in variably-saturated media, Version 2.0, *U.S. Salinity Laboratory, Agricultural Research Service, U.S. Department of Agriculture, Riverside California*, 1999.

Smith, C., and R. Carsel, A stainless-steel soil solution sampler for monitoring pesticides in the vadose zone, *Soil Science Society America Journal*, *50*, 263 – 265, 1986.

Soilmoisture, E. C., Trase System I - For Soilmoisture Measurement, *Operating Instructions*, 1993.

Spangenberg, A., G. Cecchini, and N. Lamersdorf, Analysing the performance of micro soil solution sampling devices in a laboratory examination and a field experiment, *Plant and Soil*, *196*, 59 – 70, 1997.

Sposito, G., and W. Jury, Miller similtude and generalized scaling analysis, *Scaling in Soil Physics: Principles and Applications; edited by D. Hillel and D.E. Elrick. SSSA Special Puplication*, *25*, 13 – 22, 1990.

Starr, M., Variation in the quality of tension lysimeter soil water samples from a finnish forest soil, *Soil Science*, *140*, 453 – 461, 1985.

Steffens, W., Lysimeter studies on long-term fate of pesticides: The experimental design, in *7th IUPAC International Congress of Pesticide Chemistry, Poster 07B-34, Book of Abstracts Vol. III*, p. 78, 1990.

Streck, T., On field-scale dispersion of strongly sorbing solutes in soils, *Water Resources Research*, *34*(10), 2769 – 2773, 1998.

Streck, T., and J. Richter, Field-scale study of chlortoluol movement in a sandy soil over winter: II.Modeling, *Journal of Environmental Quality*, *28*, 1824 – 1831, 1999.

Swistock, B., J. Yamona, D. Dewalle, and W. Sharpe, Comparison of soil water chemistry and sample size requirements for pan vs tension lysimeters, *Water, Air and Soil Pollution*, *50*, 387 – 396, 1990.

Talsma, T., P. Hallam, and R. Mansell, Evaluation of porous cup soil water extractors: Physical factors, *Australian Journal of Soil Research*, *17*, 414 – 422, 1979.

Thomas, A., H. Duke, D. Zachmann, and E. Kruse, Comparison of calculated and measured capillary potentials from line sources, *Soil Science Society of America Journal*, *40*, 10 – 14, 1976.

Thompson, H., C. Swanson, and A. Norman, New growth-regulating compounds. I. Summary of growth-inhibitory activities of some organic compounds as determined by tree tests, *Bot. Gaz.*, *107*, 476 – 507, 1946.

Tischner, T., G. Nützmann, and R. Pöthing, Determination of soil water phosphorus with a new Nylon suction cup, *Bulletin of Environmental Contamination and Toxicology*, *61*, 325 – 332, 1998.

Topp, G., J. Davis, and A. Annan, Electromagnetic determination of soil water content: Measurements in coaxial transmission lines, *Water Resources Research*, *16*(3), 574 – 582, 1980.

Toride, N., F. Leij, and M. van Genuchten, The CXTFIT code for estimating transport parameters from laboratory and field tracer experiments, version 2.1, *Research Report No. 137, U.S. Salinity Laboratory, Agricultural Research Service, U.S. Department of Agriculture, Riverside, California*, 1999.

Trebst, A., and E. Harth, Herbicidal N-alkylated-ureas and ringclosed N-acylamides as inhibators of phytosystem II, *Zeitschrift für Naturforschung*, pp. 232 – 235, 1974.

Trinkwasserverordnung, T., Verordnung über die Qualität von Wasser für den menschlichen Gebrauch, *Bundesgesetzblatt, Teil I Nr. 24, Novellierung vom 21. Mai 2001*, 2001.

Tseng, P.-H., M. van Genuchten, and W. Jury, Simulating the performance of a vacuum solution extraction device for measuring solute flux concentrations in field soil, in *Models for Assessing and Monitoring Groundwater Quality*, edited by B. Wagner, T. Illangasekare, and K. Jensen, no. 227, pp. 133 – 140, IAHS, 1995.

UMS, Bedienungsanleitung T4 Druckaufnehmer-Tensiometer, *UMS, Umweltanalytische Meß-Systeme GmbH, München*, 2001.

Van der Ploeg, R., and F. Beese, Model calculations for the extraction of soil water by ceramic cups and plates, *Soil Science Society of America Journal*, *41*, 466 – 470, 1977.

van Genuchten, M., A closed-form equation for predicting the hydraulic conductivity of unsaturated soils, *Soil Science Society of America Journal*, *44*, 892 – 898, 1980.

van Genuchten, M., and P. Wierenga, Mass transfer studies in sorbing porous media. I. Analytical solutions, *Soil Science Society of America Journal*, *40*, 473 – 480, 1976.

van Genuchten, M., F. Leij, and S. Yates, The RETC code for quantifying the hydraulic functions of unsaturated soils, *U.S. Salinity Laboratory, U.S. Department of Agriculture, Agricultural Research Service, Riverside, California*, 1991.

Vanderborght, J., Experimental and numerical study on non-reactive solute transport in soils, *Dissertationes de Agricultura, Landbouwkundige en Toegepaste Biologische Wetenschappen, Katholieke Universiteit Leuven, Doctoraatsproefschrift Nr.349*, 1 – 310, 1997.

Vanderborght, J., A. Timmerman, and J. Feyen, Solute transport for steady-state and transient flow in soils with and without macropores, *Soil Science Society of America Journal*, *64*(4), 1305 – 1317, 2000.

Vereecken, H., U. Jaekel, O. Esser, and O. Nitzsche, Solute transport analysis of bromide, uranin and licl using breakthrough curves from aquifer sediment, *Journal of Contaminant Hydrology*, *39*, 7 – 34, 1999.

Vetterlein, D., H. Marschner, and R. Horn, Microtensiometer technique for in situ measurement of soil matric potential and root water extraction from sandy soil, *Plant and Soil*, *149*, 263 – 273, 1993.

Vogel, T., M. Cislerová, and J. Hopmans, Porous media with linearly variable hydraulic properties, *Water Resources Research*, *27*(10), 2735 – 2741, 1991.

Wagner, G., Use of porous ceramic cups to sample soil water within the profile, *Soil Science*, *94*, 379 – 386, 1962.

Warrick, A., and A. Amoozegar-Fard, Soil water regimes near porous cup water samplers, *Water Resources Research*, *13*, 203 – 207, 1977.

Webster, C., M. Shepherd, K. Goulding, and E. Lord, Comparison of methods for measuring the leaching of mineral nitrogen from arable land, *Journal of Soil Science*, *44*, 49 – 62, 1993.

Wenzel, W., and G. Wieshammer, Suction cup materials and their potential to bias trace metal analyses of soil solutions: A review, *International Journal of Environmental Analalytical Chemistry*, *59*, 277 – 290, 1995.

Wenzel, W., R. Sletten, A. Brandstetter, G. Wieshammer, and G. Stingeder, Adsorption of trace metals by tension lysimeters: Nylon membrane vs. porous ceramic cup, *Journal Environmental Quality*, *26*, 1430 – 1434, 1997.

Wessel-Bothe, S., S. Pätzold, C. Klein, G. Behre, and G. Welp, Adsorption von Pflanzenschutzmitteln und DOC an Saugkerzen aus Glas und Keramik, *Journal of Plant Nutrition and Soil Science*, *163*, 53 – 56, 2000.

Williams, J., and E. Lord, The use of porous ceramic cup water samplers to measure solute leaching on chalk soils, *Soil Use and Management*, *13*, 156 – 162, 1997.

Winkler, R., B. Stein, D. Gottschild, and M. Streloke, Prüfung und Bewertung des Eintrags von Pflanzenschutzmitteln in das Grundwasser sowie deren Bedeutung für die Entscheidung über die Zulassung, *Nachrichtenblatt des Deutschen Pflanzenschutzdienstes*, *51*(2), 38 – 43, 1999.

Wolff, R., Weathering woodstock granite near Baltimore, Maryland, *American Journal of Science*, *265*, 106 – 117, 1967.

Worthing, C., and R. Hance, *The Pesticide Manual: A World Compendium*, 9th ed., British Crop Protection Council, Farnham, UK, 1991.

Wu, L., J. Baker, and R. Allmaras, Numerical and field evaluation of soil water sampled by suction cups, *Journal of Environmental Quality*, *24*, 147 – 152, 1995.

Wüstemeyer, A., Abbau und Transport von Ethidimuron und Methabenzthiazuron in einer Parabraunerde - Beitrag zur Validierung des Lysimeterkonzepts, *Dissertation an der Rheinischen Friedrich-Wilhelms-Universität zu Bonn*, pp. 1 – 131, 2000.

Zetler, F., Ungestörte Säulenversuche zum Sorptionsverhalten von [14C]Ethidimuron und Bromid in einer Parabraunerde aus Schwemmlöß in Abhängigkeit der Beregnungsintensität und Batchveruche zur Berechnung von Adsorptions- und Desorptionsisothermen und Verteilungskoeffizienten von Ethidimuron, *Diplomarbeit an der Fachhochschule Aachen*, pp. 1 – 62, 1998.

Zimmermann, C., M. Price, and J. Montgomery, A comparison of ceramic and teflon in situ samplers for nutrient pore water determination, *Estuarine Coastal Marine Science*, 7, 93 – 97, 1978.

Zmarsly, E., W. Kuttler, and H. Pethe, *Meteorologisch-klimtologisches Grundwissen: Eine Einführung mit Übungen, Aufgaben und Lösungen*, Eugen Ulmer GmbH & Co, Stuttgart, 1999.

Appendix A

Annex

A.1 Test site Merzenhausen

A.1.1 Soil chemical parameters

The determination of the cation exchange capacity (CEC) after Mehlich was performed through exchange of the cations with a pH = 8.2 buffered triethanolamin-solution within a glass-column. After this procedure the soil was saturated with barium and in a final step the barium was exchanges by ammonium chloride, whereby the CEC is equivalent of the reexchanged barium. The S-value was determined analogous to the CEC, whereby the equivalents of the single elements calcium, potassium, magnesium and sodium were analyzed in the eluate. The pH-value was determined electrometrically in calcium chloride ($CaCl_2$) and the calciumcarbonate content ($CaCO_3$) after the Scheibler-method. The amount of organic carbon was calculated by dividing the total humus content after annealing with an empiric factor of 1.72 (memorandum LUFA Speyer).

The decalcification depth of 225 cm falsifies the results of the profile characterization and led to an undisturbed soil genesis (Figure A.1). The humus as well as the organic carbon content was depleted below the top layer (Ap-horizont). The small increase in the Bcv and C-horizont is nontypical and may be a result of poor analytics or probe extraction. The increase of the pH-value below 225 cm is closely connected to the decalcification depth (Figure A.1).

The total salinity decreases from the topsoil continuously with depth up to the Bv-horizont and increases with higher depth to the base level (Figure 4.3). These results can be explained by fertilizations. The CEC (Cation Exchange Capacity) with its S- and T-value lies in the range for typical clay-loam soils (*Scheffer and Schachtschabel*, 1992) (Figure A.2). The enhancement of the CEC within the Bt- and Btv-horizont is closely related to the enrichment of clay, wherby the higher CEC within the C-horizont might by related to low pH-values. The high calcium allocation of interchangers reflects natural processes within the soil column.
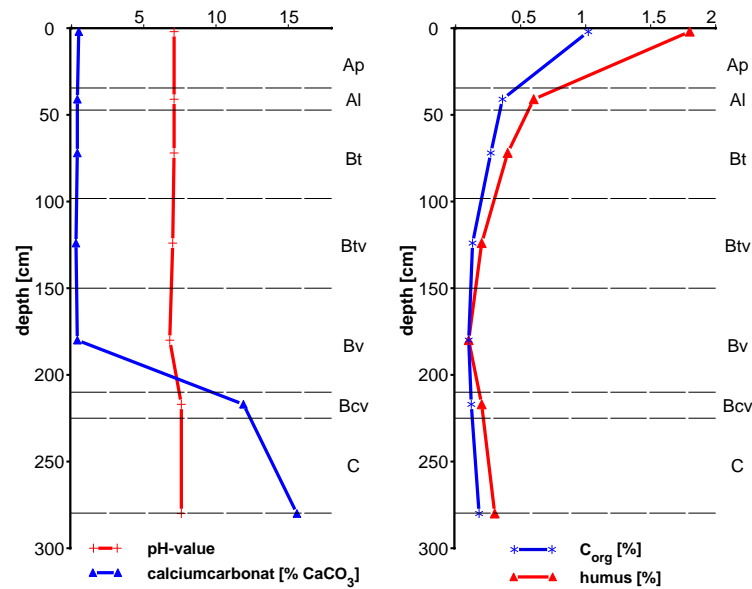
**Figure A.1: Calciumcarbonat (CaCO$_3$), pH-value, humus and C$_{org}$-content in %
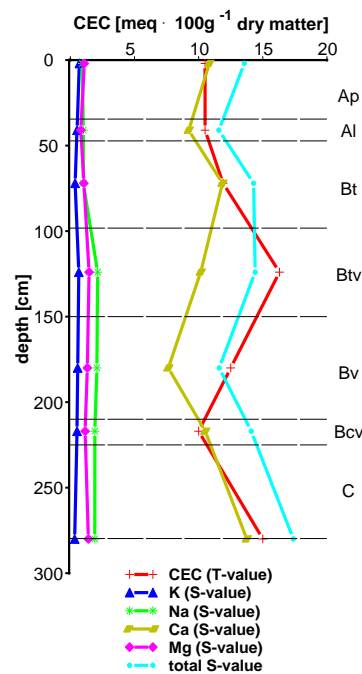by mass for the test site Merzenhausen.**

**Figure A.2: Cation exchange capacity (CEC) (S-value & T-value) in meq 100 g^{-1}
dry matter for the test site Merzenhausen.**
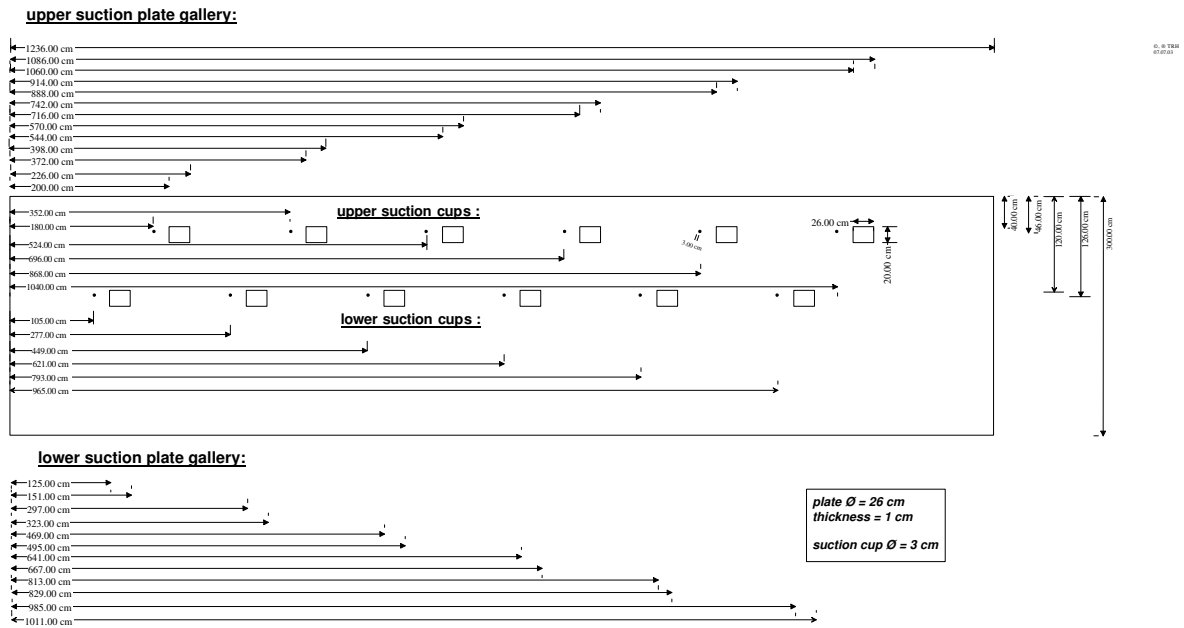
A.2   Installation

Figure A.3: Installation of the porous ceramic plates and suction cups in the sampling nests at the test site Merzenhausen. All units in cm.

A.3 Tensiometers

Table A.1: Technical data of the T4 tensiometer (*UMS*, 2001).

T4 tensiometer		
head	length	60 mm
	diameter	24 mm
	material	ceramic
shaft	length	400 mm
	diameter	24 mm
	material	plexiglas
effective range	-1000 to 850 hPa	
sensor	piezoresistive converter	

A.4 Suction cups

Table A.2: Technical data of the borosilicate-glass suction cups (*ecoTech*, 2001).

Suction cup		
cup	material	borosilicate-glass with special pores
	bubble point	at least 1000 hPa
	pore size	approximately 1 μm
	length	60 mm
	diameter	32 mm
	wall thickness	8 mm
	surface	57.3 cm^2
shaft	material	PVC
	length	300 or 500 mm
	diameter	32 mm
tubes	material	PTFE (Teflon)
	diameter	2 mm inner / 3 mm outer

A.5   Ceramic plates

Table A.3: Technical data for the porous ceramic plates (*Dressel*, 2003).

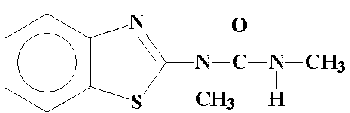| *Porous ceramic plate*	
diameter	276 ± 3 mm
surface	0.0593 m^2
wall thickness	9.5 ± 0.8 mm
bubble point	1 bar
porosity	45 %
saturated hydraulic conductivity	$8.6 \cdot 10^{-8}$ m s^{-1}
tubes	PTFE (Teflon)

A.6   Test substances

A.6.1   Methabenzthiazuron

Physicochemical properties

Methabenzthiazuron or MBT is the active ingredient formulated as 70 % of the wettable powder of the herbicide Tribunil™, which controls a broad spectrum of weeds in cereal crops. Synthesis (*Franz et al.*, 1962) and herbicidal activity of MBT are discribed in detail by *Searle* (1956) and *Hack et al.* (1967). The herbicide is nontoxic to bees (*Kidd and James*, 1991) and of minimal mammal toxicology (*Kimmerle and Löser*, 1969; *Bayer*, 1982). The physicochemical properties of MBT are given in Table A.4.

Table A.4: Physicochemical properties of Methabenzthiazuron (*Bayer*, 1982; *IVA*, 1990; *Kidd and James*, 1991).

chemical description	1-benzothiazol-2yl-1,3-dimethylurea	
CAS-register-number	18691-97-9	
structural formula		
molecular formula	$C_{10}H_{11}N_3OS$	
molecular weight	221.3 g mol^{-1}	
vapour pressure	5.9×10^{-8} hPa at 20 °C	
melting point	119 - 121 °C	
water solubility at 20° C	water: 0.059	dichloro methane: >200
[g L^{-1} solvent]	methanol: 66	n-hexane: 1 - 2
	acetone: 115.9	toluene: 50 - 100
	methylene chloride: 560	isopropanol: 20 - 50
octanol/water- partition coefficient (log$_{10}$ K$_{ow}$)	2.64	
stability:	hydrolysis:	
	pH 5 stable	photodegradation:
	pH 7 stable	stable
	pH 9 stable	thermal persistance:
		stable

Environmental fate

The compound Methabenzthiazuron, respectively the herbicide Tribunil™ 70 WP, was in use for pre- and post-emergence selective weed control in winter- and spring wheat, vegetable plantations and nurserys (*Hack*, 1968; *Kolbe and Zimmer*, 1969; *Kolbe*, 1974; *Bayer*, 1982). The recommended amount of Tribunil™ varies between 2 up to 5 kg ha^{-1}, where time of application, soil properties, kind of crop and the actual climate (soil moisture and air temperature) determines the amount of herbicide. The uptake of the active compound takes place over the root system and translocation via the transpiration

process. The uptake via the plant leaves is limited to a small proportion (*Hack*, 1968, 1969; *Bayer*, 1982). Batch-experiments with a *Parabraunerde* (FAO = luvic orthosol) showed K_{oc} -values for MBT from 247 up to 587. In addition to a classification from *Hock et al.* (1995) after *McCall and Laskowski* (1980) and *Kenaga* (1980) these values indicate low to moderate mobility. *Brumhard* (1991) also determined a K_f-value Freundlich-constant) for the *Parabraunerde* with 7.01 and a Freundlich-exponent with 0.69. In lysimeter studies the low migratory tendency of the substance confirmed the immobile character of this pesticide (*Brumhard et al.*, 1987; *Pütz*, 1993; *Printz*, 1995). A detailed description of the substance and its behaviour in soils is given by *Brumhard* (1991) and *Wüstemeyer* (2000).

A.6.2　Ethidimuron

Physicochemical properties

Ethidimuron or ETD is the active compound formulated as 70 % of the wettable powder of the total herbicide Ustilan™. Synthesis and herbicidal activity of ETD are described in detail by *Kubo et al.* (1970), *Metzger and Eue* (1970) and *Nüsslein and Arndt* (1972). The substance is nontoxic to bees and of minimal mammal toxicology (*Kidd and James*, 1991). The physicochemical properties of ETD are given in table A.5.

Table A.5: Physicochemical properties of Ethidimuron (*Bayer*, 1975; *Jarczyk*, 1979; *IVA*, 1990; *Worthing and Hance*, 1991).

chemical description	1,3-dimethyl-3(5-ethylsulfonyl-1,3,4-thiadiazol-2-yl)-urea
CAS-register number	30043-49-3
structural formula	
molecular formula	$C_7H_{12}N_4O_3S_2$
molecular weight	264.3 g mol^{-1}
vapour pressure	8.0×10^{-10} hPa at 20°C
meltingpoint	155.9 - 156.0°C

water solubility at 20° C	water: 3.04	dichloro methane: 10 - 20
[g L^{-1} solvent]	methanol: 2.0	n-hexane: ¡ 0.1
	acetone: 240	chloroform: 10.8
(log$_{10}$ K$_{ow}$)	0.43	
stability	hydrolysis:	
	pH 5 stable	photodegradation:
	pH 7 stable	UV-light sensitive
	pH 9 stable	thermal persistence:
	NaOH$_{(aq)}$:	decomposition at 217.8° C
	decomposition of 70 % in 24 h	

Environmental fate

The compound Ethidimuron, respectively the herbicide Ustilan™ 70 WP, was in use as a total herbicide on non cultivated land without any forestation as well as on railway tracks and industrial areas, squares and lanes. The recommended amount of Ustilan™ varies from 5 to 10 kg ha^{-1} at beginning of the growing season (*Bayer*, 1975) and on agricultural land an amount of 3.5 kg ha^{-1} showed good effect on vegetation for over six months (*Moore*, 1976). The uptake of the active compound takes mainly place over the root system and translocation via the transpiration process (*Bayer*, 1975), whereby the herbicid inhibits the photosystem II within the chloroplasts (*Trebst and Harth*, 1974). Batch-experiments determined K$_{oc}$-values for ETD in a *Parabraunerde* from 37.1 up to 149 (*Zetler*, 1998). In addition to a classification from *Hock et al.* (1995) after *McCall and Laskowski* (1980) and *Kenaga* (1980) these values indicate a high to very high mobility,

where as *Puhl and Hurley* (1978) determined a K_f-value from 2.37 and a Freundlich-exponent from 0.89 in a loamy soil. A detailed description of the substance and its behaviour in soils is given by *Wüstemeyer* (2000).

A.7   Equipment of the climatic station

Table A.6: Instrumentation of the climatic stations at the test site Merzenhausen (MRZ) and the lysimeter at the Agrosphere Institute, with installation high over ground in meters. All data means of minute with datalogging intervall $\Delta t = 10$ min.

Equipment	Decive	Manufacturer	MRZ	ICG-IV
windspeed	cup anemometer Porton A100	Walz, Effeltrich	0.2 & 2 m	2 m
	anemometer Typ 8470	TSI Aachen	0.02 m	
precipitation	ombrometer	Thies, Göttingen	1 m	1 m
global radiation	pyranometer Li-200 SA	Li-COR, Lincoln	2 m	2 m
net radiation	pyrradiometer	Thies, Göttingen	2 m	1m
humidity	psychrometer	Thies, Göttingen	2 m	2 m
	hygrometer	Thies, Göttingen	2 m	2 m
soil surface temperature	infrared thermometer R22	Ultrakust, Gotteszell	2 m	2 m
soil temperature	thermometer Pt100	Thies, Göttingen	-0.05 to -1 m	

A.8 Agricultural practice on lysimeters and test site Merzenhausen

Table A.7: Agricultural practice before experiments on the lysimeters at the Agrosphere Institute and the test site Merzenhausen (MRZ = test site Merzenhausen; Lys = lysimeters Agrosphere Institute).

| vegetation	date	practice
sugar beet	summer 2001	withdrawal of the lysimeters
	14.11.2001	harvest
	03.04.2002	tillage (grubing) MRZ
	10.04.2002	tillage (milling) MRZ
	22.05.2002	irrigation Lys with 40 l
	10.06.2002	tillage Lys
	14.06.2002	irrigation Lys with 32 l
	18.06.2002	irrigation Lys with 32 l
	24.06.2002	tillage & irrigation Lys with 48 l
	25-28.06.2002	irrigation Lys with 32 $\mathrm{l \cdot d^{-1}}$
	05.07.2002	tillage & irrigation Lys with 32 l
	08.07.2002	irrigation Lys with 32 l
	08.07.2002	tillage field lysimeter MRZ
	09.07.2002	irrigation Lys with 32 l
	11.07.2002	irrigation Lys with 32 l
	29.07.2002	irrigation Lys with 32 l
	11.09.2002	settling into lysimeter station
	10.09.2002	tillage (grubing) MRZ
	16.09.2002	tillage Lys
	30.09.2002	suction of 25 mbar constant head Lys
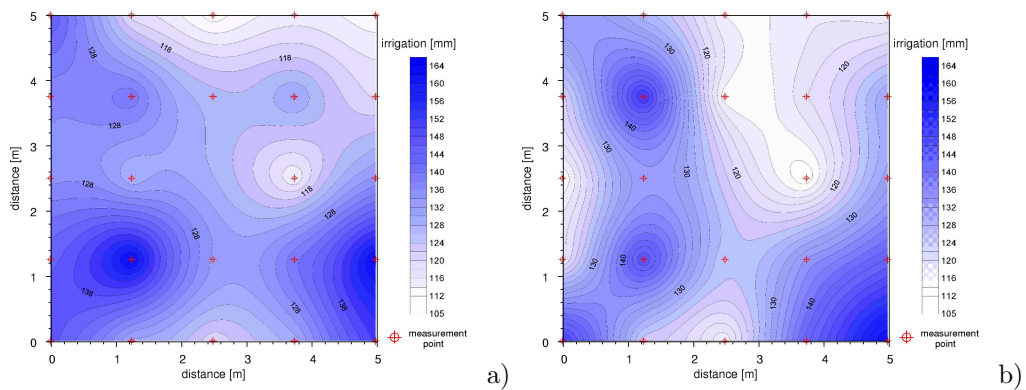
Figure A.4: Homogeneity of the irrigation process at the test site Merzenhausen.

Table A.8: Agricultural practice on the lysimeters at the Agrosphere Institute and the test site Merzenhausen (MRZ = test site Merzenhausen; Flys = field-lysimeter; Lys = lysimeters Agrosphere Institute).

date	practice	compounds
03.04.03	application MRZ/Flys/Lys	MBT/ETD/bromide
06.05.03	application Flys	round up ultra 2 % (0.4 ml m^{-2} solved in 20 ml H$_2$O)
30.06.03	application MRZ	Taifun forte (2.5 l ha^{-2} solved in 200 l H$_2$O)
08.07.03	application MRZ	Taifun forte (2.5 l ha^{-2} solved in 200 l H$_2$O)
08.09.03	irrigation	tab water: 11.45 mm in 111 min
09.09.03	irrigation	tab water: 18.20 mm in 125 min
09.09.03	tillage (max 5 cm)	
10.09.03	irrigation	tab water: 13.99 mm in 80 min
16.09.03	tillage (max 5 cm)	
16.09.03	irrigation	tab water: 6.02 mm in 96 min
17.09.03	irrigation	tab water: 8.04 mm in 115 min
01.10.03	irrigation	tab water: 28.84 mm in 183 min
14.10.03	irrigation	tab water: 10.31 mm in 75 min
11.11.03	irrigation	tab water: 18.34 mm in 135 min
31.03.04	tillage (max 5 cm)	
31.03.04	irrigation	tab water: 13.03 mm in 135 min
17.05.04	application MRZ	Taifun forte (2.5 l ha^{-2}solved in 200 l H$_2$O)

A.9   Background concentrations

Table A.9: Background bromide concentration [mg l^{-1}] in the field lysimeter, sampling pits and lysimeters Agrosphere Institute.

location	bromide concentration [mg l^{-1}]
field lysimeter	0.000110
suction cups sampling pits 40 cm depth	< 0.00002
suction cups sampling pits 120 cm depth	0.000115
suction plates sampling pits 40 cm depth	0.000035
suction plates sampling pits 120 cm depth	0.000160
lysimeter 1 suction cups 40 cm depth	0.000040
lysimeter 1 suction cups 120 cm depth	0.000215
lysimeter 2 suction cups 40 cm depth	0.000100
lysimeter 2 suction cups 120 cm depth	0.000190
lysimeter 1	0.000340
lysimeter 2	0.000265

A.10   Application of the test substances

Table A.10: Distribution of the **63** petridishes and homogeneity of the spraying process of bromide on the test site Merzenhausen. Mean value = **15.20 g m^{-2}** with a standard deviation = **2.29 g m^{-2}**. Mean value for sampling pit 2 (points **39 to 53**) = **15.39 g m^{-2}** with standard deviation = **1.80 g m^{-2}**). Mean value for sampling pit 4 (points **9 to 23**) = **16.67 g m^{-2}** with standard deviation = **2.14 g m^{-2}**.

no.	x-axis	y-axis	Br$^-$ [g m^{-2}]	no.	x-axis	y-axis	Br$^-$ [g m^{-2}]
1	0	0	16.4530	33	22.5	3.75	16.0820
2	0	7	11.8798	34	25	0	11.3191
3	2.5	3.75	15.8126	35	25	2.5	17.8114
4	5	0	17.0435	36	25	3.75	13.5336
5	5	2.5	18.4095	37	25	5	14.7666
6	5	3.75	13.1732	38	25	7.5	12.1919
7	5	5	14.6575	39	27.5	1.25	15.3901
8	5	7	10.6590	40	27.5	2.5	15.9589
9	7.5	1.25	17.5693	41	27.5	3.75	14.0154
10	7.5	2.5	17.9691	42	27.5	5	16.0262
11	7.5	3.75	15.1866	43	27.5	6.25	16.5975
12	7.5	5	17.6664	44	30	0	14.7651
13	7.5	6.25	15.5812	45	30	1.25	17.8491
14	10	0	16.6478	46	30	3.75	15.1682
15	10	1.25	18.0309	47	30	6.25	15.8524
16	10	3.75	17.1315	48	30	7	10.5433
17	10	6.25	17.3341	49	32.5	1.25	14.4929
18	10	7	11.4337	50	32.5	2.5	18.3457
19	12.5	1.25	13.8226	51	32.5	3.75	14.4961
20	12.5	2.5	19.6579	52	32.5	5	16.2800
21	12.5	3.75	19.7444	53	32.5	6.25	15.0374
22	12.5	5	15.7717	54	35	0	14.8564
23	12.5	6.25	16.4811	55	35	1.25	11.9286
24	15	0	14.0582	56	35	2.5	14.4911
25	15	2.5	16.5490	57	35	3.75	15.3238
26	15	3.75	15.6204	58	35	5	13.2325
27	15	5	15.6377	59	35	6.25	16.1895
28	15	7	11.0464	60	35	7	10.6388
29	17.5	3.75	14.5396	61	37.5	3.75	14.5727
30	20	1.25	17.3886	62	40	0	16.7711
31	20	3.75	16.1702	63	40	7	9.7237
32	20	5	14.3634				

A.11   Sorption experiments of the borosiligate-glass suction cups
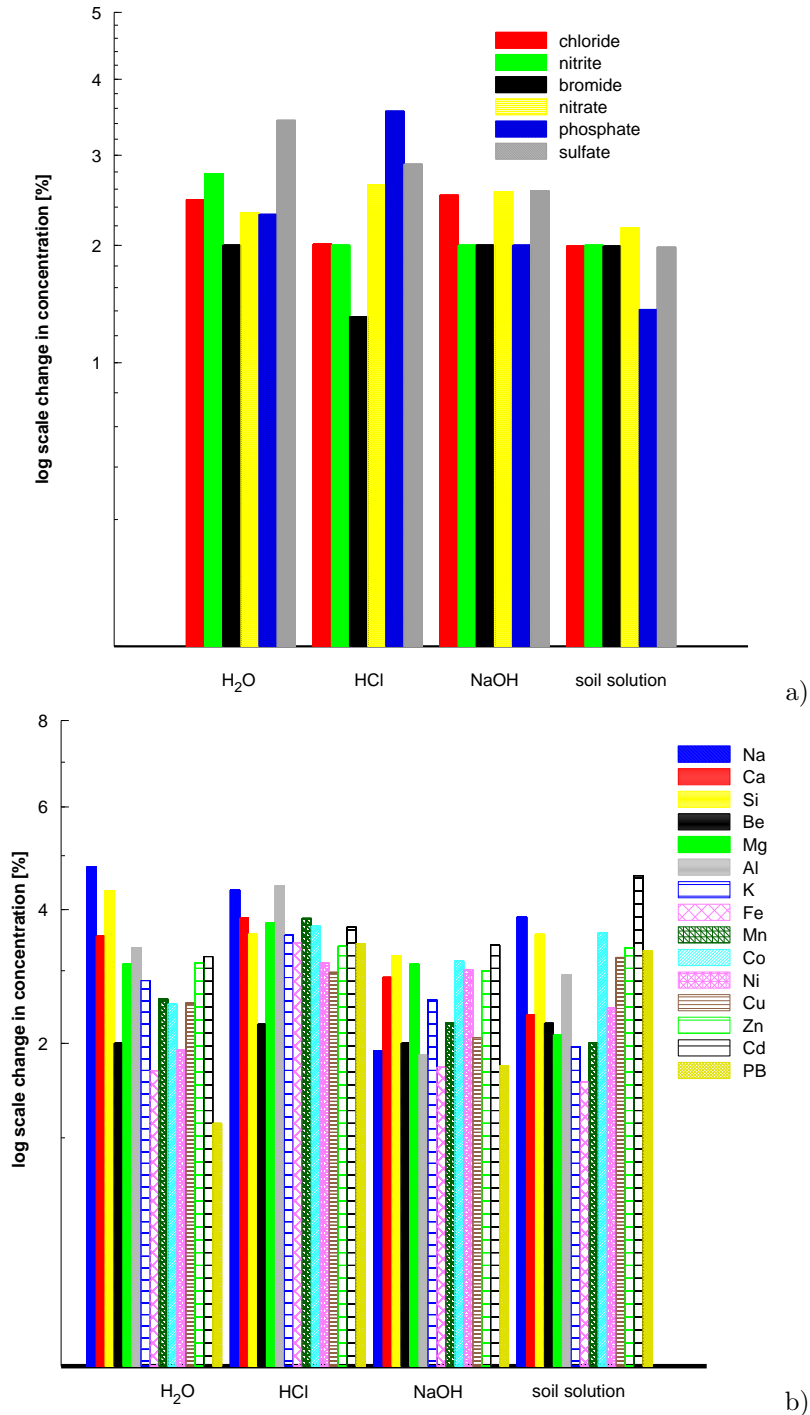

Figure A.5: Change of concentration in percent for a sorption test for a) anions and b) cations using the raw material of the borosilicate-glass suction cups.
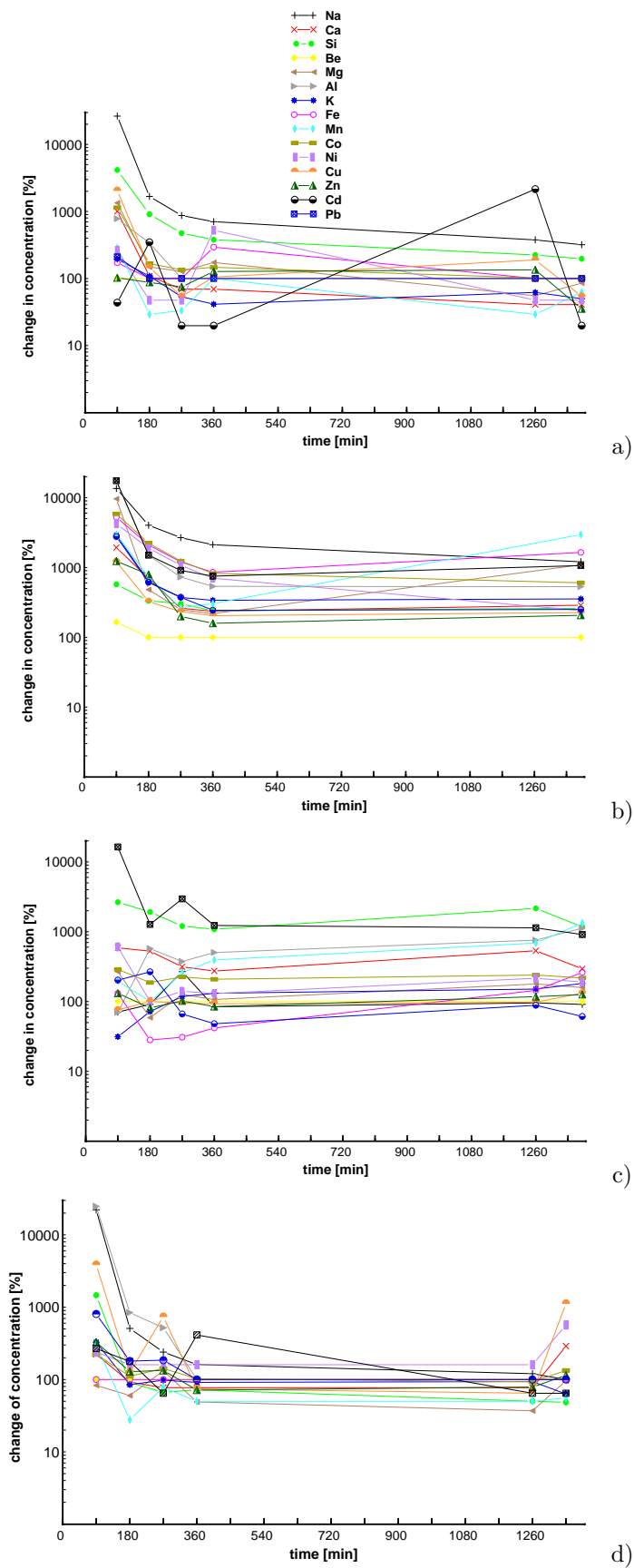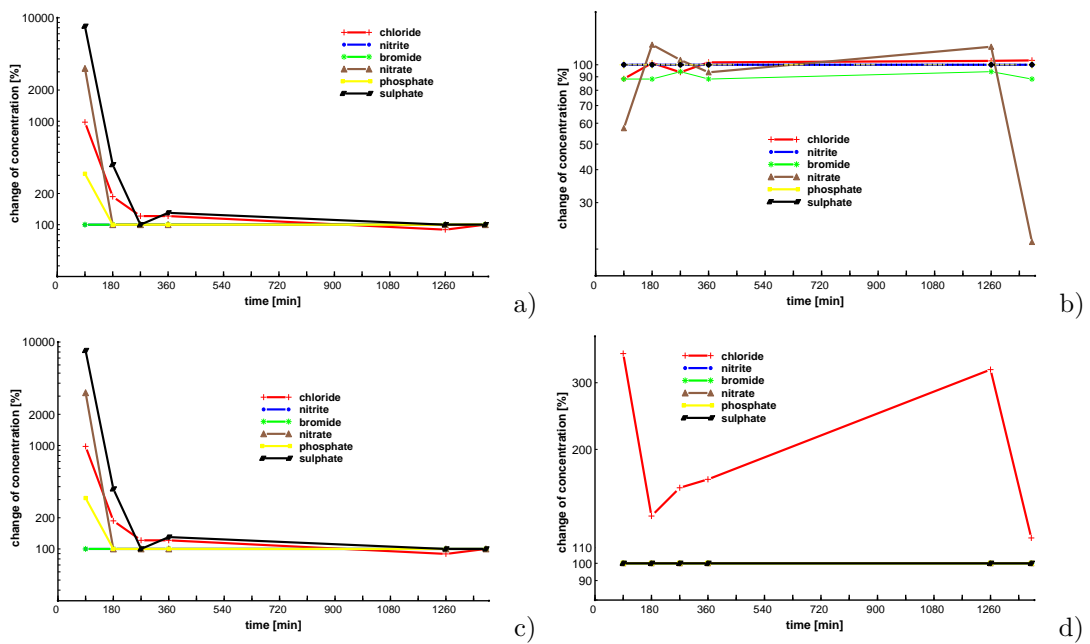
Figure A.6: Change in concentration in percent for the cleaning test of the borosilicate-glass suction cups. Rinsing with a) distilled water b) 1 N HCl$_{(aq)}$ c) 1 N NaOH$_{(aq)}$ and d) distilled water. Note: All y-axes values in log scale. No changes equals 100 %.

Figure A.7: Change of anion concentration in percent for the cleaning test of the borislicate-glass suction cups. rinsing with a) distilled water, b) 1 N HCl$_{(aq)}$, c) 1 N NaOH$_{(aq)}$ and d) distilled water.

A.12   Analytics

MBT and ETD analysis

The analysis of the herbicides MBT and ETD in aqueous solution was accomplished at the Institute Agrosphere at the Forschungszentrum Jülich GmbH using LC-MS-MS (Liquid Chromatography - Mass Spectrometry - Mass Spectrometry) technology. The LC-MS-MS contains a triple quadrupole mass spectrometer (model TSQ Quantum, year 2002) from Thermo Finnigan with an ESI (electro spray ionization) source. Argon 5.0 was chosen as collision gas. A HPLC column type LiChrospher 60 RP Select-B (CS Chromatographie Service Langerwehe) with a length of 250 mm, an inner diameter of 4 mm and a particle size of 5 μm was used. As a mobile phase in the HPLC eluenten deionized water (Millipore Milli Q Plus 185) 0.1% methanol and 0.1 % formic acid, and acetonitrile for HPLC (ACN) (For UV Gradient Grade J.T.Baker 99.8 % purity) was used. The HPLC boundary condition (gradient) was set to a flow rate of 0.25 ml min^{-1} with time 0 min with 70 % H$_2$0 and 30 % ACN, time 5 min 70 % H$_2$0 and 30 % ACN, time 13 min 0 % H$_2$0 and 100 % ACN, time 23 min 0 % H$_2$0 and 100 % ACN, time 24 min 70 % H$_2$0 and 30 % ACN and time 35 min 70 % H$_2$0 30 % ACN, respectively. The MS conditions were set to an acquire time of 35 min, whereby a divert valve was used with 0 - 15 min to waste, 15 - 27 min to ESI source and 27 - 35 min to waste.

The SRM (Selected Reaction Monitoring) mode was set to a MBT parent with a mass of 221.8 m z^{-1} ESI positive mode (ESI + mode) and an ETD parent mass of 264.9 m z^{-1} in ESI + mode. The MBT product mass of 165 m z^{-1} with an CE (collision energy) of 24 V, MBT product mass of 150 m z^{-1} with an CE of 40 V and MBT product mass of 96 m z^{-1} with CE of 58 V was selected. For ETD product mass 208 m z^{-1} with an CE of 30 V, ETD product mass of 161.9 m z^{-1} with an CE of 26 V and ETD product mass of 114 m z^{-1} with an CE of 24 V was chosen. For an injection volume of 100 μl the retention time was 19.3 min for ETD and 22.8 min for MBT. All samples were dissolved in blank soil solution.

Bromide analysis

The analysis of the bromide content in aqueous solution was accomplished by the ZCH (Zentralabteilung für Chemische Analysen) at the Forschungszentrum Jülich GmbH using ion chromatography (system: DIONEX Series 4000i). The analytical error is ±3 % and the limit of detection is 0.02 μ g ml^{-1}.

A.13   Simulated temperature distribution in lysimeters
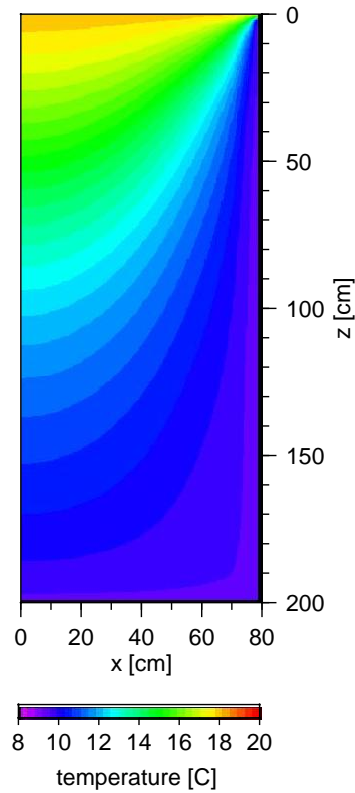

Figure A.8: Simulated HYDRUS-2D (*Simunek et al.*, **1999) temperature distribution in a sandy soil lysimeter. Upper boundary = constant temperature of 20° C. Lower and lateral boundary = constant temperature of 10° C. Axisymmetrical simulation mode. (Memorandum Tina Neef Forschungszentrum Jülich GmbH 2003).**
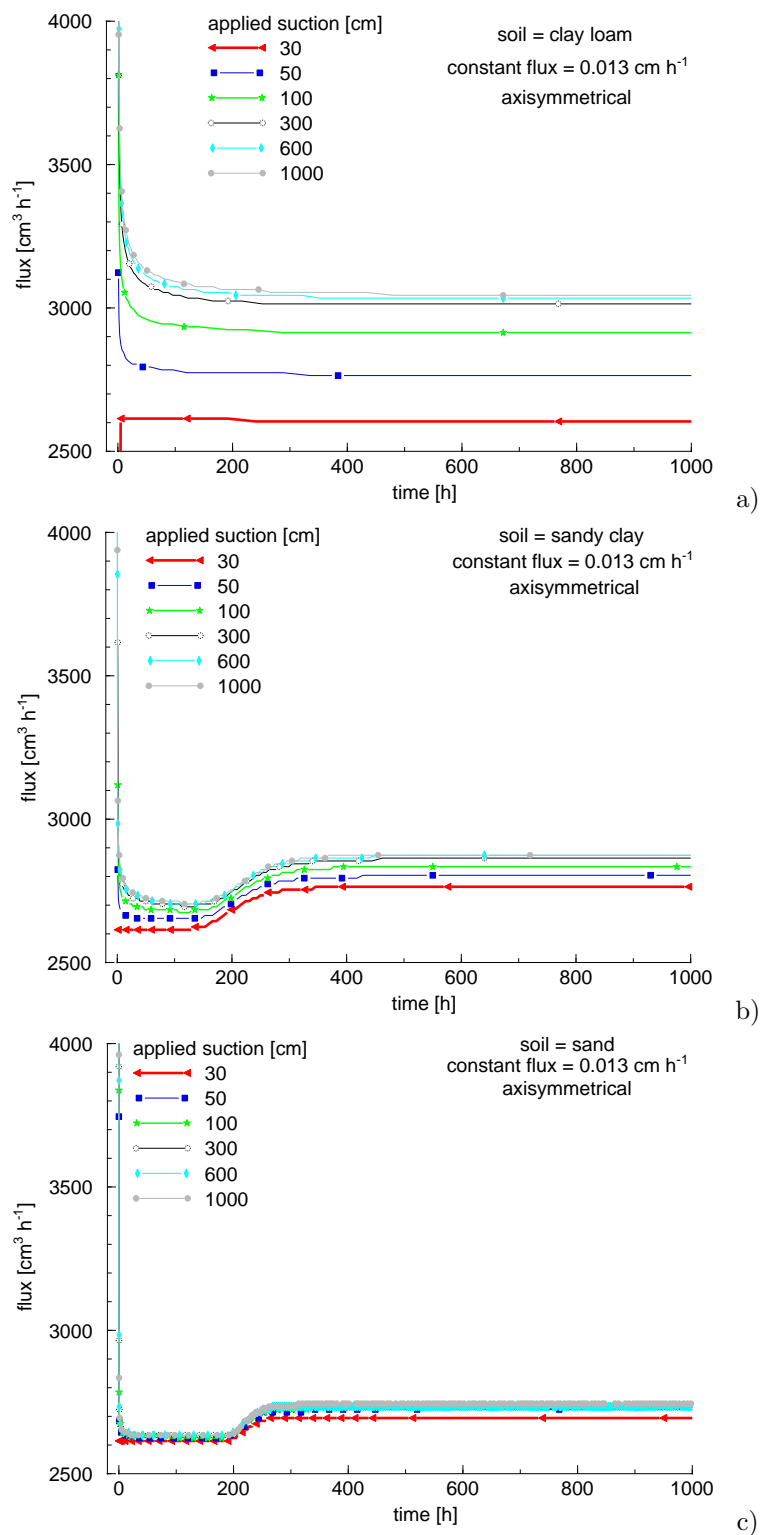
A.14   Extraction rates of the suction cup

Figure A.9: Extraction rates $[\mathrm{cm}^3\ \mathrm{h}^{-1}]$ of the suction cup for a constant flux $J_w = 0.013\ \mathrm{cm}\ \mathrm{h}^{-1}$ and different soils. a) clay loam, b) sandy clay, and c) sandy soil.

A.15 Calculation of the moments

When the data are measured, Equation 4.12,4.14 and 4.15 can be evaluated numerically using the trapezoidal rule. The integrals can approximated as:

$$\tau_0 = \sum_{i=1}^{n-1} [\frac{1}{2}(C_i + C_{i+1})]\Delta I \tag{A.1}$$

for the 0. moment. With C_i are a set of concentrations at the measured amount of water I_i. For the 1. moment Equation A.2 can be solved.

$$\tau_1 = \frac{\sum_{i=1}^{n-1} [\frac{1}{2}(I_i + I_{i+1})]^1 [\frac{1}{2}(C_i + C_{i+1})]\Delta I}{\sum_{i=1}^{n-1} [\frac{1}{2}(C_i + C_{i+1})]\Delta I} \tag{A.2}$$

The 2. moment can be solved by Equation A.3.

$$\tau_2 = \frac{\sum_{i=1}^{n-1} [\frac{1}{2}(I_i + I_{i+1})]^2 [\frac{1}{2}(C_i + C_{i+1})]\Delta I}{\sum_{i=1}^{n-1} [\frac{1}{2}(C_i + C_{i+1})]\Delta I} \tag{A.3}$$

Out of the 2. moment the variance, τ can be calculated by $\sigma^2 = \tau_2 - \tau_1^2$. The standard deviation is therefore $\sqrt{\sigma^2}$. For the flux concentration in the CDE, evaluation of the sample moments with Equation A.2 and A.3 yields to:

$$v = \frac{z}{\tau_1} \tag{A.4}$$

v is the mean pore water velocity [L T^{-1}] and z is the sampling depth [L]. The dispersion coefficient D_{eff} is calculated by:

$$D_{eff} = \frac{v^3}{2z} \sigma^2 \tag{A.5}$$

The dispersivity [L] results by dividing the dispersion coefficient D by the mean pore water velocity v.

The solution of the CDE can be written as a probability density function (pdf) ((*Jury and Roth*, 1990)):

$$C^f(z, I) = f^f(z, I) = \frac{z}{2\sqrt{\pi D I^3}} \exp(-\frac{(z - vI)^2}{4DI}) \tag{A.6}$$

with the cumulative amount of extracted water I [L]. To calculate the CDE for concentrations Equation A.6 has to be multiplied by the recovery R (see Chapter 4.12).
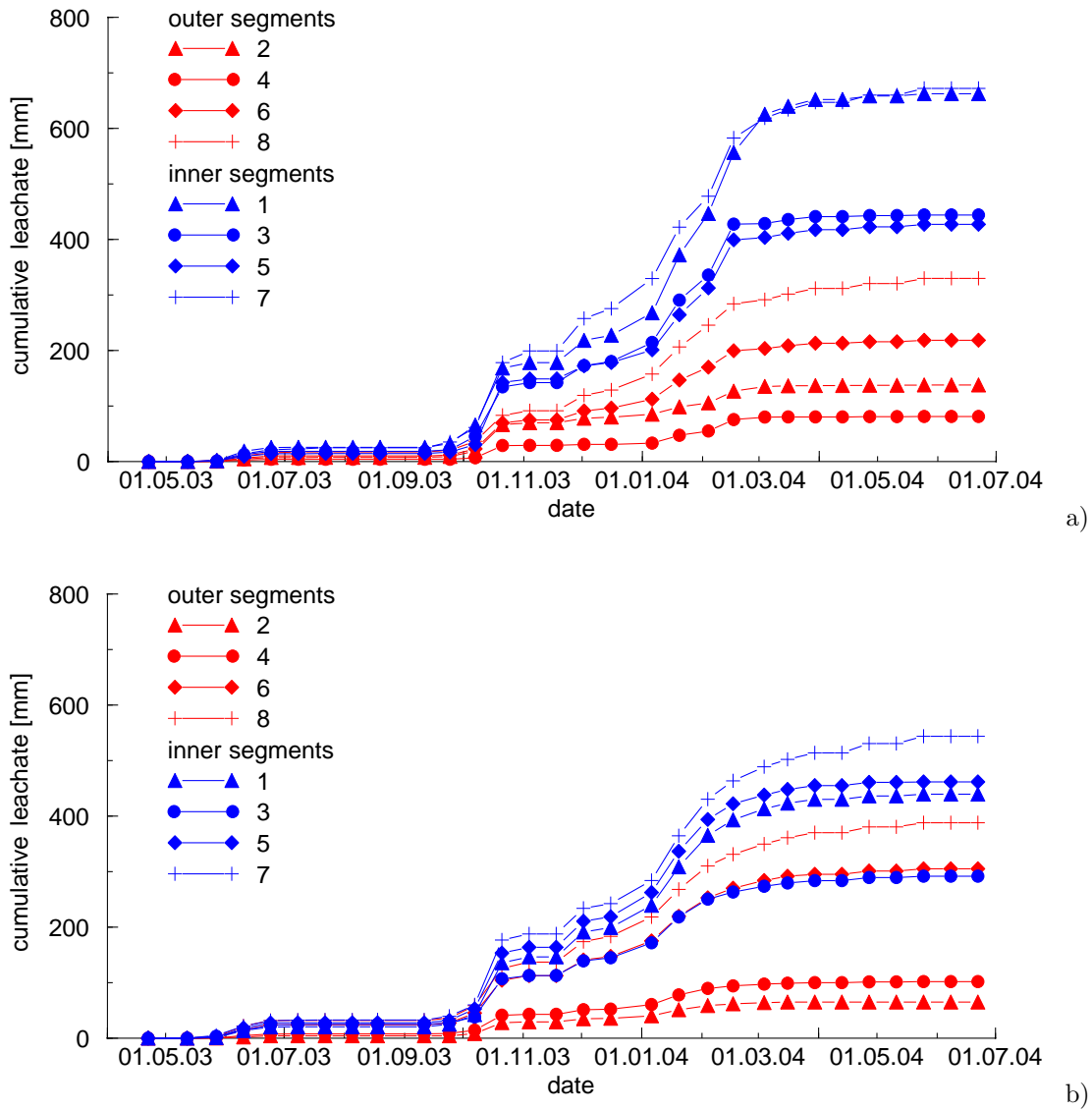
A.16 Field and lysimeter experiments

Figure A.10: Cumulative leachate at the bottom of the lysimeters at the Agrosphere Institute for a) lysimeter 1 and b) lysimeter 2. Size of the inner segments and outer segments are 1046 cm^2 and 3954 cm^2, respectively.
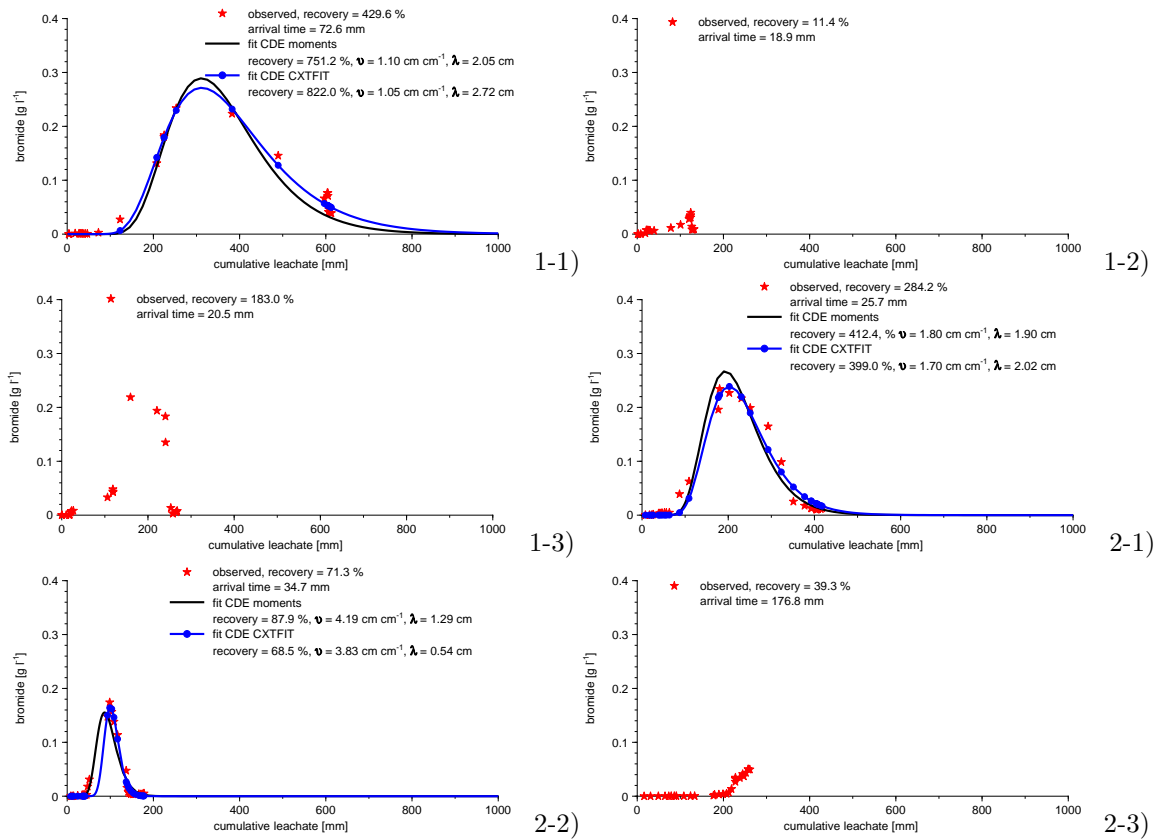
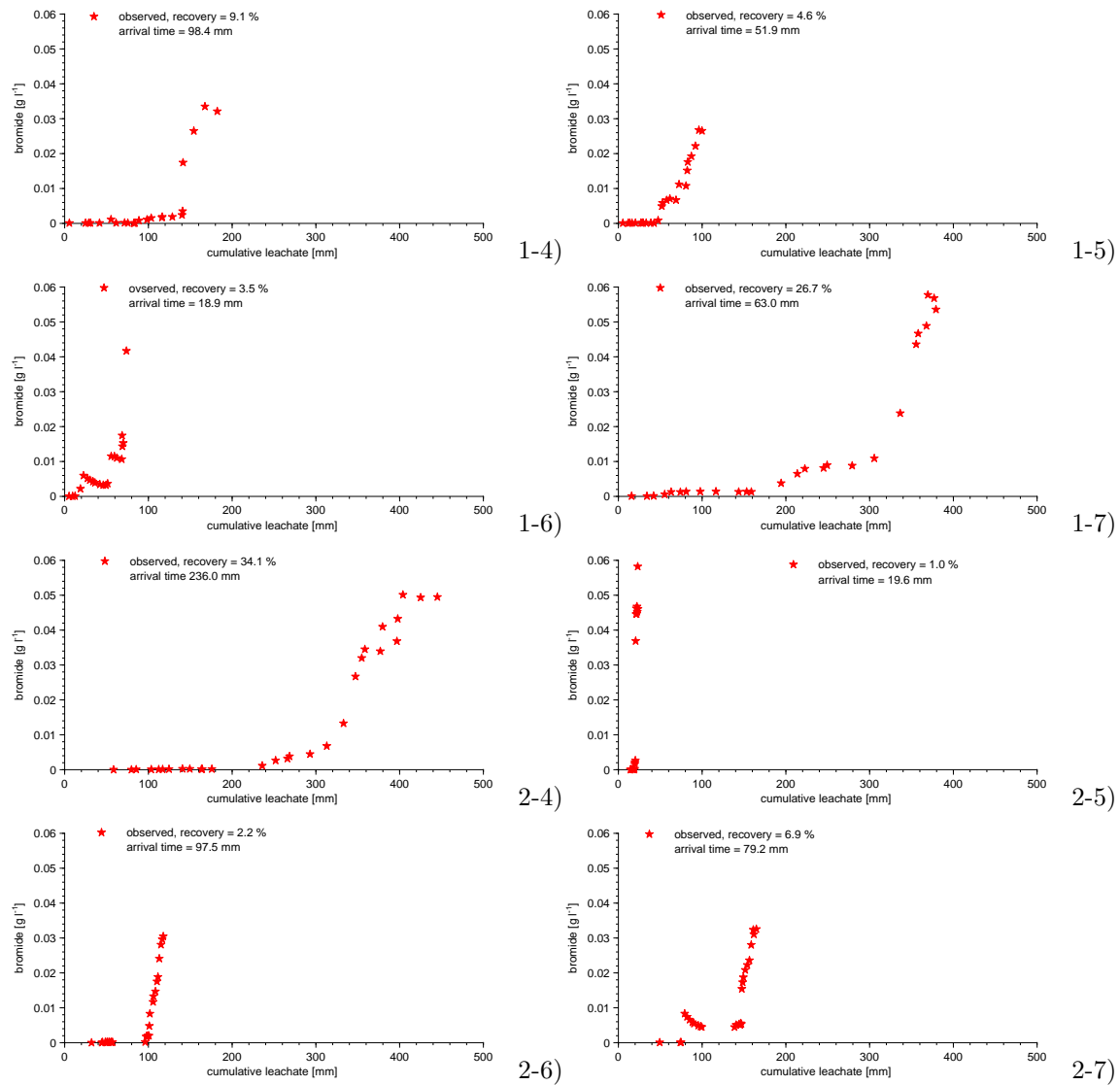## A.16.1 Bromide BTC lysimeters at the Agrosphere Institute

Figure A.11: Bromide breakthrough for the suction cups at 40 cm depth in the lysimeters 1 (1-1 to 1-3) and lysimeter 2 (2-1 to 2-3) at the lysimeter station at the Agrosphere Institute. Arrival time was determined using the measured concentration >0.001 g l^{-1}. Mass recovery was calculated using the measured concentration. CDE was calculated by methods of moments and fitted with CXTFIT (*Toride et al.*, 1999).

Figure A.12: Bromide breakthrough for the suction cups at 120 cm depth in the lysimeters 1 (1-4 to 1-7) and lysimeter 2 (2-4 to 2-7) at the lysimeter station at the Agrosphere Institute. Mass recovery was calculated using the measured concentration. Arrival time was determined using the measured concentration >0.001 g l^{-1}.
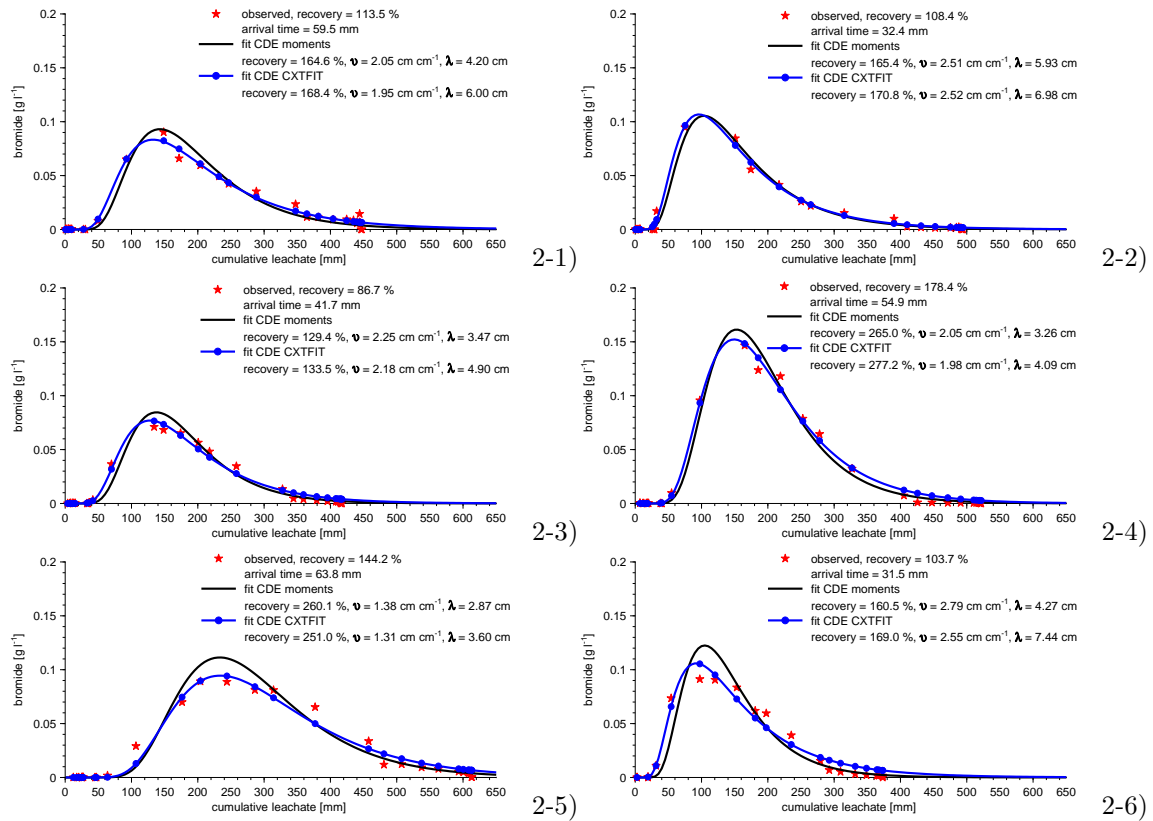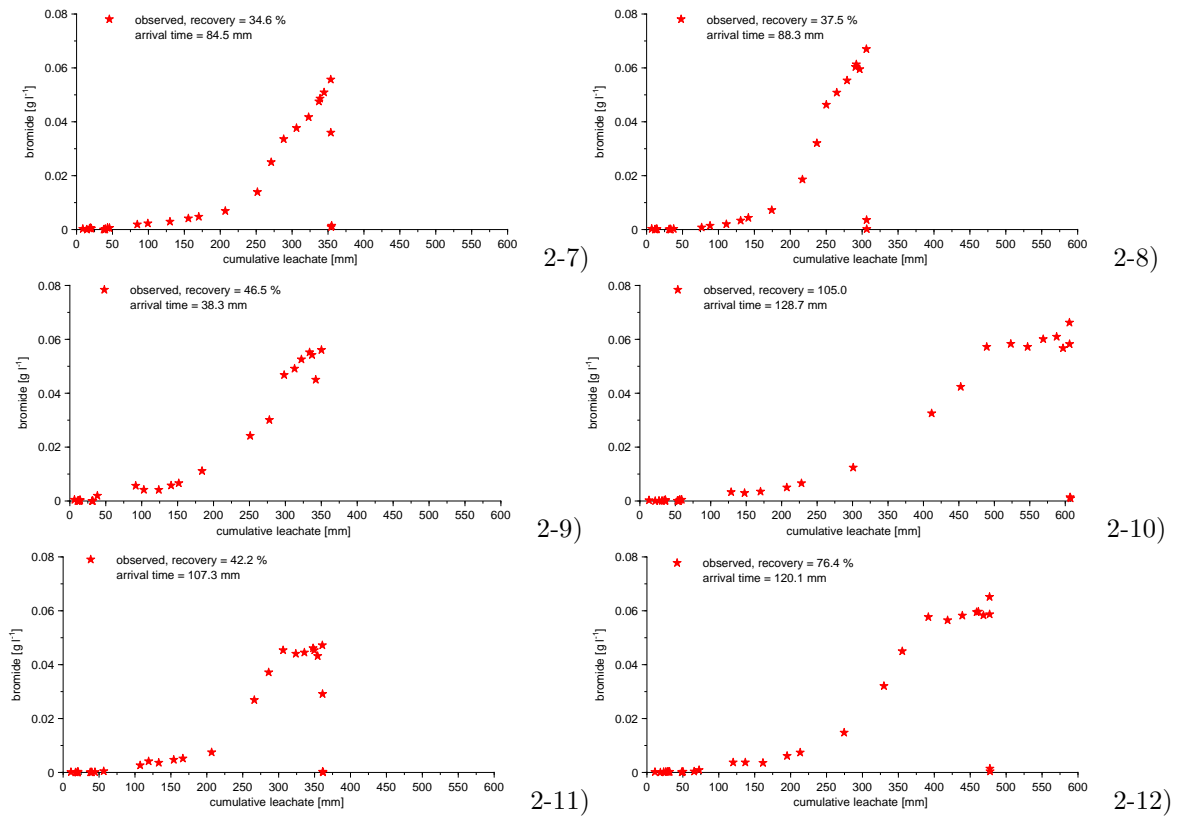
A.16.2   Bromide BTC test site Merzenhausen

Figure A.13: Bromide breakthrough for the ceramic plates at 40 cm depth in the sampling pit 2 at the test site Merzenhausen. Mass recovery was calculated using the measured concentration. CDE was calculated by methods of moments and fitted with CXTFIT (*Toride et al.*, 1999).
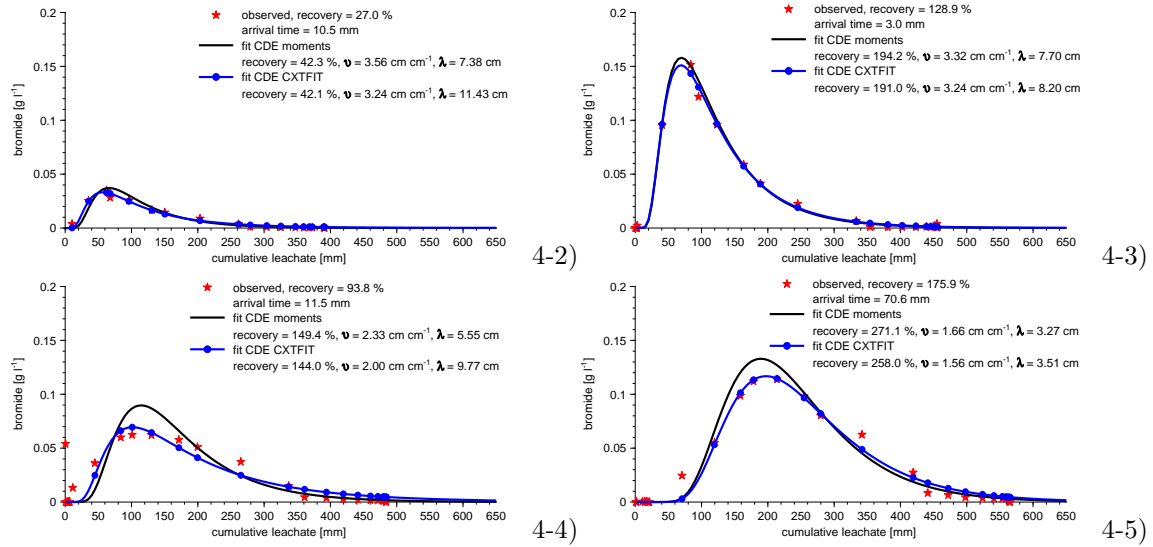
Figure A.14: Bromide breakthrough for the ceramic plates at 120 cm depth in the sampling pit 2 at the test site Merzenhausen. Mass recovery was calculated using the measured concentration. Arrival time was determined using the measured concentration >0.001 g l^{-1}.
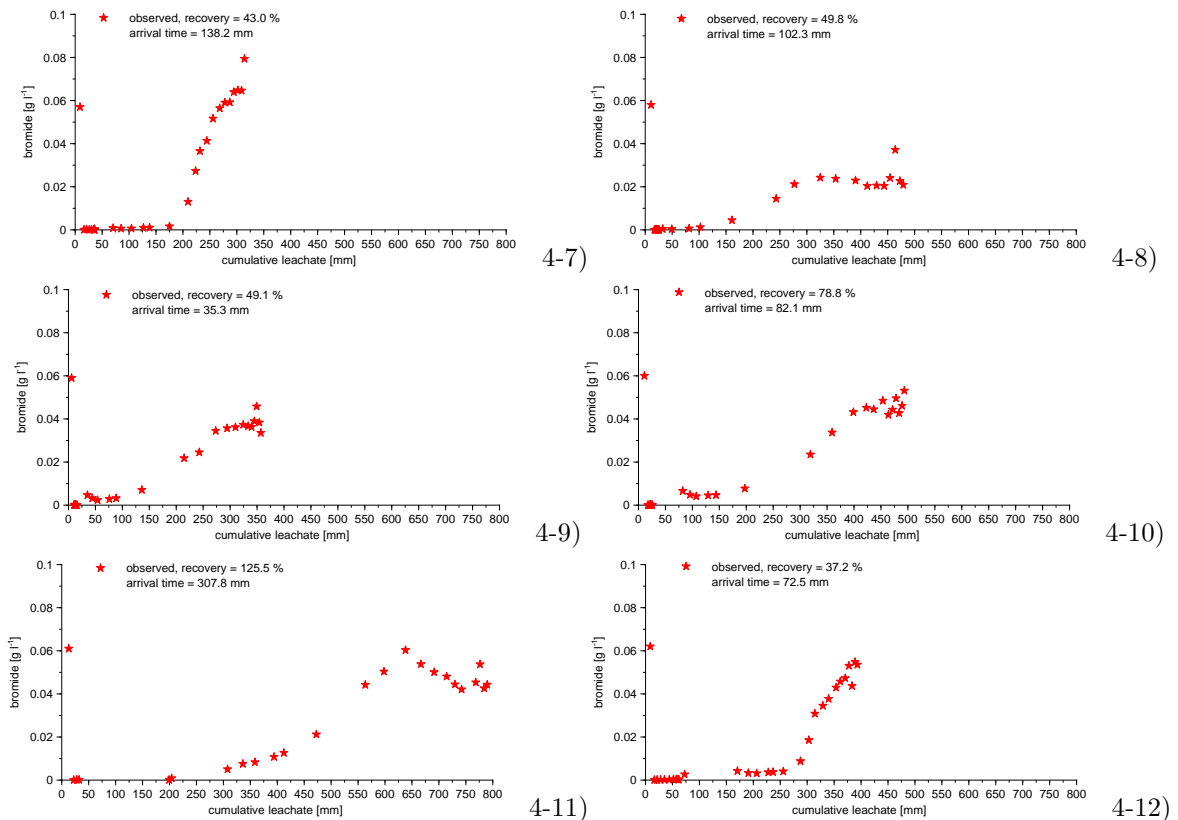
Figure A.15: Bromide breakthrough for the ceramic plates at 40 cm depth in the sampling pit 4 at the test site Merzenhausen. Mass recovery was calculated using the measured concentration. CDE was calculated by methods of moments and fitted with CXTFIT (*Toride et al.***, 1999).**

Figure A.16: Bromide breakthrough for the ceramic plates at 120 cm depth in the sampling pit 4 at the test site Merzenhausen. Mass recovery was calculated using the measured concentration.
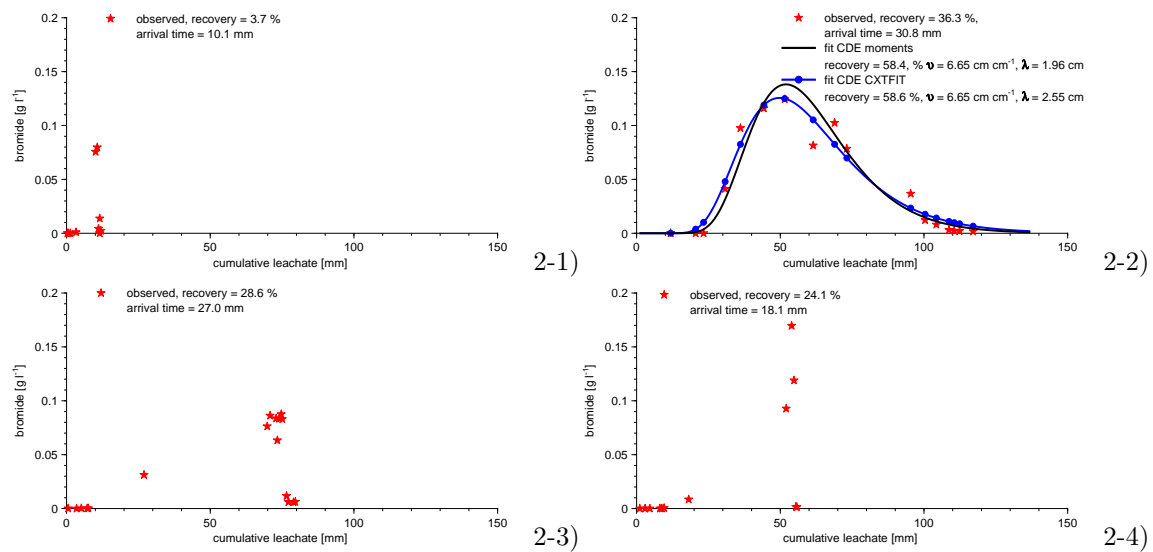
Figure A.17: Bromide breakthrough for the suction cups at 40 cm depth in the sampling pit 2 at the test site Merzenhausen. Mass recovery was calculated using the measured concentration. Arrival time was determined using the measured concentration > 0.001 g l^{-1}. CDE was calculated by methods of moments and fitted with CXTFIT (*Toride et al.,* **1999).**
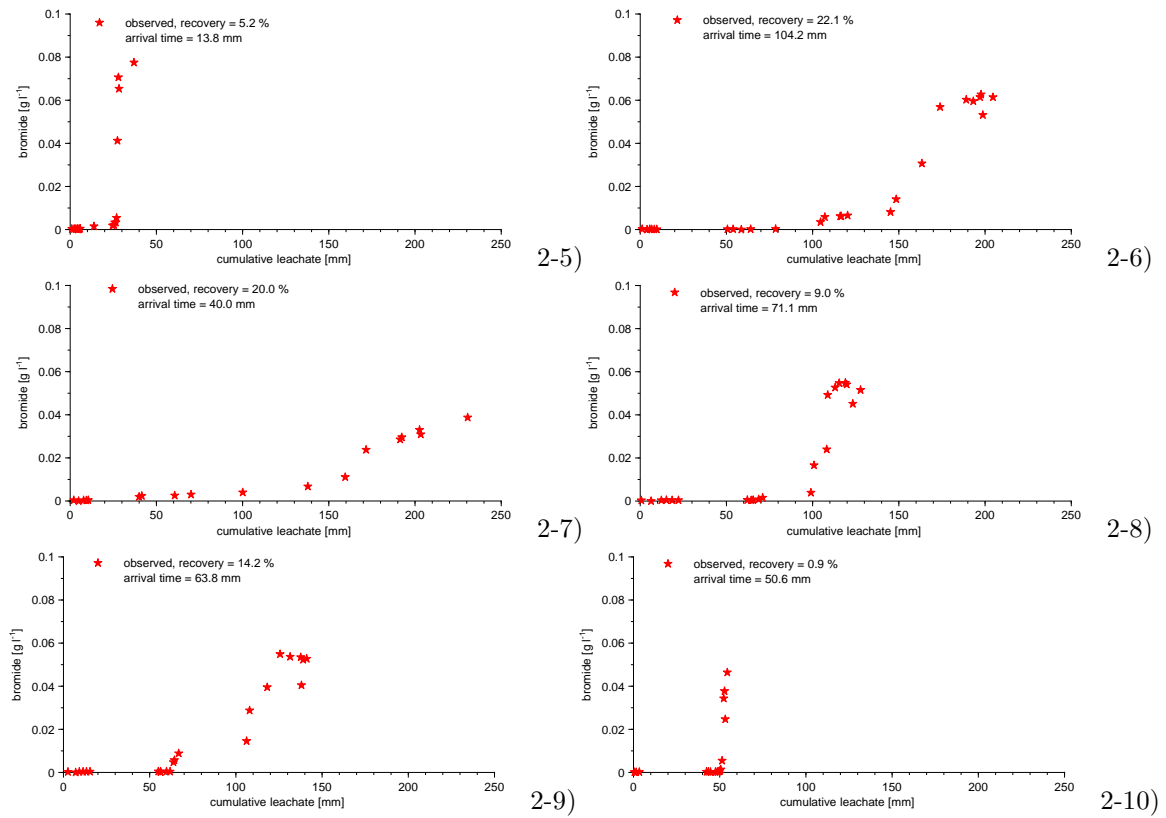
Figure A.18: Bromide breakthrough for the suction cups at 120 cm depth in the sampling pit 2 at the test site Merzenhausen. Mass recovery was calculated using the measured concentration. Arrival time was determined using the measured concentration > 0.001 g l^{-1}.
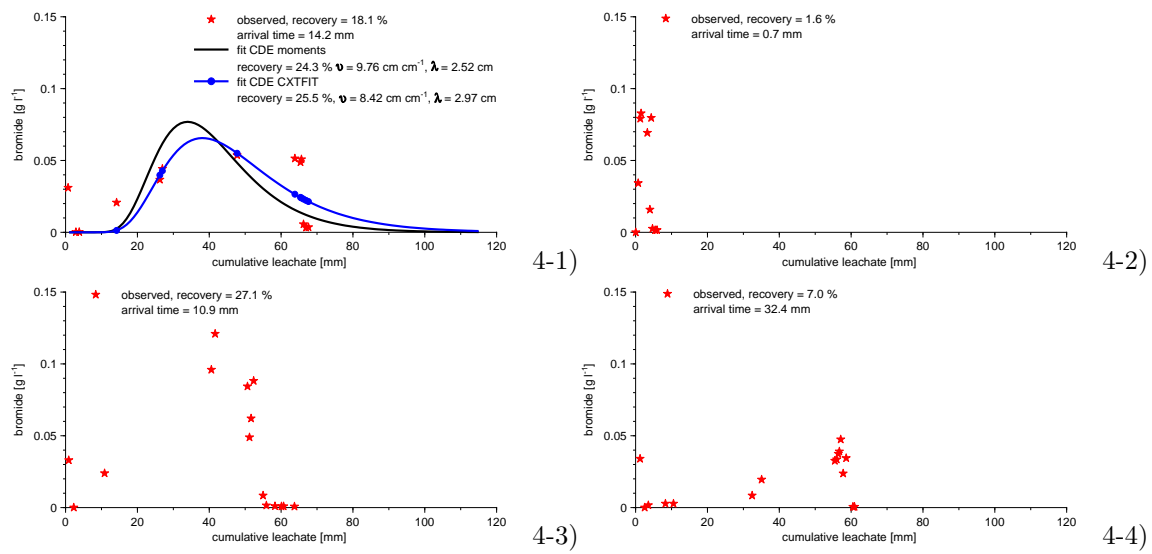
Figure A.19: Bromide breakthrough for the suction cups at 40 cm depth in the sampling pit 4 at the test site Merzenhausen. Mass recovery was calculated using the measured concentration. CDE was calculated by methods of moments and fitted with CXTFIT (*Toride et al.*, 1999).
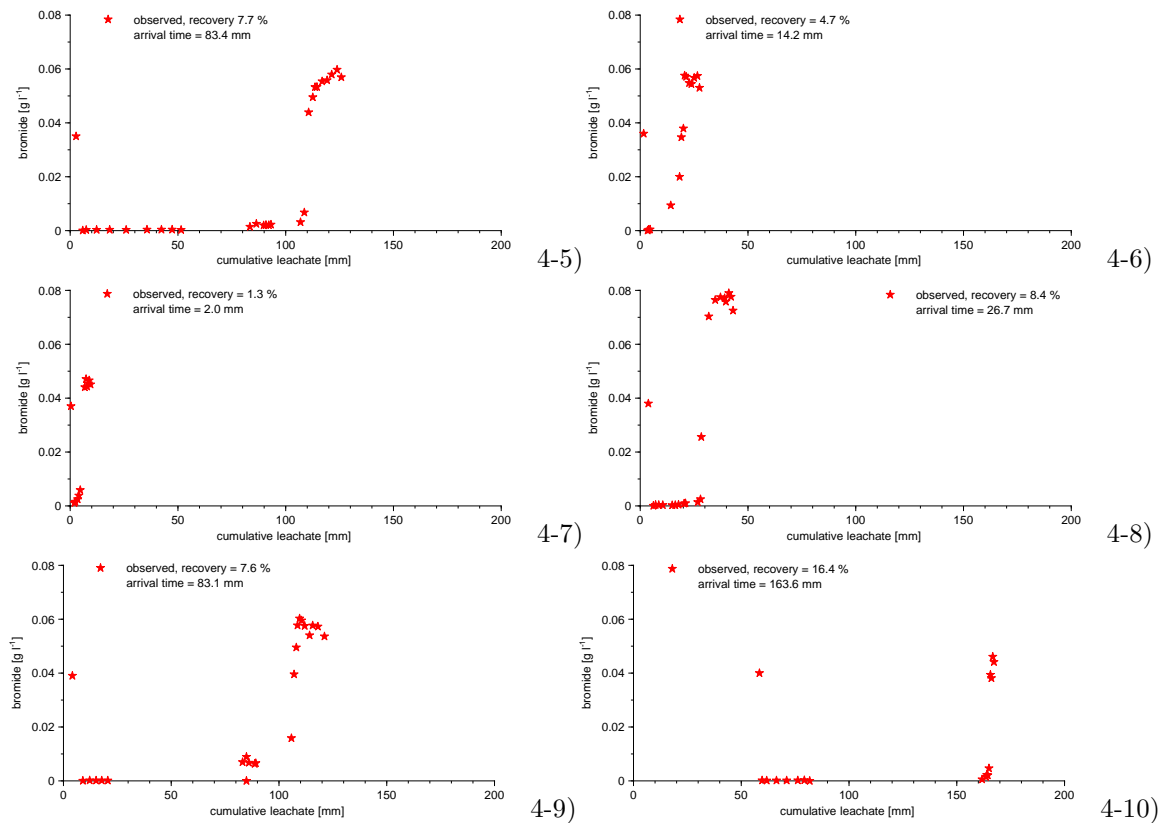
Figure A.20: Bromide breakthrough for the suction cups at 120 cm depth in the sampling pit 4 at the test site Merzenhausen. Mass recovery was calculated using the measured concentration. Arrival time was determined using the measured concentration > 0.001 g l⁻¹.

Curriculum Vitae

<u>Persönliche Angaben</u>

Name: Lutz Weihermüller

Geburtsdatum: 18. Januar 1973

Geburtsort: Hamburg

Familenstand: Verheiratet seit dem 30. August 1999
mit Claire Isabelle Weihermüller (geb. Petetin)

<u>Schulausbildung</u>

1979 - 1982 Grundschule Wettstetten

1982 - 1983 Grundschule Altkloster (Buxtehude)

1983 - 1985 Orientierungsstufe Nord (Buxtehude)

1985 - 1992 Gymnasium der Halepaghen Schule Buxtehude

<u>Studium</u>

1992 - 1996 Studium der Geographie und Sport auf Lehramt an der
Universität Bremen

1996 - 1997 Studium der Geologie und Geographie an der
Keele University (England)

1997 - 2001 Studium der Diplomgeographie and der Universität Bremen

2000 - 2001 Diplomarbeit im Niedersächsischem Landesamt für
Bodenforschung / Bodentechnologisches Institut Bremen bei
Herrn Dr. Schäfer

<u>Berufliche Tätigkeit</u>

1999 - 2001 Tätigkeit als studentische Hilfskraft im Niedersächsischem
Landesamt für Bodenforschung / Bodentechnologisches Institut Bremen

2001 Tätigkeit als wissenschaftliche Hilfskraft (Doktorand) and der
Gesamthochschule Essen Abteilung Landschaftsökologie / Stadtklimatologie

2001 - 2004 Tätigkeit als wissenschaftliche Hilfskraft (Doktorand) im Institut
für Chemie und Dynamik der Geosphäre, Institut IV: Agrosphäre.
Erstellung der vorliegenden Arbeit unter Anleitung von
Prof. Dr. H. Vereecken